12-2018

Photoreception and Eye Regeneration Mechanisms in Planarians

Taylor R. Birkholz
Western Michigan University

PHOTORECEPTION AND EYE REGENERATION MECHANISMS IN PLANARIANS

by

Taylor R. Birkholz

A dissertation submitted to the Graduate College
in partial fulfillment of the requirements
for the degree of Doctor of Philosophy
Biological Sciences
Western Michigan University
December 2018

Doctoral Committee:

Wendy S. Beane, Ph.D., Chair
John A. Jellies, Ph.D.
John M. Spitsbergen, Ph.D.
Kelly Ai-Sun Tseng, Ph.D.

ACKNOWLEDGEMENTS

First and foremost, I want to thank my advisor Dr. Wendy Beane. Wendy is a great scientist who has shown me what it takes to be a successful scientist and mentor. I had a few life-changing experiences during my time in Wendy's lab and I honestly don't know if I would have been able to complete my degree without her understanding and support. I feel so grateful that I had the opportunity to learn from Wendy and believe that her advice, guidance, and support will help me to succeed in whatever path I choose to follow.

I would also like to thank the members of my committee: Dr. John Jellies, Dr. John Spitsbergen, and Dr. Kelly Ai-Sun Tseng. I truly appreciate the input, direction, and encouragement they have given me and believe their advice and support was an important part of my progression and completion of the program. I want to thank my fellow Beane lab members who have been there to talk about and relate to situations that were unique and could only be understood in our lab.I would also like to acknowledge and thank my brother and Abbie for letting me work at their apartment on many occasions when I needed a change of scenery while writing papers and my dissertation.

Finally, I want to thank my wonderful husband, Patrick, for all of his support. He's been there for me through many, many years of graduate school with all the ups and downs. Patrick has supported me not only emotionally but also being there for Kira during times of high stress. I couldn't have done this without him and can't thank him enough for everything.

Taylor R. Birkholz

PHOTORECEPTION AND EYE REGENERATION MECHANISMS IN PLANARIANS

Taylor R. Birkholz, Ph.D.

Western Michigan University, 2018

Although humans lack the ability to regenerate complete organs and limbs following amputation or injury, there are many other species (both vertebrates and invertebrates) that can. Significant advances have been made in understanding the genetic mechanisms that regulate organ regeneration in these species, including regeneration of eye tissues such as the lens and retina. Planarians are an established historical model used to study regeneration due to their ability to regenerate any organ, including the eye. With recent advances in molecular genetic analyses, planarians are now an emerging model for the specific study of eye regeneration mechanisms. Furthermore, regeneration of the planarian eye is an ideal system for investigating regenerative morphology, in other words how tissue size, shape, and placement is established during regeneration. However, comparatively little is known about the physiology of planarian photoreception or the mechanisms that regulate eye regrowth. These fundamental aspects must be understood in order to increase the effectiveness of the planarian eye regeneration model.

Our data has revealed that planarians have complex phototactic responses and display differential behaviors to specific wavelengths of light, including ultraviolet and infrared. This information is critical because regeneration studies previously determined functional recovery of the visual system based on planarian responses to white light. As white light is a composite of

many wavelengths, this may have masked complex behaviors or resulted in inconsistent results between studies. We also found that similar to other invertebrates, planarians are capable of responding to light using mechanisms outside of the eye, inputs that could also confound analyses of ocular responses. Our data show that extraocular behavioral responses in planarians are regulated in part by a homolog of the transient receptor potential channel A1 (TRPA1), a mechanism previously only identified in *Drosophila*.

Using this expanded understanding of planarian photoreception, we investigated the cellular mechanisms required for planarian eye regeneration. We have identified a potential cell signaling pathway that includes the vacuolar ATPase (V-ATPase) ion channel, Notch, and apoptosis. We found that similar pathway components were also required for eye regrowth in developing tadpoles, suggesting evolutionarily conserved mechanisms are required for eye regeneration in two very different animal models. Together, the data presented in this work increases our understanding of planarian photoreception and provides evidence that ancestral mechanisms may be required for eye regeneration.

TABLE OF CONTENTS

Table of Contents–continued

Table of Contents–continued

CHAPTER

Table of Contents–continued

CHAPTER

Table of Contents–continued

LIST OF FIGURES

List of Figures – continued

LIST OF ABBREVIATIONS

RNAi:	RNA interference
ASC:	adult stem cell
TRPC:	transient receptor potential cation
CNG:	cyclic nucleotide gated
UV:	ultraviolet
H_2O_2:	hydrogen peroxide
TRPA1:	transient receptor potential ion channel A1
AP:	anterior-posterior
hpa:	hours post amputation
PCG:	position control gene
DV:	dorsal-ventral
BMP:	bone morphogenetic protein
ML:	medial-lateral
dpa:	days post amputation
Dap-1:	death-associated protein
FGF:	fibroblast growth factor
GJC:	gap junction communication
CaV:	voltage-gated calcium channel
ER:	endoplasmic reticulum

SERCA:	sarcoplasmic/endoplasmic reticulum calcium ATPase
PCP:	planar cell polarity
IR:	infrared
ND:	neutral density
dsRNA:	double-stranded RNA
ROS:	reactive oxygen species
O3:	ozone
V-ATPase:	vacuolar ATPase
DMSO:	dimethyl sulfoxide
NICD:	Notch intracellular domain

CHAPTER I: INTRODUCTION

The Planarian Model System

Planarians have fascinated scientists for hundreds of years due to their extreme tissue plasticity. One remarkable example of this plasticity is the ability of the planarians to constantly remodel their bodies based on food supply and proportionally grow when food is abundant and "degrow" when starved (Baguñá and Romero, 1981; Lillie, 1900). This tissue plasticity also allows planarians to completely regenerate into new, proportional animals from tiny tissue fragments (Fig. 1). This has historically made planarians a powerful model system for examining regeneration (Morgan, 1900; Stevens, 1909). In 1814, the early investigator John Dalyell stated that planarians appear to be "immortal under the knife" (Dalyell, 1814). Although early planarian studies were largely observational, recent molecular and genomic advances have added a wealth of knowledge to our understanding of this model organism. This includes a completely sequenced genome of one of the most common species used, *Schmidtea mediterranea* (Grohme et al., 2018; Robb et al., 2015; Robb et al., 2008), RNA interference (RNAi) techniques (Rouhana et al., 2013; Sánchez Alvarado and Newmark, 1999), and *in situ* hybridization and immunohistochemistry protocols (Forsthoefel et al., 2014; King and Newmark, 2013; Pearson et al., 2009). Their unique characteristics, along with the available molecular toolkit, have made planarians an important model system for understanding a range of biological processes including stem cell biology and regeneration (Adell et al., 2010; Elliott and Sánchez Alvarado, 2013; Reddien, 2013; Rink, 2013; Umesono et al., 2011; van Wolfswinkel et al., 2014), reproduction (Rouhana et al., 2017), toxicology (Grebe and Schaeffer, 1991; Van Huizen et al., 2017; Wu and Li, 2018), evolution (Labbé et al., 2012; Nakazawa et al., 2003), and tissue

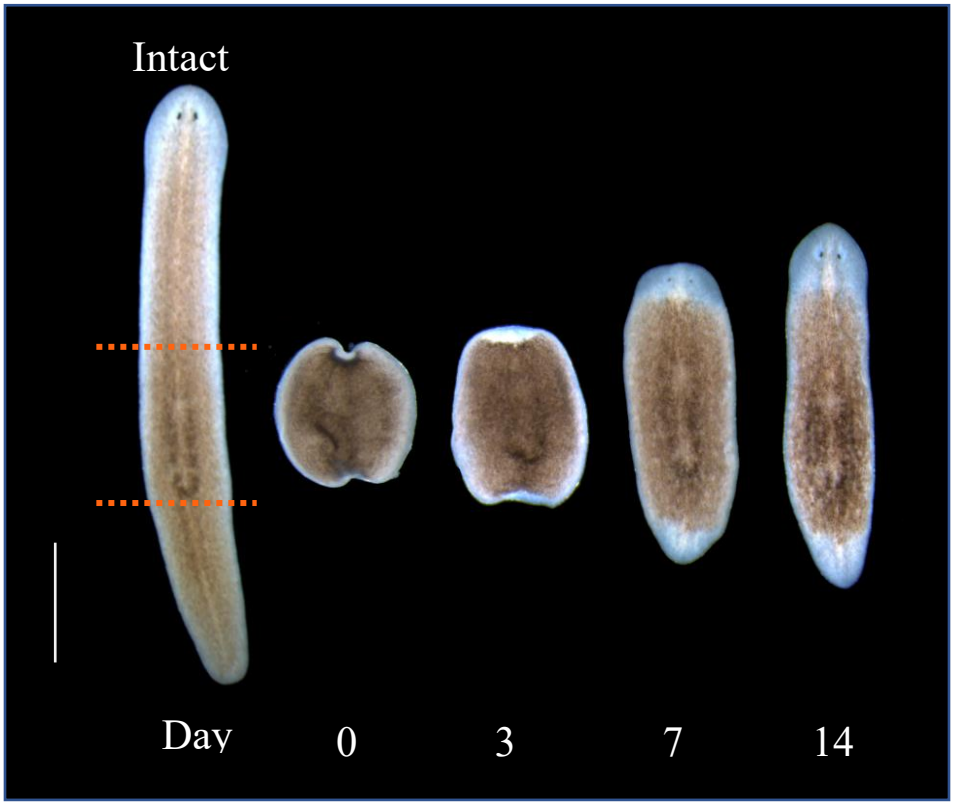

Figure 1. Planarian Regeneration. Composite image showing planarian regeneration over 14 days following amputation into a trunk fragment. Anterior is up, dotted line=amputation plane, scale bar=1 mm.

morphogenesis (Birkholz et al., 2018; Emmons-Bell et al., 2015).

Planarians are nonparasitic flatworms that are found in both fresh and salt water streams and ponds throughout the world. They are members of the phylum Platyhelminthes (order Tricladida), which includes simple bilateral animals that have discreet organ systems and tissues derived from all three germ layers. Planarians are small, soft bodied animals that lack a respiratory or circulatory system and instead obtain oxygen by diffusion. This results in their characteristic flattened morphology, since tissues must remain thin for diffusion to occur across all cells. Planarians have a sophisticated central nervous system that consists of bi-lobed anterior cephalic ganglia (true brain) and two ventral nerve cords that run along the length of the body (Fig. 2) (Agata et al., 1998). The anterior region of the animal also contains photoreceptors (Carpenter et al., 1974) and numerous chemoreceptors (MacRae, 1967). Planarians eat and defecate using a single muscular tube, called the pharynx, which connects to the three-branched (triclad) digestive system (Fig. 2) (Newmark and Sanchez Alvarado, 2002). The protonephridial excretory system functions to remove waste products and facilitates osmoregulation and has been found to have homologies to vertebrate kidneys (Fig. 2) (Ishii, 1980; Rink et al., 2011). Planarian reproduction occurs either sexually, as cross-fertilizing hermaphrodites (Chong et al., 2011), or asexually through transverse binary fissioning.

The process of fissioning, which is a form of asexual reproduction, is another striking example of planarian plasticity. To fission, a planarian stretches until it tears in half, resulting in head and tail fragments that will subsequently grow into two new animals. The head fragment will grow a new tail, while the tail fragment will grow a new head including completely new brain. This ability to regenerate entire organ systems is due to the large population of adult stem

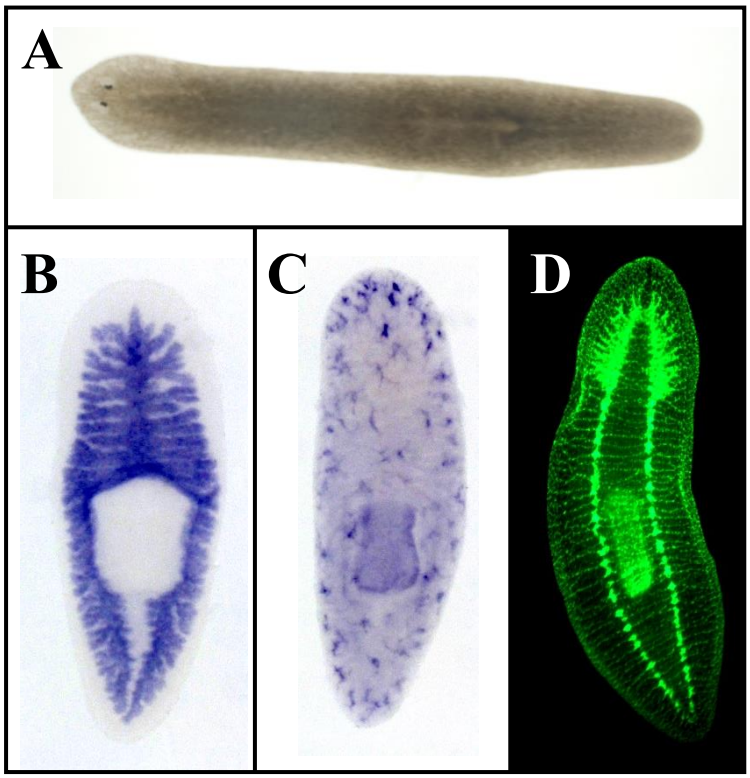

Figure 2. Planarian Model System and Anatomy. (A) The planarian species *Schmidtea mediterranea* (anterior is left). **(B)** Digestive system visualized innexin-9. **(C)** Excretory system visualized with innexin-10. **(D)** Central nervous system labeled with anti-synapsin. B-D anterior is up. Dorsal is up in all.

cells (ASC), historically known as neoblasts, found throughout the body. ASCs are the only known dividing cells in planarians and represent ~25-30% of all cells (Baguñà et al., 1989; Reddien and Sánchez Alvarado, 2004). Following tissue removal, regeneration begins with an initial wound response that triggers an increase in apoptosis at the injury site (Wenemoser et al., 2012). This is followed by apoptosis-induced proliferation of ASCs throughout the body (Pellettieri et al., 2010; Wenemoser and Reddien, 2010). The ASCs then migrate to the wound where they form a mass of unpigmented newly differentiating cells, called the blastema (Baguñà et al., 1989; Eisenhoffer et al., 2008). Most of the lost tissue will emerge from the blastema and by approximately 2 weeks, a completely regenerated, proportional animal will be produced (Beane et al., 2013).

Photoreception and the Planarian Visual System

Unlike most other animals, planarians have the ability to regenerate their entire eye, making them excellent model organisms for eye regeneration. Although simpler than vertebrate eyes, planarian eyes still have several phylogenetically conserved characteristics. For example, both planarians and vertebrates rely on common genes for eye development such as *Sine oculis*, *Eyes absent*, and *Otx* (Martín-Durán et al., 2012; Pineda et al., 2000). Planarian eyes are located dorsally and consist of two cell types: pigment cells and photoreceptor neurons (Fig. 3). The pigment cells form a semi-lunar optic cup that faces the photoreceptor organelles in a similar orientation as vertebrate photoreceptors with respect to the retinal pigment epithelium (Lapan and Reddien, 2011). The primary function of pigment cells in simple eyes is to absorb photons of light, which creates shade and provides information about the direction of incoming light (Nilsson, 2009). The photoreceptor cell bodies are located outside of the optic cup and extend

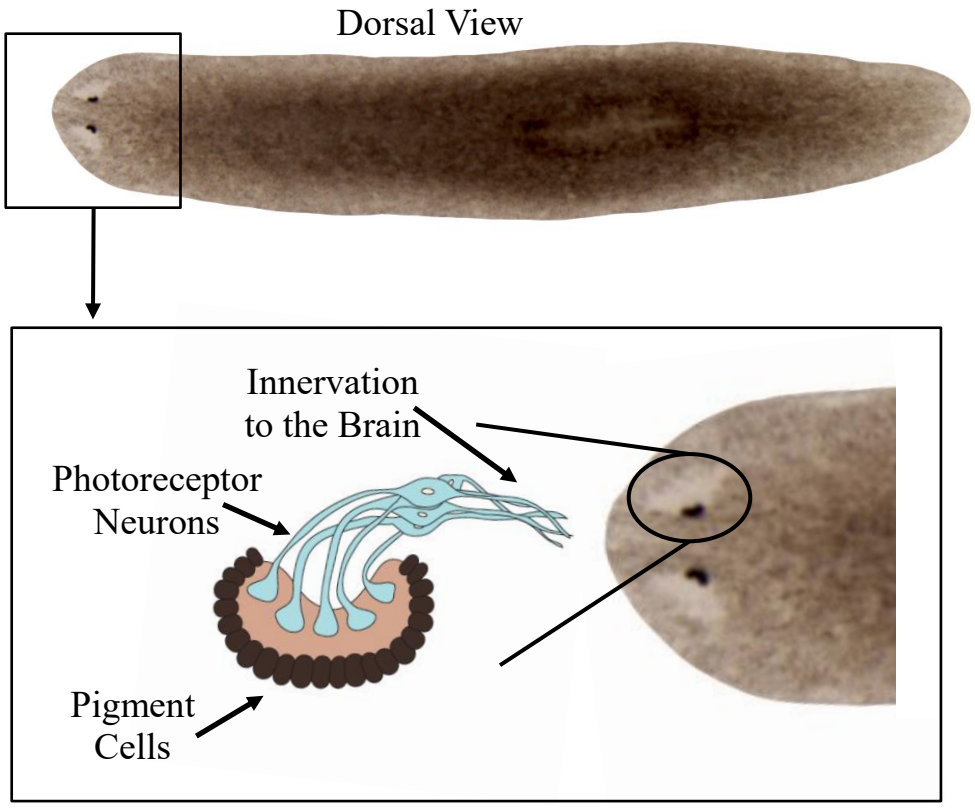

Figure 3. Planarian Eye Anatomy. The planarian species *Schmidtea mediterranea* was used. Boxed region shows a close up of the eyes, with an inset diagram of the light-sensing structures of the optic cup. The eye consists of two tissue types: the light capturing pigment cells and the photoreceptor neurons that transduce photons into signals sent to the brain. Figure taken from (Paskin et al., 2014).

dendrites into the cup forming a rhabdomeric structure where opsin accumulates (Azuma and Shinozawa, 1998; Carpenter et al., 1974; Orii et al., 1998). Photoreceptor cell axons project posteriorly to the brain with some fibers forming a partial optic chiasma allowing photosensory information from both sides of the animal to be integrated (Agata et al., 1998; Okamoto et al., 2005; Sakai et al., 2000).

The molecular mechanisms used in ocular phototransduction (i.e. the ability of cells found specifically in the eye organ to detect light) have been elucidated in numerous model organisms, highlighting that many of the transduction components are highly conserved throughout the Bilateria (Arendt, 2003). For example, opsins, which are a group of G-protein coupled receptors that bind to chromophores, are responsible for ocular light detection in all known animal systems (Wald, 1968). Although a few exceptions do exist (Vöcking et al., 2017), the invertebrate eye has rhabdomeric photoreceptors that use r-opsins while vertebrates have ciliary photoreceptors and use c-opsins (Arendt, 2003). In the presence of photons, the activation of r-opsins initiates a pathway that results in the opening of transient receptor potential cation (TRPC) channels (Hardie, 2001) while c-opsins lead to the closing of cyclic nucleotide gated (CNG) ion channels (Kaupp and Seifert, 2002). The result of both cascades is a signal that is sent to the brain for interpretation so that an appropriate behavioral response can be elicited.

Planarians possess rhabdomeric photoreceptors and express components of the r-opsin phototransduction pathway including two r-opsin orthologs, Gα-q, PLC, and two TRPC orthologs (Lapan and Reddien, 2012; Orii et al., 1998). Interestingly, it has also been shown that the planarian eye contains genes such as CNG, that are typically found in the c-opsin pathway (Lapan and Reddien, 2012). However, the function of these genes remains to be identified. Lacking camera eyes, planarian ocular photoreception is not involved in image formation but

instead is most likely required for detection of luminal contrast. Planarians are negatively phototactic (Parker, 1900; Reynierse, 1967), a behavior that is commonly used to evaluate regeneration of the visual system (Arees, 1986; Dasheiff and Dasheiff, 2002; Inoue et al., 2004; Takano et al., 2007). Although planarians possess a well-documented photophobic response to white light, little is known about how their behavior is affected by various wavelengths. This is despite the fact that many animals exhibit wavelength-specific behaviors. For example, zebrafish larvae will swim toward ultraviolet (UV), blue, and red light but are only weakly attracted to green light (Orger and Baier, 2005). Conversely, leeches display complex negative phototactic responses to green and UV light (Jellies, 2014a, b) while *Drosophila* larvae avoid exposure to blue, violet and UV wavelengths (Xiang et al., 2010).

Extraocular Photoreception

In addition to ocular photoreception, many animals are also able to detect and respond to light using light-sensitive structures located outside of the eye. This type of light detection, called extraocular photoreception, has been recorded in both vertebrates and invertebrates (Cronin and Johnsen, 2016; Lees, 1948; Porter, 2016; Steven, 1963). The function of extraocular photoreception is diverse and ranges from phototaxis and/or shadow-induced withdrawal in mollusks and Cnidaria (Lukowiak and Jacklet, 1972; Pankey et al., 2010; Ramirez et al., 2011; Taddei-Ferretti and Musio, 2000), dorsal-ventral body orientation in leeches (Jellies, 2014b), detection of polarized light and magnetic orientation in amphibians (Adler and Taylor, 1973; Phillips et al., 2001), and regulation of circadian and reproductive cycles in birds (Menaker, 1968).

The molecular pathways used for extraocular photoreception are also wide-ranging and include both opsin and non-opsin-based mechanisms. For example, c- and r-opsins are used for extraocular photoreception in cuttlefish (Mathger et al., 2010) and pond snails (Pankey et al., 2010), respectively, while light perception in the purple sea urchin is mediated by both c- and r-opsins (Delroisse et al., 2014). Gs-opsins (or "cnidops") are another group of opsins used for extraocular photoreception in Cnidarians and are believed to activate CNG channels in *Hydra* (Plachetzki et al., 2010).

A few mechanisms for extraocular photoreception have also been identified that do not rely on opsins. Although the transduction pathway is poorly characterized, cryptochromes are UV-A/blue light sensitive photoreceptors that regulate behaviors such as circadian rhythms in plants and animals (Chaves et al., 2011; Haug et al., 2015) and magnetoreception (Bazalova et al., 2016; Gegear et al., 2008). Another non-opsin-based mechanism for extraocular light detection involves gustatory-related receptor proteins. In *C. elegans*, two gustatory-related receptor genes, LITE-1 and GUR-3, are responsible for the detection and avoidance of UV light (Bhatla and Horvitz, 2015; Edwards et al., 2008). It is thought that the mechanism of photodetection may be UV light-generated hydrogen peroxide (H_2O_2) (Bhatla and Horvitz, 2015). Similarly, in *Drosophila* larvae, the gustatory receptor GR28b (its closest homolog to LITE-1) mediates negative phototactic behavior to UV, violet, and blue light through the activation of the transient receptor potential ion channel A1 (TRPA1) (Xiang et al., 2010). TRPA1 also plays a role in light sensing in human melanocytes. In response to UV light, melanin production is increased via rhodopsin-mediated TRPA1 activation (Bellono et al., 2014). While the previous examples require G-protein coupled receptors or light-sensitive chromophores for extraocular photoreception, a subset of neurons in *Drosophila* have been shown to detect light

using direct activation of the TRPA1 ion channel by UV light-produced H_2O_2 (Guntur et al., 2015).

Planarians as a Model for Regenerative Morphology

Eye regeneration is an excellent system for understanding regenerative morphology, or the ability to induce appropriate shape *in situ*. Regenerated structures need to be integrated with pre-existing ones, through the combined regulation of new tissue growth and the scaling of surrounding tissues. Eye regeneration, for example, requires not only that the animal detects and regenerates the appropriate tissue types and produces the correct number of cells, but also that the new eyes are proportional, the correct shape, and in the right location. Correct eye morphology is critical for planarians for many reasons. Planarians are highly photophobic, and the semi-lunar shape formed by the pigment cells provides directional information about incoming light so that the animal can respond accordingly. Additionally, planarians possess true cerebral eyes, making the location of eye regeneration (near the brain) important for axonal projections.

While great strides have been made in elucidating cell growth and differentiation mechanisms, how overall shape is generated during regeneration remains largely unknown. This is because a significant gap remains in our understanding of how cell behaviors are coordinated at the level of tissues and organs. The main processes that are currently known to regulate tissue and animal shape during planarian regeneration include adult stem cell regulation, the reestablishment of body axes, tissue remodeling in pre-existing structures, organ scaling and the maintenance of body proportion, and the bioelectrical regulation of animal morphology. An

important step for the field of regenerative biology will be to uncover how all these separate processes are synchronized to produce the worms' final shape.

Overview

The goal of this work is to investigate some of the fundamental properties of planarian photoreception and eye regeneration. This will be accomplished by providing a review of what is currently known about planarian regenerative morphology, describing how planarians respond to different wavelengths of light using both ocular and extraocular mechanisms, and investigating potential signaling pathways involved in planarian eye regeneration.

Our data show that planarians have complex behavioral responses to light and respond differently to different wavelengths, including UV and infrared wavelengths. These behaviors were not previously known and will be important for functional studies that use planarian photophobic behavior to examine eye regeneration. Also important for behavioral assays used in regeneration studies is our finding that planarians are able to respond to UV light using mechanisms outside of the eye. These extraocular behavioral responses involve the TRPA1 ion channel, as our data shows that RNAi to *Smed-TrpA* reduces extraocular behavioral responses to UV.

Finally, we investigate a potential signaling pathway required for planarian eye regeneration that involves the ion channel V-ATPase, Notch, and apoptosis. This signaling pathway is especially fascinating because similar pathway components have been found to be required for eye regrowth in the vertebrate, *Xenopus laevis*. Taken together, our work significantly increases our understanding of planarian photoreception and provides the

groundwork that is needed for a deeper understanding of the mechanisms that are involved in eye regeneration.

CHAPTER II: STAYING IN SHAPE: PLANARIANS AS A MODEL FOR UNDERSTANDING REGENERATIVE MORPHOLOGY

Introduction

Planarians have fascinated scientists and non-scientists alike for hundreds of years due to their remarkable regenerative abilities. What could be more intriguing than regrowing a whole new animal from the tiniest of fragments? But these freshwater, non-parasitic flatworms are remarkable not merely because they can replace any and all tissues following injury, but because of the manner in which they do so. The tissue plasticity of planarians is astounding, allowing them to restore body shape almost regardless of the type of injury, maintaining proper proportions even when the newly regenerated worm is significantly smaller than the original (Fig.4A). This level of plasticity is important, allowing them to reproduce not only sexually but also asexually by means of transverse fissioning. When worms fission, they literally rip themselves into two, after which head fragments regenerate new tails and tail fragments regenerate new heads. Except the two resulting worms are now much smaller than the original, requiring the scaling of body parts to the new body size. Researchers have co-opted this remarkable ability in the laboratory to study regenerative mechanisms following injury, demonstrating that regeneration on the organismal scale requires not only new tissue production but also reorganization of pre-existing tissues to ensure correct size and proportion of the regenerated animal.

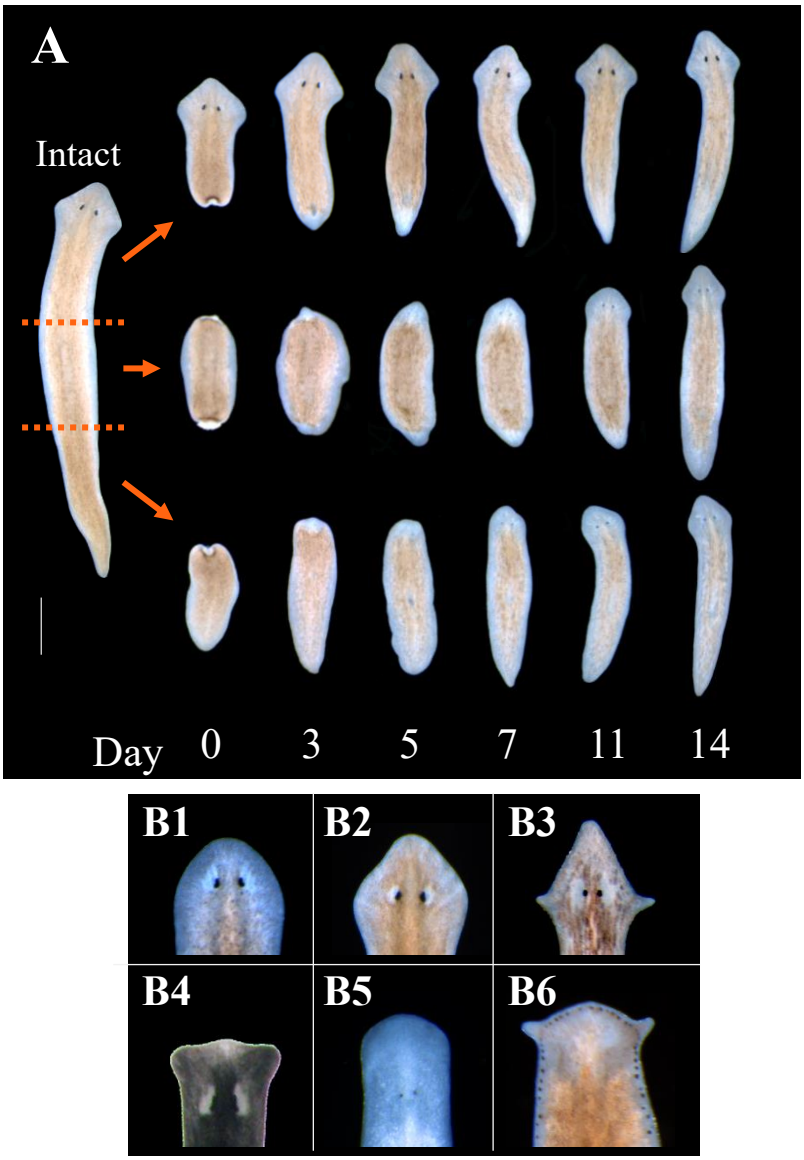

Figure 4. Planarians as a Model for Regenerative Shape. (A) Composite image showing regeneration in a single *Dugesia japonica* worm over 14 days following amputation into head, trunk, and tail fragments. Anterior is up, dotted line=amputation plane, scale bar=1 mm. **(B)** Head morphologies of different planaria. **(B1)** *Schmidtea mediterranea, (B2) Dugesia japonica*, **(B3)** *Girardia dorotocephala*, **(B4)** *Phagocata gracilis*, **(B5)** *Phagocata morgani*, **(B6)** *Polycelis felina*.

For this reason, planarians make an outstanding model for investigating the mechanisms of regenerative shape, defined here as the establishment of normal form (or animal-wide morphology) during regrowth. In addition, there are hundreds of known species, many with morphologically distinct features (such as differing head shapes) that facilitate understanding of organismal shape mechanisms (Fig.4B). Along with a wealth of historical data, significant progress has been made in understanding the molecular and genetic mechanisms that underlie planarian regenerative capabilities. On a certain level almost all processes associated with regeneration could be considered part of shape establishment; the ultimate goal of regeneration is the restoration of functional tissues and organs, and shape is integral to function. Here we provide an overview of just those mechanisms that have been shown to be most critical for morphology during planarian regeneration. The reader is directed to the many excellent reviews that delve into each subject more thoroughly (see (Adler and Sánchez Alvarado, 2015; Cebrià, 2016; Cutie et al., 2017; Elliott and Sánchez Alvarado, 2013; Mathews and Levin, 2017; Roberts-Galbraith and Newmark, 2015; Ross et al., 2017; Zhu and Pearson, 2016)). Furthermore, we provide a brief historical context of the study of regenerative shape in planaria, as well as highlight the most important future directions for this field.

Historical Studies: Questions Without Answers

Planarian regeneration has been studied for centuries (for review see (Elliott and Sánchez Alvarado, 2013)), and their ability to reform into the correct shape following a myriad of injury types was the focus of much of the early historical literature. Rooted in classical embryological methods, the earliest studies of planarians explored changes in shape following virtually every conceivable type of injury and after exposure to a wide range of chemicals, compounds, and

environmental conditions. These studies were largely observational, but led to the discovery of many of the characteristics that make planarians a great model for regenerative shape. Harriet Randolph's work in the late 1890's noted that the amount of new tissue (*i.e.* the blastema) that was regenerated in planarians was less than what was originally removed (Randolph, 1897). Furthermore, the amount of new tissue produced was proportional to the new smaller worm size (rather the larger original worm) leading to restoration of normal body proportions (Randolph, 1897). Around the same time, Thomas Hunt Morgan noted that planarian heads always regenerated from anterior facing wounds (and tails from posterior facing wounds), and that new pharynges arose not in new tissues but within the old pre-existing tissues (Morgan, 1898). Morgan termed this reorganization of pre-existing tissues "morphallaxis," and suggested it was the result of "an active migration of old tissue" (Morgan, 1900, 1901). Thus, the study of critical shape processes such as new tissue growth, axial polarity establishment, and tissue remodeling were the focus of planarian research from the beginning.

In his studies, Morgan described how the tiniest of fragments—1/100 or 1/279 of the original worm—were able to regenerate but interestingly not with the correct overall morphology (Morgan, 1898). A few years later (in 1909) Morgan's former graduate student Nettie Stevens concluded, after researching disruptions of regenerative shape (from different amputation schemes that gave rise to ectopic structures such as heads and pharynges), that "an unlimited amount of work on the readjustments in nerve cords and digestive tract" are required to regenerate a symmetrical worm (Stevens, 1909). These kinds of observations led researchers to postulate on the level and mechanisms of regulation that controlled morphogenesis during planarian regeneration.

Morgan hypothesized the existence of a "graded distribution of materials" that determined the polarity of tissues during regeneration, stating that "The phenomena of regeneration are, in part, the outcome of this gradation" (Morgan, 1905). Morgan would eventually discard this line of investigation. Not long after, Charles Manning Child built on these ideas to propose his now famous gradient theory for polarity establishment along the anterior-posterior (AP) axis during planarian regeneration (Child, 1911). Child's hypothesis was that a morphogenetic gradient (in this case regulated by metabolic factors rather than particles) controlled shape decisions in regenerating tissues (Child, 1911). However, subsequent decades failed to identify a definitive gradient. As stated in 1901 by another planarian researcher, Frank Lillie, the "phenomena of regeneration offer many problems, some of which not only appear insoluble in the present state of our knowledge, but actually offer no point of attack" (Lillie, 1901). The question of whether or not the gradient predicted by Morgan and Child regulated planarian shape would be left to modern researchers.

Modern Era: New "Points of Attack"

Molecular and genomic advancements have significantly improved our understanding of planarian regenerative processes, uncovering mechanistic explanations for many historical observations. The modern planarian toolkit includes the sequenced genome of the species *Schmidtea mediterranea* (Grohme et al., 2018; Robb et al., 2015; Robb et al., 2008), RNAi techniques (Rouhana et al., 2013; Sánchez Alvarado and Newmark, 1999), and *in situ* hybridization and immunohistochemistry protocols (Forsthoefel et al., 2014; King and Newmark, 2013; Pearson et al., 2009; Umesono et al., 1997). Not surprisingly, the data reveal that regeneration of functional tissues of the correct size and shape is a rich, complex process

requiring communication and feedback at the cellular, tissue and organism levels. Here we highlight the main components that have been identified as key regulators of regenerative shape (Fig.5). It is likely that these are not the only factors involved in shape establishment, particularly since very little is known about how these disparate processes are coordinated on an animal-wide scale. However, the planarian model system provides one of the best platforms for investigating the natural ability to scale and reorganize the body plan to the correct geometry. And importantly, researchers now have the tools to be able to answer: What do you need to regenerate an animal of the right shape?

Getting the Right Number of Organs In the Right Place

To regenerate with proper shape, the correct tissues must be replaced in the correct location following injury. In planarians this process requires: (1) the regulation of stem cells to promote new tissue growth and (2) the establishment of axial polarity in those new tissues. But how does the animal determine what tissues need to be restored and where these new tissues should go? Understanding the signals that regulate these early decisions is essential for regenerative shape and has been the focus of much of the current planarian literature.

In planarians, wounding triggers an increase in apoptosis at the injury site 1-4 hours post amputation (hpa) (Pellettieri et al., 2010) and a body-wide increase in mitosis that peaks between 4-6 hpa (Wenemoser and Reddien, 2010). This early proliferation reflects the mobilization of a heterogeneous planarian ASC population, also known as neoblasts. In addition to this generic wound response, a regeneration-specific response follows by 12-24 hpa, leading to the upregulation of ASC-associated transcription factors and patterning genes known as position control genes (PCGs)

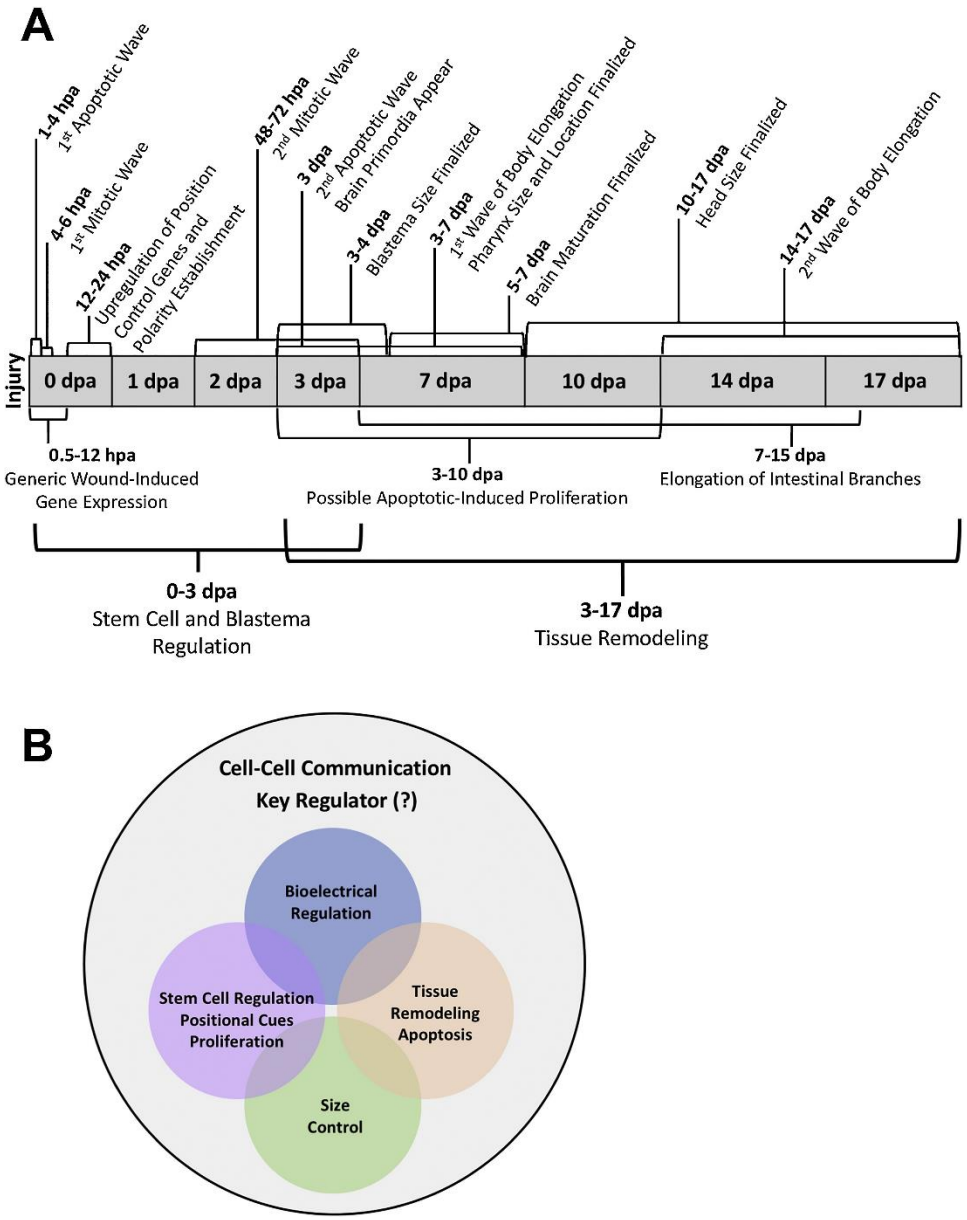

Figure 5. The Regulation of Regenerative Shape. (A) Timeline of shape establishment events during the regeneration of trunk fragments in *S. mediterranea.* Based on data from (Beane et al., 2013; Forsthoefel et al., 2011; Pellettieri et al., 2010; Roberts-Galbraith et al., 2016; Wenemoser et al., 2012; Wenemoser and Reddien, 2010; Wurtzel et al., 2015). Note that the timeline will be skewed for other species and/or fragment types. (B) Diagram of potential interactions between the central processes regulating regenerative shape during planarian regeneration.

(Scimone et al., 2014a; Wenemoser et al., 2012; Witchley et al., 2013; Wurtzel et al., 2015). Between 48-72 hpa, a second peak of mitotic activity occurs following ASC migration to the wound site (Wenemoser and Reddien, 2010). This gives rise to the regeneration blastema, an unpigmented structure comprised of ASC progeny that will eventually differentiate into many of the missing tissues (Baguñà et al., 1989; Eisenhoffer et al., 2008; Wenemoser and Reddien, 2010).

Establishment of axial polarity in the new tissues is controlled by PCGs expressed in muscle cells (Reuter et al., 2015; Scimone et al., 2016; Witchley et al., 2013). Each of the main planarian body axes is regulated by common developmental signaling pathways. The AP axis is regulated by PCGs involved in Wnt/β-catenin signaling (Gurley et al., 2008; Iglesias et al., 2008; Kobayashi et al., 2007; Petersen and Reddien, 2008; Rink et al., 2009). Inhibition of β-catenin signaling causes head regeneration at all wounds (regardless of normal polarity), while upregulation of β-catenin signaling results in regenerates with multiple tails and no head (Adell et al., 2009; Gurley et al., 2008; Iglesias et al., 2008; Petersen and Reddien, 2008, 2011). Hedgehog signaling is upstream of this β-catenin signaling, and modulation of the Hedgehog pathway leads to similar regenerative AP defects (Rink et al., 2009). A growing number of other transcription factors have also been found to regulate the AP axis during planarian regeneration (Blassberg et al., 2013; Chen et al., 2013; Currie and Pearson, 2013; Felix and Aboobaker, 2010; Fraguas et al., 2014; Hayashi et al., 2011; März et al., 2013; Scimone et al., 2014b; Vásquez-Doorman and Petersen, 2014; Vogg et al., 2014), suggesting that establishment of the AP axis is a central and early requirement and that many redundancies/parallel mechanisms likely exist to ensure AP polarity is correctly patterned.

The planarian dorsal-ventral (DV) axis is regulated by bone morphogenetic protein (BMP) signaling. BMP is expressed along the dorsal midline, and inhibition of pathway members results in ventral genes and structures being ectopically located on the dorsal side of the animal (Molina et al., 2007; Orii and Watanabe, 2007). The BMP pathway also plays an important role in medial-lateral (ML) polarity. Disruption of BMP signaling results in regenerative midline defects, such as duplicated eye tissues (Gaviño and Reddien, 2011; Reddien et al., 2007). Additionally, the Slit family of guidance cues functions reciprocally with *Wnt5* to pattern the ML axis, and its inhibition during regeneration results in collapse of the midline (Cebrià et al., 2007; Gurley et al., 2010). The involvement of BMP in both DV and ML axial patterning suggests polarity establishment includes crosstalk between each of the individual axial control programs. It is intriguing that AP axis establishment appears to require significantly more regulation than the other axes, perhaps suggesting AP polarity plays a greater initial role in regenerative patterning.

Ensuring Organs Are Scaled to the Right Size

An important step in regenerative shape is to ensure that all structures are proportional to the new worm's body size. This requires: (1) tissue remodeling of pre-existing structure, (2) apoptotic pruning of organs that are too large for the smaller regenerate, and (3) size control mechanisms to scale both new and old tissues. The planarian ability to scale tissue and organ size in both regenerative and non-regenerative contexts makes them one of the best model organisms for the study of shape establishment. Intact planaria undergoing starvation will reduce their body size while still maintaining correct body proportions, in an unusual process known as degrowth (Fig.6). The process of growth and degrowth is thought to be a balance between cell

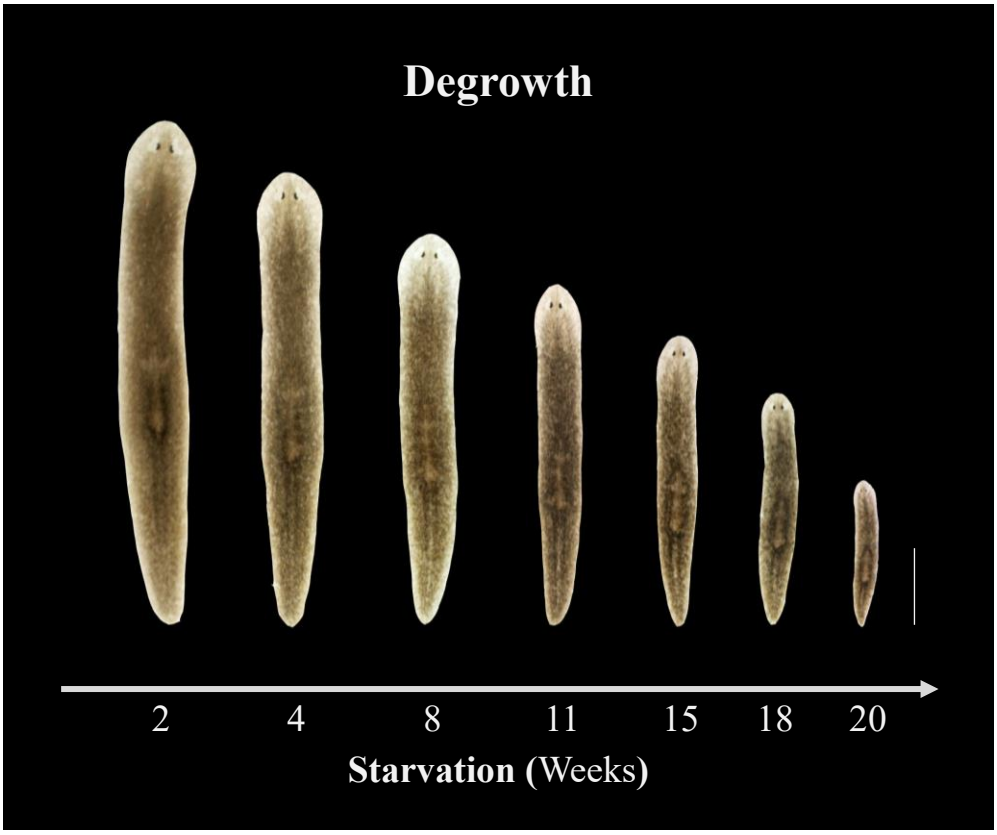

Figure 6. Starvation-Induced Degrowth in an Intact Planarian. Tissue plasticity in planarians illustrated by a composite image of a single *S. mediterranea* worm over 20 weeks of starvation. Note that as the body size decreases, tissues are scaled proportionally. Anterior is up, scale bar=1 mm.

division and cell death, much like size control during vertebrate development (Conlon and Raff, 1999). During degrowth, planarians maintain basal levels of proliferation (González-Estévez et al., 2012) but show an increase in cell death that leads to an overall loss of cells (Baguñá and Romero, 1981). In contrast, growth as a result of feeding causes more proliferation to occur than cell death, thus resulting in larger animals (Baguñá and Romero, 1981). This "allometric scaling" of body proportions, where organs have proportionally fewer cells than they previously did, is seen in both degrowth and regeneration (Oviedo et al., 2003), suggesting carefully controlled mechanisms specifically scale cell number relative to body size.

As in other regenerative organisms, tissue remodeling during planarian regeneration is mediated largely or in part by apoptosis (Bergmann and Steller, 2010; Fogarty and Bergmann, 2017; Jäger and Fearnhead, 2012). Also known as programmed cell death, apoptosis is characterized by a defined set of biochemical pathways that activate the caspase family of apoptotic regulators and lead to stereotypical cellular changes including chromatin condensation and membrane blebbing (Elmore, 2007). Following self-destruction, cell remnants are scavenged by phagocytic cells, resulting in a process that disposes of damaged, infected, or unwanted cells (Bergmann and Steller, 2010). The apoptotic machinery, and the signaling that regulates it, appears to be highly conserved in planarians (Almuedo-Castillo et al., 2014; Dhanasekaran and Reddy, 2017; Hwang et al., 2004; Pellettieri et al., 2010). There are two main waves of apoptosis that occur during regeneration. The first apoptotic peak is localized to the wound site at 1-4 hpa and is part of the generic wound response (Pellettieri et al., 2010), while the second wave of apoptosis occurs 3 days post amputation (dpa) throughout the body of the worm (Pellettieri et al., 2010). During the first 3 days post injury (which are associated with blastema formation and polarity establishment), very little to no shape changes in the original tissues are observed.

Measurements of trunk regenerates (where both the head and tail were removed) showed no change in pharynx size during the first 3 dpa (Beane et al., 2013). It is only on day 3, coincident with the second peak of apoptosis, that regenerative remodeling of pre-existing tissues begins (Pellettieri et al., 2010).

Signals from apoptotic cells are able to stimulate proliferation non-cell autonomously (Fogarty and Bergmann, 2017; Pérez-Garijo and Steller, 2015), and apoptosis-induced proliferation has been reported in multiple regenerative contexts (Chera et al., 2009; Gauron et al., 2013; Li et al., 2010; Tseng et al., 2007; Wells et al., 2006). The first wave of planarian apoptosis does not appear to regulate proliferation, as caspase inhibition does not prevent either the first peak of proliferation (González-Estévez and Saló, 2010) nor the formation of the regeneration blastema (Beane et al., 2013). There is evidence, however, that the second apoptotic wave does function in apoptosis-induced proliferation, as conditions which blocked this peak reduced proliferation levels at 3 dpa in pre-existing tissues (Beane et al., 2013). Additionally, studies of the re-establishment of the planarian intestinal track report that intestinal remodeling in pre-existing tissues was dependent on ASC activity—as irradiation (which kills ASCs) prevented intestinal remodeling from occurring (Forsthoefel et al., 2011). Together these data implicate apoptosis-induced proliferation as an important possible mechanism during tissue remodeling in planarians and suggest the need for further investigation.

A few studies (including ours) have looked specifically at shape changes and body scaling during planarian tissue remodeling. We tracked organ size during the regeneration of trunk fragments and found that blastema size was finalized between 3-4 dpa, pharynx reduction to its new smaller size occurred from 3-7 dpa, and head size was not established until 10-17 dpa (Beane et al., 2013). We also observed two waves of body elongation: the first from 3-7 dpa,

during which the regenerate lengthened from its original square shape (although it was still wider than pre-amputation); and a second round of elongation that was not finalized until 17 dpa, which further thinned the regenerate to its correct proportions (Beane et al., 2013). Characterization of neural regeneration has determined that brain primordia arise by 3 dpa (Roberts-Galbraith et al., 2016), with brain maturation continuing through 5-7 dpa (reviewed in (Ross et al., 2017)). Analyses of regeneration in trunk fragments revealed intestinal branches undergo elongation beginning at 7 dpa (Forsthoefel et al., 2011), concurrent with the second wave of body elongation. It was also shown that along with new intestinal cell proliferation, existing intestinal cells are repurposed during regeneration; for instance anterior enterocytes were found to contribute to the regenerating posterior intestines (Forsthoefel et al., 2011).

We are only just now beginning to elucidate the molecular mechanisms behind tissue remodeling and organ scaling in planarians. For instance, inhibition of insulin signaling in intact worms disrupts proliferation and results in phenotypes that resemble body size reduction during degrowth (Miller and Newmark, 2012). A homolog of the death-associated-protein (*Dap-1*) is upregulated upon starvation and regulates autophagy during both degrowth and regeneration (González-Estévez et al., 2007), while the H^+,K^+-ATPase ion pump is required for both the second apoptotic peak and subsequent tissue remodeling starting at 3 dpa (Beane et al., 2013). The Hippo signaling pathway is required for regenerative size control; its inhibition leads to a failure of head fragments to prune the pre-existing brain down to the regenerate's smaller size, while eye removal alone results in disproportionally larger eyes that continue to increase in size beyond the normal regenerative timeframe (Lin and Pearson, 2014) (Lin and Pearson, 2017).

These data indicate there are rigorous control mechanisms to maintain body proportions during planarian regeneration, many of which have begun to be identified. After fissioning, head

and tail fragments use different mechanisms to control size during regeneration (Yang et al., 2017). Size control of the brain compartment is regulated in part by Fibroblast Growth Factor (FGF) signaling and its inhibition leads to a dramatic posterior expansion of the brain (Cebrià et al., 2002). A feedback loop of positive Wnt signaling (*Wnt11-6)* in the posterior brain and Wnt inhibition in the anterior, has been shown to modulate the number of brain progenitors needed (Hill and Petersen, 2015). Furthermore, regulation of the brain/anterior compartment appears to be linked to regulation of the neighboring trunk compartment through FGF signaling. In this case, FGF combines with additional Wnt signaling (*WntP-2)* to restrict the trunk compartment, and inhibition of this regulation results in expansion of the trunk and ectopic posterior pharynges (Lander and Petersen, 2016). These data provide evidence for cooperation between size control mechanisms, PCG regulation, and polarity establishment.

Making All These Tissues Talk to Each Other

The blastema alone does not replace all missing tissues—remodeled pre-existing tissues also contribute to regenerated structures in planarians (for example, see (Beane et al., 2013)). Following organ loss, proper regenerative shape requires the incorporation of both new blastemal cells and repurposed pre-existing cells, which combine to produce the final regenerated structure (Baguñà et al., 1994; Beane et al., 2013; Forsthoefel et al., 2011). For these tissues to be integrated, as well as for polarity information to be conferred, there must be communication between the old pre-existing tissues and the new tissues of the blastema. This is required to functionally connect organ systems across the two tissues. In addition to this inter-tissue communication, there must also be a high level of intra-tissue communication to coordinate

tissue remodeling within pre-existing tissues, as well as regulate ASC differentiation within the blastema. Clearly, regulated cell-cell communication is a top priority for regenerative shape.

The exact means by which cells communicate shape information during regeneration is an important area of research that is poorly understood. One mechanism that has been investigated during planarian regeneration is gap junction communication (GJC) (Skerrett and Williams, 2017). Gap junctions are integral membrane channels that allow the direct passage of ions and small molecules between neighboring cells; in vertebrates these channels are made of connexin proteins, while in invertebrates gap junctions are comprised of functionally homologous innexin proteins (Phelan, 2005; Skerrett and Williams, 2017). Data has shown that planarian innexin genes are expressed in the blastema (Nogi and Levin, 2005), and disruption of GJC can lead to polarity and patterning defects (Emmons-Bell et al., 2015; Peiris and Oviedo, 2013). Importantly, blocking GJC is capable of driving brain and head regeneration at posterior wounds, even when the regenerate still contains the original head (Nogi and Levin, 2005; Oviedo et al., 2010). These data allude to the possibility that brain/head formation might be a sort of "default" state for regeneration in the absence of other signals and suggest GJC is required for regenerating tissues to determine what tissues are missing and need to be replaced.

Interestingly, the two main organ systems that have been implicated in regulating such communication are the muscles and the nervous system. Some of this cell-cell communication is clearly between ASCs and muscle cells during axial establishment in general and AP polarity in particular (Scimone et al., 2016; Witchley et al., 2013). The data have also suggested that the brain (like muscle) may function as a signaling center, although the molecular mechanisms remain to be identified. However, simple modulation of neurotransmitter levels such as dopamine and serotonin is sufficient to disrupt regenerative morphology, leading to double-

headed or headless phenotypes respectively (Chan et al., 2014). And it is inhibition of innexins specifically expressed in the central nervous system that are required for GJC regulation of regenerative polarity (Nogi and Levin, 2005; Oviedo et al., 2010). As a whole, the existing data overwhelmingly point to a significant amount of cellular communication that must occur both within and between tissues to establish proper regenerative shape.

Coordinating These Mechanisms Across the Animal

During the restoration of shape in regenerating planarians, there are a lot of distinct processes happening—often at the same time. Some processes are obviously interconnected (for instance expansion of anterior regions requires that posterior regions are decreased), but it is harder to connect-the-dots with others (how do eye number and pharynx size relate to each other). However, in order to establish body proportion across the entire animal, there must be some sort of regulation that coordinates all these disparate processes. A growing body of research from several model systems suggests that bioelectrical signaling mechanisms (such as membrane voltage and ion transport) may serve this function during regeneration in general and the establishment of regenerative shape in particular (Adams et al., 2007; Beane et al., 2011; Beane et al., 2013; Chan et al., 2014; Ferreira et al., 2016; Monteiro et al., 2014; Tseng et al., 2010; Tseng and Levin, 2012; Zhang et al., 2011).

Endogenous bioelectrical signaling relies on ion channels and pumps to mediate ion transport, most frequently across the plasma membrane. One function of this ion flux is to establish a steady-state transmembrane potential, which is found in all non-excitable cells and is in contrast to the rapid changes that occur in neurons (Tseng and Levin, 2013). Regulation of membrane voltage has been shown to play a role in many processes during development and

growth, including proliferation, apoptosis, and importantly, animal-wide patterning (Adams et al., 2007; Adams et al., 2006; Barghouth et al., 2015; Blackiston et al., 2009; Levin et al., 2017). Bioelectrical signals can also regulate organ size, such as with K^+ flux during zebrafish fin growth (Perathoner et al., 2014). Studies have found direct links between membrane voltage and downstream transcriptional and epigenetic targets (Levin and Stevenson, 2012; Tseng and Levin, 2012). In addition, the flux of individual ions such as Ca^{2+} and Na^+ has been shown to play signaling roles in regeneration irrespective of membrane voltage (Beane et al., 2011; Chan et al., 2014; Chan et al., 2017; Tseng et al., 2010).

The field is just beginning to focus on the downstream effectors of identified bioelectrical signals. For example, H^+ flux mediated by the V-ATPase proton pump during zebrafish fin regeneration has been shown to be required for the expression of FGF and retinoic acid pathway members, which in turn are required for blastema cell proliferation and outgrowth (Monteiro et al., 2014). V-ATPase is also necessary for *Xenopus* tail regeneration, where early H^+ flux-dependent membrane voltage changes are required for regenerative proliferation (Adams et al., 2007). Specifically, these membrane voltage changes control the later expression of voltage-gated sodium channels in the regeneration bud; and the resulting Na^+ flux is required for the expression of signaling genes such as Notch and BMP, as well as cell proliferation (Tseng et al., 2010). In both zebrafish fin and *Xenopus* tail regeneration, bioelectrical signaling is also essential for proper innervation during regeneration (Monteiro et al., 2014; Tseng et al., 2010).

Planarians are one of the few model systems where the contributions of bioelectrical signaling in regeneration are best characterized (Durant et al., 2016). For instance, membrane depolarization of anterior tissues is required for anterior polarity and head regeneration in planarians. H^+,K^+-ATPase plays an endogenous role in maintaining this depolarization, and its

inhibition leads to hyperpolarized animals that fail to regenerate heads (Beane et al., 2011; Beane et al., 2013). However, it is the depolarization itself that is important rather than the individual ion channels that achieve it, as ectopic depolarization of the blastema is sufficient to induce head regeneration even at posterior-facing wounds (Beane et al., 2011). Anterior membrane depolarization is an early step in planarian regeneration (within the first 24 hpa) and is required for the upregulation of Ca^{2+} into the blastema (Beane et al., 2011). Ca^{2+} signaling itself is an important regulator of many planarian regenerative shape processes. Early activation of voltage-gated calcium channels (CaVs) is sufficient to induce head regeneration at posterior wounds, and functions in part to regulate neuronal signaling (Chan et al., 2014; Nogi et al., 2009; Zhang et al., 2011).

We investigated the effects of inhibition of the sarcoplasmic/endoplasmic reticulum (ER) calcium ATPase (SERCA), which controls Ca^{2+} storage into the ER. Our data showed that SERCA inhibition from 0-3 dpa results in double-headed regenerates due to increased intracellular Ca^{2+} levels (Fig.7A1,B1). In contrast, SERCA inhibition from 3-10 dpa (after blastema formation and polarity establishment) resulted in a complete block of tissue remodeling, perhaps due to the eventual depletion of intracellular Ca^{2+} levels (Fig.7A2,B2). These data demonstrate that tissue remodeling during shape establishment is a distinct process from earlier polarity establishment and initial stem cell regulation. Our preliminary hypothesis is that ER-mediated Ca^{2+} release is required for apoptotic tissue remodeling. Further investigation is needed to determine the actual role of SERCA channels during regeneration.

As in other organisms, bioelectrical signals appear to function during the initiation of regenerative processes in planarians. In some cases, such as the membrane depolarization of the anterior region, bioelectrical signaling appears to be used to define broad anatomical boundaries

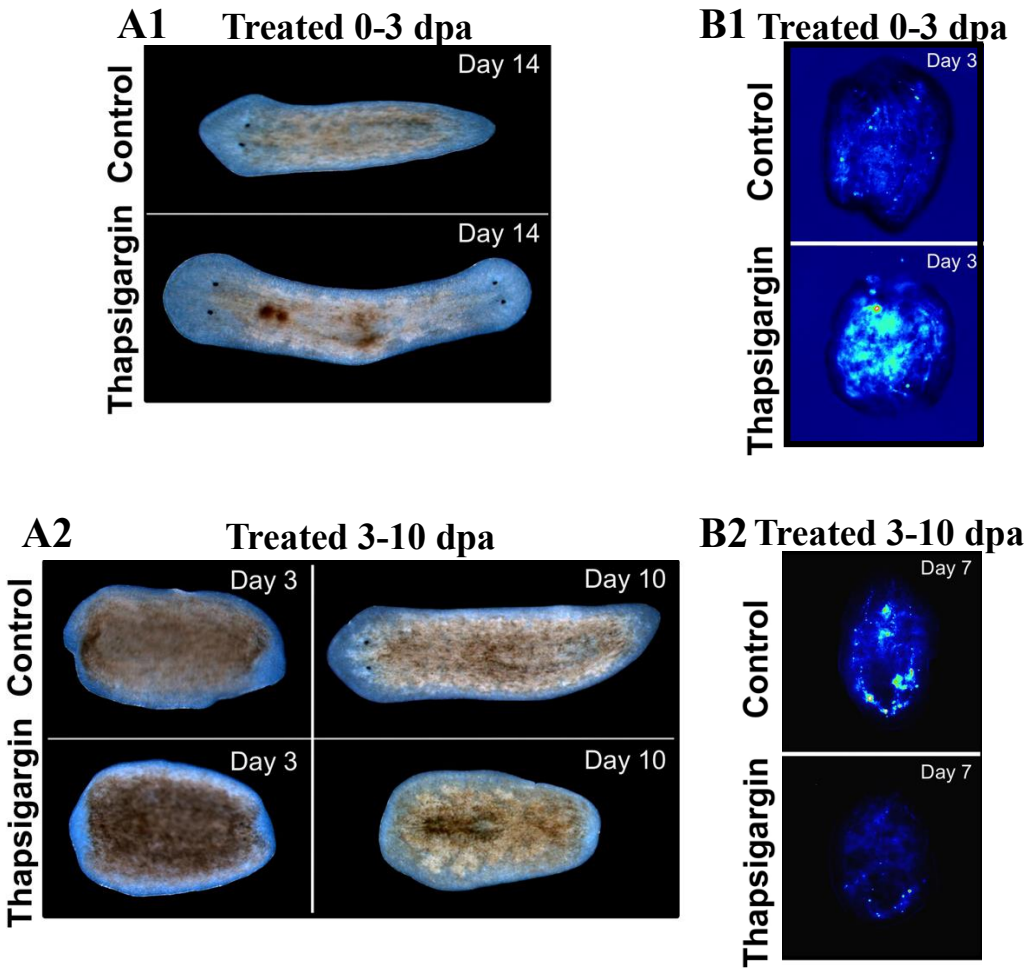

Figure 7. Ca^{2+} Flux has Distinct Roles in Polarity Establishment vs. Tissue Remodeling. *D. japonica* trunk fragments treated with 1 μM Thapsigargin (Sigma), which inhibits SERCA-mediated ER Ca^{2+} storage, or DMSO as a vehicle control. Inhibition of ER Ca^{2+} storage from 0-3 days post amputation (dpa) results in **(A1)** double-headed regenerates due to **(B1)** an increase in intracellular Ca^{2+} levels, as measured by Flou-3 (Molecular Probes). Inhibition from 3-10 dpa results instead in **(A2)** a complete lack of tissue remodeling, perhaps due to **(B2)** depleted Ca^{2+} stores. Anterior is left for morphology (n=10), and up for Flou-3 (n=5).

(*e.g.* regenerate head here). As such, bioelectrical regulation is an important component of regenerative shape and functions to regulate morphology at multiple points during this process. This makes bioelectrical signals a strong candidate for coordinating communication across multiple tissues. In fact, it is highly likely the signals being transmitted via GJC are bioelectrical in nature (ions)—pointing to the need to integrate stem cell regulation, bioelectrical signaling, and cell-cell communication during the establishment of regenerative polarity in planarians.

Conclusions and Future Directions: Identifying More Shape Mutants

The planarian field has made great strides in elucidating the molecular mechanisms behind many of the most important processes that regulate shape during regeneration. It has even provided evidence for the existence of Morgan's gradation of polarity that he proposed back in the early 20th century. It is true that we still have not identified a single regulator that functions as a gradient, either to promote or inhibit anterior fates in planarians. But we have found that there is a gradient of PCG expression along the AP axis that directly correlates with core components of the Wnt pathway (Reuter et al., 2015; Stückemann et al., 2017). This gradient is comprised not of a single molecule but the combined expression of all Wnt/β-catenin signaling regulators taken as a whole, that results in Wnt ligands and positive drivers of β-catenin being expressed more posteriorly, while inhibitors of β-catenin signaling are expressed more anteriorly (Adell et al., 2009; Gurley et al., 2010; Gurley et al., 2008; Petersen and Reddien, 2009, 2011; Stückemann et al., 2017). The modern toolkit has enabled us to answer some of the mechanistic questions posed by the earliest planarian researchers.

Despite this, as a field the investigation of regenerative shape is somewhat still in its infancy. We have a wealth of observational and phenomenological data from the historical

literature. And we have begun to make inroads on the molecular-genetic pathways regulating stem cells, tissue patterning, apoptotic remodeling, organ scaling, cell-cell signaling, and even bioelectrical regulation. But many important black boxes remain. One of the biggest unknowns, not just for regenerative shape but regeneration in general, is how the termination of regeneration is regulated. This is a particularly important question for planarian regeneration, where unlike development, the growth of tissues is not constrained by outside physical forces (such as by an egg capsule) and there are no outside patterning cues (such as from surrounding yolk cells). Internal mechanisms must exist that function to tightly restrict growth in order to produce tissues of the correct shape and size. Only a few studies have begun to elucidate these control mechanisms. For example, a negative feedback loop (in which *wnt11-6* activates the expression of its own inhibitor *notum*) appears regulate brain growth, functioning to restrict brain size (Hill and Petersen, 2015; Kobayashi et al., 2007). In addition, our research has shown that the Planar Cell Polarity (PCP) pathway is required for the termination specifically of neural growth in planarians, as disruption of PCP results in the continual production of new nerves month(s) after controls have stopped proliferating (Beane et al., 2012). However, whether this regulation is direct or indirect and the exact mechanisms that are involved are not known, and much research remains to be done.

The most important future direction for the field of regenerative shape is to determine how all of the individual processes involved are coordinated at the macro level—such that the entire animal regenerates with the correct size, number, and placement of organs needed to maintain body proportionality. The data already reveal that there is much crosstalk between the individual processes regulating shape (Fig.5B). One hypothesis is that there is a "key regulator" of regenerative shape, and it has been postulated that bioelectrical cell-cell communication

mechanisms could serve this function; but no one mechanism has been found to date that coordinates all the known processes involved. Therefore a critical direction for the field will be to uncover the "upper" level regulative mechanism(s) that serve to establish overall animal patterning and shape.

One barrier to this research has been the need for a different class of shape mutants. Although examples of dysmorphia result from the disruption of most regenerative processes, to date most of these mutants have consisted of the replacement of one organ with another (e.g. regrowth of a head instead of a tail), the presence of supernumerary organs (such as ectopic eyes or pharynges), or the deletion of organs (as in headless regenerates). While these mutants have been critical in uncovering the mechanisms that regulate individual structures, they mostly do not provide the opportunity to investigate animal-wide regulation of shape. What is needed are mutants in which the correct organ has regenerated in the correct place, but with the incorrect shape. A few such shape mutants exist, for instance the "shrunken" heads we observed following RNAi to H^+,K^+ ATPase, which result from a lack of apoptotic remodeling of preexisting tissues (Beane et al., 2013) (Fig.8A,B). Similarly, inhibition of GJC in *G. dorotocephala* was found to produce regenerates with incorrect head morphologies that more closely resembled head shapes found in other planarian species (Emmons-Bell et al., 2015) (Fig.8C). But there are not enough examples in the literature to resolve the mechanisms involved at the organism level. What is required are large-scale RNAi or chemical screens to identify phenotypes that result in a failure to produce overall regenerative shape. Such investigations will be important for regenerative medicine going forward, so that induction of appropriate organ shapes *in situ* can serve as a complement to the controlled *in vitro* regulation of stem cells.

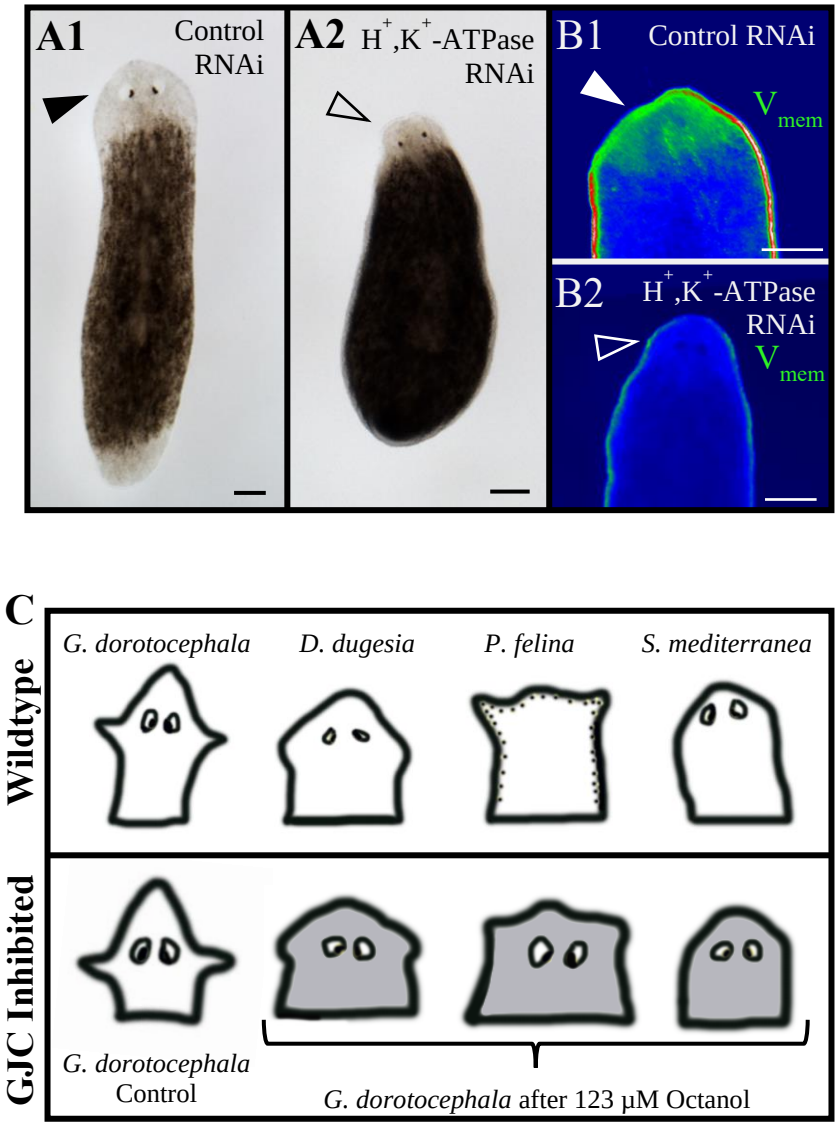

Figure 8. Example of Shape Mutants for Investigating Regenerative Morphology. (A,B) Inhibition of the H^+,K^+-ATPase ion pump via RNAi results in regenerates with shrunken heads, due to ectopic loss of membrane depolarization (green) of the anterior region. V_{mem}=membrane voltage, visualized with $DiBAC_4(3)$. Control RNAi=VenusGFP. Anterior is up, scale bar=200 µm. **(C)** Graphic representation of the effects of gap junction inhibition. Octanol treatment causes *G. dorotocephala* to regenerate with head morphologies characteristic of different species. Based on (Emmons-Bell et al., 2015).

All data and figures presented in chapter II were published in the journal *Seminars in Cell & Developmental Biology* with the title, “Staying in Shape: Planarians as a Model for Understanding Regenerative Morphology” (Birkholz et al., 2018).

CHAPTER III: PLANARIAN PHOTOTACTIC ASSAY REVEALS DIFFERENTIAL BEHAVIORAL RESPONSES BASED ON WAVELENGTH

Introduction

Planarians are non-parasitic flatworms that are an important model system for understanding stem cell biology (Reddien, 2013; Rink, 2013; van Wolfswinkel et al., 2014), regeneration (Adell et al., 2010; Elliott and Sánchez Alvarado, 2013; Umesono et al., 2011), toxicology (Grebe and Schaeffer, 1991; Pra et al., 2005), and evolution (Labbé et al., 2012; Nakazawa et al., 2003). Additionally, with their true central nervous system and cerebral eyes connected to the brain, planarians have been used as a model for eye research. Several basic features found in planarian eyes are phylogenetically conserved such as photoreceptor cells containing opsin, a pigmented cup structure, and a host of eye-specific developmental genes that are essential for eye formation (Lapan and Reddien, 2011, 2012; Orii et al., 1998; Taliaferro, 1920). These common features, combined with the relative simplicity of the planarian visual system, make flatworms a valuable addition to the models used for investigating the basic features of eye biology and increasing our understanding of eye evolution and development.

Located on the dorsal side of the body, planarian eyes are composed of two cell types: pigment cells and photoreceptor neurons (Fig.3). The pigmented cells form a semi-lunar optic cup and function to absorb incoming light. Thus, each eyecup confers a left-right directional selectivity to visual information while the rostral location confers an anterior dimension to visual information transduced by the ocelli. The photoreceptor cells are bipolar neurons whose cell bodies are located outside of the optic cup (Carpenter et al., 1974). Axons from the

photoreceptor neurons project posteriorly into the brain, with some fibers forming a partial optic chiasma to integrate photosensory inputs from both sides of the animal (Agata et al., 1998; Okamoto et al., 2005; Sakai et al., 2000). The dendrites of the planarian photoreceptors extend inside the optic cup and form a rhabdomeric structure where opsin accumulates (Asano et al., 1998; Orii et al., 1998). Opsins are a highly conserved class of G-protein coupled receptors that covalently bond to a chromophore forming the visual pigment rhodopsin (Wald, 1968). Transcriptome analyses reveal that the rhodopsin signaling pathway is conserved in planarians, including two R-opsin homologs (Lapan and Reddien, 2012).

Planarians are photophobic and when exposed to light they seek cover (Arees, 1986; Parker, 1900; Reynierse, 1967). This negative phototaxis has been used to evaluate regeneration of the visual system (Arees, 1986; Dasheiff and Dasheiff, 2002; Inoue et al., 2004; Takano et al., 2007), as well as memory storage and transference (McConnell, 1967; Shomrat and Levin, 2013). In these planarian behavioral studies, analyses have been conducted with white light, which consists of an amalgamation of multiple wavelengths. However, many animals have been shown to have different behavioral responses to different wavelengths of light. For example, zebrafish larvae will swim toward UV, blue, and red light but are only weakly attracted to green light (Orger and Baier, 2005). Conversely, leeches detect and exhibit complex negative phototactic responses to UV and green wavelengths, with UV producing the maximal response (Jellies, 2014a, b). In *Drosophila* larvae, exposure to blue, violet, and UV wavelengths elicits negative phototaxis, while green and red light produces no behavioral response (Xiang et al., 2010). Similarly, the movement of *C. elegans* increases under blue or shorter wavelengths of light, again with maximum responses to UV (Edwards et al., 2008).

A further complication of using white light for phototactic studies is that different sources of white light (e.g. halogen, Light-Emitting Diode or LED, and fluorescent) have varying spectral compositions. Even within a single source, such as the commonly used halogen light, substantial differences exist in the wavelengths included (Zukauskas et al., 2009). Additionally, regulation of intensity by controlling current also alters the spectral composition, giving rise to yet another poorly controlled variable. Therefore, we suggest that use of white light to study planarian photophobia may mask important behaviors associated with different wavelengths of light. We hypothesize that rather than a general photophobic response, planarians have differential responses across a range of wavelengths both within and outside of the visible spectrum. Here, we describe a novel planarian behavioral assay developed to test behavioral responses to individual wavelengths including UV and infrared (IR), which to the best of our knowledge have not previously been examined in these flatworms. Our data show that planarians display a complex, hierarchal photophobic response to specific ranges of wavelengths, in addition to a brief general response that appears to be more wavelength-independent. Furthermore, similar to leeches and *C. elegans*, planarians display the most robust responses to UV wavelengths. These results serve to improve our understanding of the basic biology of planarian eye function and suggest a previously underappreciated visual richness in these animals.

Materials and Methods

Colony Care

Asexual *Schmidtea mediterranea* were maintained as previously described (Beane et al., 2012), except worm water was comprised of 0.5g/L of Instant Ocean salts. 6-9 mm worms were starved at least one week prior to experimentation before use.

Light Sources

Ambient lighting was generated by directing two 100 watt LED flashlights onto the walls on either side of an otherwise completely dark room to produce diffuse background illumination of 50-55 lux ("Light Meter–Lux Measurement Tool" Version 1.2, iPhone application). LED wands (fixed resistor and RCA plug attached to a 9 volt battery with switch) were constructed as previously described (Jellies, 2014a, b). Each wand delivered roughly equivalent numbers of photons $cm^{-2}s^{-1}$ (flux), with the following nominal wavelength ranges: near IR (700-850 nm), red (615-640 nm), green (515-520 nm), blue (460-470 nm), and 2 wavelengths of near UV (395-405 nm and 360-365 nm). White light was obtained using a standard LED fiber optic illuminator with goosenecks from a dissecting scope setup. Approximate relative luminosity in the testing dish was assessed using a phototransistor coupled to a 2 mm diameter fiber optic (Jellies and Kueh, 2012). As expected, intensity was greatest in quadrant 1 (Q1) and steadily decreased, with quadrant 4 (Q4) being the darkest. For the avoidance assay, commercially available red, green, and UV laser pointers with nominal peak wavelengths of 650 nm, 532 nm, and 405 nm (+/- 10 for all) were used. In order to obtain a spot of light that was smaller than the worm itself, a piece

of tape was placed on the end of the laser and punctured to create a pinhole that produced a circle of light approximately 2.5 mm in diameter.

Photophobia Assay

A rectangular 7.6 cm x 3.4 cm x 1.1 cm testing dish, made from the top of a standard coverslip box, was placed over a sheet of white paper containing a template marked with the perimeter of the testing dish (for dish placement) and lines dividing the dish into four equal quadrants (1.9 cm x 3.4 cm). There was also a half circle at the origin, with its apex midway through Q1, for directing light placement. LED wands were secured above the testing dish with a clamp attached to a ring stand, while a second clamp secured the battery pack to prevent unintended movement of the wand. The end of the LED wand was positioned about 5 cm above the top of the testing dish with the light directed into the half circle in Q1. An SLR camera was positioned over the testing dish using a tripod. On each experimental day, batteries were replaced in both flashlights and the LED wand. The testing dish was filled to a depth of 0.5 cm with worm water for each trial and emptied and wiped clean between wavelength presentations. In a single day, one wavelength was applied to total of 60 worms (10 groups of 6 worms, or 10 trials), repeated 3 times. For each trial, all worms were placed into Q1 before the camera was turned on. Except for controls, the light was switched on (time 0) at 5 seconds after recording started. Behavior was recorded for 2 minutes. Animals were allowed to rest at least overnight before the next wavelength. Wavelengths were generally tested in the order: control, IR, red, green, blue, UV 395, and UV 360.

Neutral Density (ND) Filters

Filters used were 25.4 mm diameter nickel chromium coated fused silica (7980) as previously described (Jellies, 2014a, b). A holder was designed from stiff foam pipe insulation to position the LED wand above the filter such that all emitted light passed through the filter. ND filters attenuating 95% of light (optical density = 1.3) and 99% of light (optical density = 2.0) were used.

Avoidance Assay

White paper was placed on the microscope stage so that laser light could be seen. A 100 mm Petri dish filled with 20 mL of worm water was positioned over the paper, and the microscope base's brightfield light was turned to the lowest setting that allowed for recording. Individual worms were transferred to the middle of the dish and recording was started when the worm began traveling on the bottom of the dish. The laser beam was directed in front of the animal at a distance equal to one diameter of the circle of light (approximately 2.5 mm). Only a single wavelength was tested each day (with 30 worms repeated twice, for a total of 60 trials), and animals were allowed to rest at least overnight before the next wavelength (in the following order: red, green, and UV).

Imaging and Recording

For the photophobia assay, imaging was done using a Canon EOS Rebel T5i SLR camera mounted to a tripod. For the avoidance assay, imaging was done using a Zeiss V20 fluorescent stereomicroscope with AxioCam MRc camera and Zen Lite software. Recordings from all behavioral trials were examined using Windows Media Player.

Assay Analyses and Statistics

For the photophobia assay, the three repeat trials for each group were first averaged to compensate for individual animal variability. When determining location, at least 50 percent of the worm had to be in the quadrant. To examine the location of worms across all quadrants, all wavelengths were compared using a Kruskal-Wallis test, with Dunn's Q corrected for tied ranks. The escape index was calculated as 1-(number of worms in Q1 at time X/number of worms in Q1 at time 0), and significance was determined using two-way repeated-measures ANOVA. A Bonferroni post hoc multiple comparisons test was conducted to examine differences between means. $P \leq 0.01$ was considered significant for all tests.

Results

A Novel Planarian Photophobia Assay to Test Responses to Individual Wavelengths

Planarian flatworms possess a well-documented negative phototactic (photophobic) behavioral response in the presence of light, as tested using various sources of multi-wavelength "white" light (Arees, 1986; Dasheiff and Dasheiff, 2002; Davidson et al., 2011; Harden Jones, 1971; Inoue et al., 2004; Reynierse, 1967; Takano et al., 2007). However, from available data, it is unclear whether planarians have a single general photophobic response or if their behavioral responses actually vary by wavelength as has been shown in other animals (Aksoy and Camlitepe, 2012; Edwards et al., 2008; Jellies, 2014a, b; Orger and Baier, 2005; Xiang et al., 2010). To distinguish between these possibilities, we developed a novel behavioral assay (Materials and Methods). Because the LED wand was exchangeable, our setup allowed not only

for testing behavioral responses to different visible wavelengths, but provided a means to investigate planarian responses to UV and IR wavelengths as well.

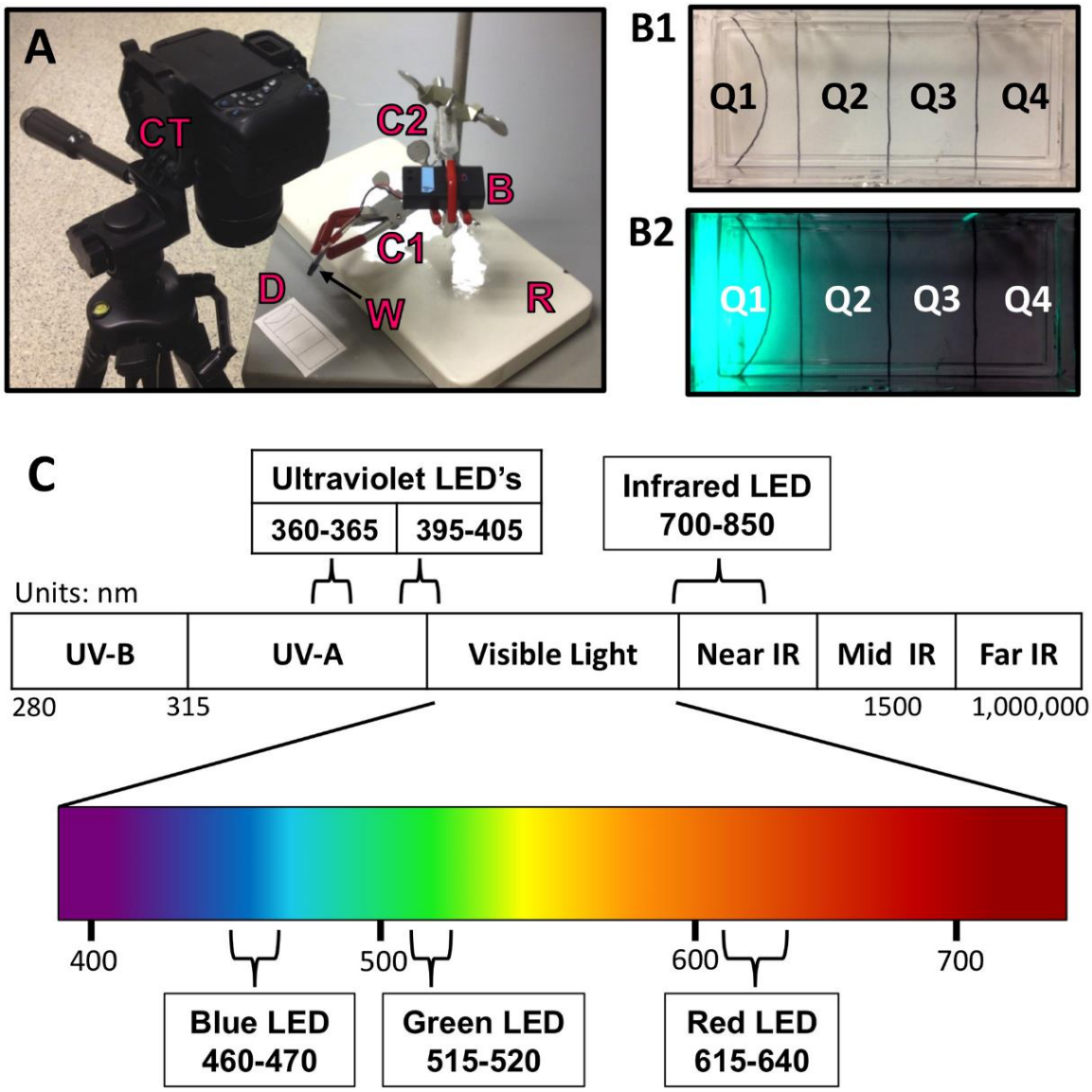

Figure 9. Photophobia Assay. (A) The imaging setup. CT = Camera mounted on tripod. W = LED wand. D = Testing dish. C1/C2 = Clamps. B = Battery pack. R = Ring stand. **(B)** Close-up of testing dish. (B1) The labeled guide placed underneath the dish marks the 4 quadrants (Q1-Q4) and the semi-circle where the LED light will be directed. (B2) Image of testing dish during a trial, showing the resulting light-to dark gradient. **(C)** The spectral composition of the LEDs used, and their location on the electromagnetic spectrum. UV = Ultraviolet. IR = Infrared.

One objective was to establish an easily reproducible photophobia assay with standardized testing parameters in order to improve comparability. Therefore, each LED wand was clamped above the testing dish at a fixed distance of about 5 cm (Fig.9A). Additionally, a sheet of white paper was placed beneath the testing dish, with four equal quadrants (Q1 to Q4) demarked (Fig.9B). To verify that the amount of light gradually decreased from Q1 to Q4, the intensity of light in each quadrant was estimated with a phototransistor. Finally, the assay used easily-constructed LED wands powered by 9 volt batteries, as previously described (Jellies, 2014a, b), which allowed for some control of the ranges of wavelengths tested. Each wand was also designed to deliver roughly equivalent numbers of photons $cm^{-2}s^{-1}$ (flux)(Jellies, 2014a, b). For our experiments, the nominal wavelengths used were (Fig.9C): near IR (700-850 nm), red (615-640 nm), green (515-520 nm), blue (460-470 nm), and two distinct wavelengths of near UV light (395-405 nm and 360-365 nm). In addition, we also tested worm responses to white light using a standard LED fiber optic illuminator (with goosenecks) as typically used with a dissecting scope. The use of white light, even though there are certainly different spectra involved using LED or halogen sources, allowed us to compare responses from more restricted and narrow ranges of wavelengths with the non-specific white light typically used in planarian photophobia studies.

The photophobia assay was performed under ambient background lighting of approximately 50 lux ("no light" or controls), which was just sufficient to allow photography without agitating worms but not be completely dark. For the assay, the behavioral responses of 60 worms were tested (in 10 groups of 6 worms) for each wavelength (a single trial). Trials were repeated 3 times and the data averaged, to compensate for variability in individual worm responses. Trial parameters were as follows: camera recording was turned on, a group of 6

worms was placed in Q1, after 5 seconds the LED wand was turned on, and behavior was recorded for 2 minutes (the initial time was scored as when the light was first turned on). The 2 minute assay length was chosen based on preliminary data indicating the average time for worms to traverse the testing dish was ~45 seconds (n=36). Because of the remote possibility that the brief exposure to very weak UV light might cause damage, UV trials were performed last. Generally, worms were tested in order from longest to shortest wavelengths.

Planarian Behavioral Responses Varied by Wavelength

Using the above parameters, we performed our photophobia assay with control (ambient light only), IR, red, green, blue, and UV (395 nm and 360 nm) wavelengths, as well as with white light (Fig.10). Worm location by quadrant was scored at 30 second intervals (Fig.10A), with photophobia being assessed after 2 minutes (Fig.10B). Statistical significance (asterisks in Fig.10B) was assayed for the overall pattern of worm location throughout the entire dish (across all four quadrants), rather than for individual quadrants. Control groups explored the dish in an apparently random manner (Fig.10A), such that by 1 minute animals were evenly distributed between all quadrants and remained so for the duration of the trial (with an average of 24.75% of worms in each quadrant at 2 minutes). This random exploration is consistent with initial exploratory behavior in new environments previously noted in planarians (Beane et al., 2011; Beane et al., 2013; Stevenson and Beane, 2010).

In contrast, exposure to green, blue, and both UV wavelengths resulted in strong photophobic responses, such that the majority of worms ($\geq$ 80%) ended up located in the darkest quadrant (Q4, black bars in Fig.10B). In most of the UV trials, the worms congregated on the wall of the dish furthest from the light (Fig.10A). As expected, worms exposed to white light

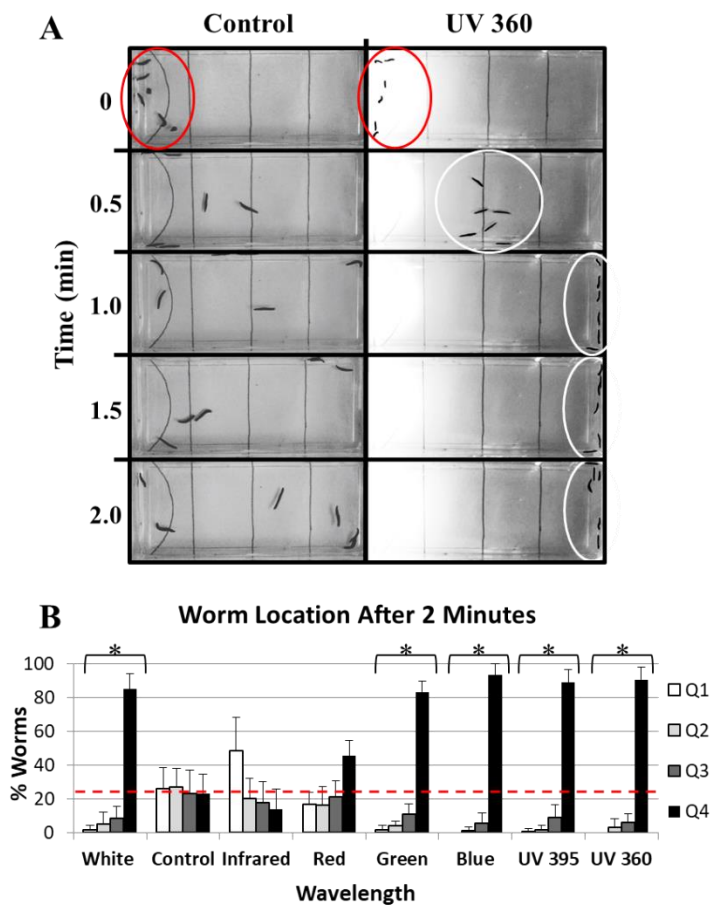

Figure 10. Planarian Photophobic Responses Vary by Wavelength. (A) Images of the photophobia assay showing single trials (one group, n = 6) for control (ambient light, left) and UV 360 (right) wavelengths. All worms begin in quadrant 1 (Q1, red circles). While control worms randomly explore the dish, in UV 360 trials worms move rapidly away from the light (white circles). Images enhanced for visualization. **(B)** Graph showing overall photophobic responses for each wavelength, as measured by worm location in each of the four quadrants (Q1-Q4) after 2 minutes. Photophobic responses are indicated by increased presence in Q4 (black bars) which is farthest from the light. Significance (asterisks = $p<0.001$ as compared to controls) was calculated by Mann-Whitney (with Dunn's Q), which takes into account worm location across all four quadrants simultaneously. Red dashed line = average control value.

also displayed strong negative phototaxis, with a striking correlation across all quadrants between white light (Q1: 1.67%, Q2: 5.00%, Q3: 8.33%, Q4: 85.00%) and green light (Q1: 1.67%, Q2: 3.89%, Q3: 11.11%, Q4: 83.33%). On the other hand, neither of the IR or red wavelength responses were statistically different from controls by the end of the trial (Fig.10B). Although the (small) majority of worms exposed to red wavelengths were in fact located in Q4 farthest from the light, worm location compared to controls was not statistically significant across all quadrants ($p>0.20$). Interestingly, although there was also no statistical significance in the location of worms exposed to IR across all quadrants as compared to controls ($p\geq0.50$), a reverse trend was observed where the majority of worms were located in Q1 directly under the light (Fig.10B). Overall, these results suggest that our novel planarian photophobia assay is able to recapitulate the strong photophobia previously demonstrated by other methods.

To confirm that the observed behavioral responses resulted from visual detection of specific wavelengths and not other variables such as heat or nociception, we repeated our photophobic assay with neutral density filters. If responses to light are in fact a result of visual detection, we would expect worm responses to diminish in a predictable fashion as light attenuation increases (and the behaviorally relevant stimulus decreases). For the first trial, all LED lights were attenuated to 95%, so that only 5% of the light reached the testing dish, while in the second trial 99% of the light was attenuated (Fig.11). The results confirmed that the number of worms displaying photophobia steadily decreased with increased light attenuation, suggesting that the behavioral responses were the result of visual responses to specific ranges of wavelengths and not uncontrolled variables.

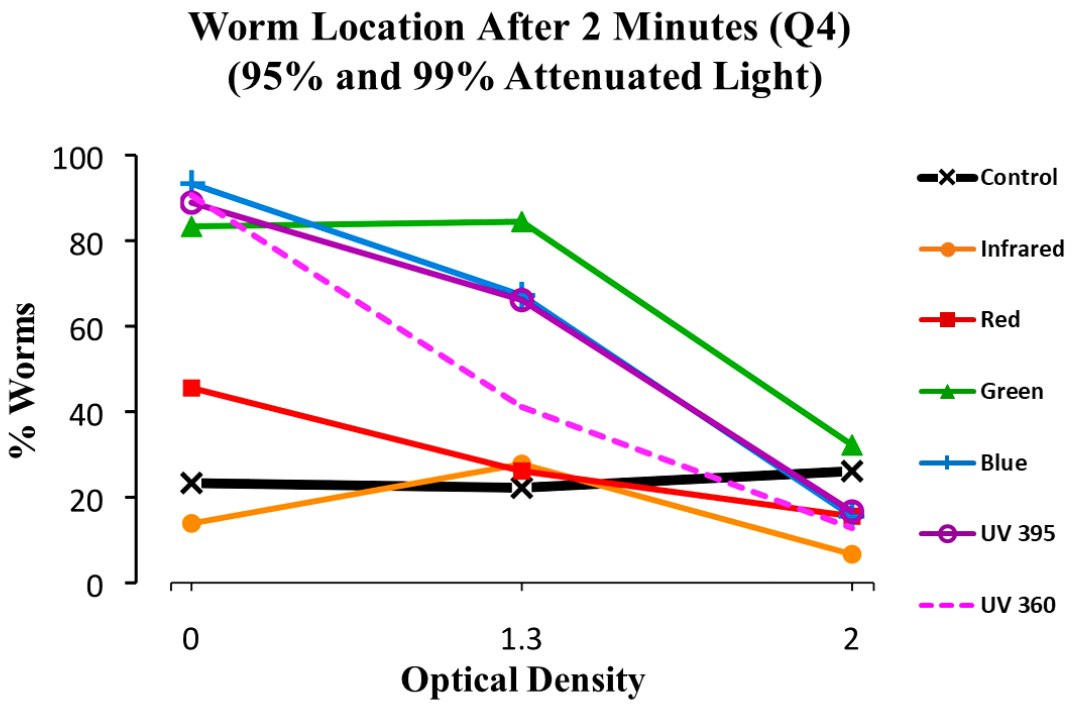

Figure 11. Photophobic Responses Result from Light Stimulus. Graph showing behavioral responses over increasingly attenuated light, as measured by the number of worms in Q4 at 2 minutes. Worms were exposed to full light, 95% attenuated light, and 99% attenuated light (or optical densities of 0, 1.3 and 2.0 respectively). The trend shows that phototactic responses decreased along with diminished behavioral stimuli (light).

Planarians Displayed the Severest Escape Responses to UV Light

Although our data revealed that green, blue and UV light all resulted in robust photophobic responses (Fig.10B), we observed that worms exposed to near UV light appeared to move away from the light faster than for other wavelengths tested. This suggested that more complex differences exist between the photophobic responses than our scoring for photophobia at 2 minutes revealed. Thus, we next examined the rate at which worms escaped direct light (in Q1) by tracking both the number of worms that left Q1, and the number that returned, throughout the trial (Fig.12). To do this, we calculated an escape index (Θ), where 0 indicated all worms remained in Q1 while 1 indicated all worms had left Q1. Therefore, higher values represented stronger photophobic responses. It should be noted that an important difference exists between the analyses in Figure 10 and the analyses here in Figure 12 that represent how fast worms escape from direct light exposure. Because of this, the escape index as used here is a measure of the initial intensity of the response rather than a measure of overall strength of the response.

At 30 seconds, the escape indices for all wavelengths were statistically different ($p<0.001$) from controls (Fig.12), including red and IR (which were not significantly different in overall photophobic response (Fig.10). However, analyses revealed that escape responses to the UV light were significantly faster ($p<0.01$) than for all other wavelengths, confirming our observations that UV light caused the most extreme initial photophobic response. Additionally, the escape indices highlighted that reactions to green, blue, and white light at 30 seconds represented an intermediate behavioral response, which (while still strongly photophobic) was statistically different from both the UV responses ($p<0.01$) and the random exploration of controls ($p<0.001$). Interestingly, white light was more similar to (though not statistically

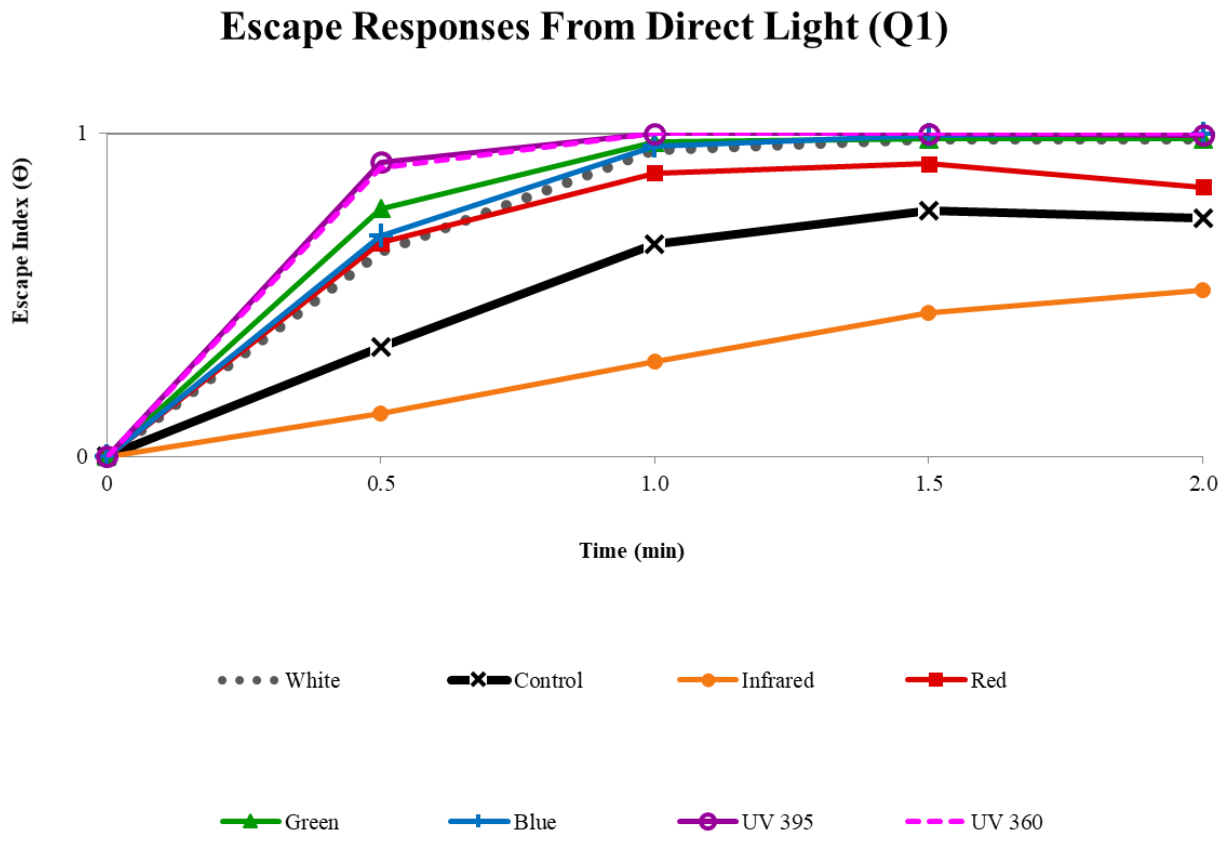

Figure 12. Escape Responses Vary by Wavelength. Graph showing escape responses as a measure of the severity of phototactic behavior. The escape index (Θ) is based on the number of worms that leave Q1 (direct light), where a value of 1 indicates all worms have left Q1. Thus, higher values indicate stronger photophobic responses. At 30 seconds, the data indicate that UV wavelengths elicited a significantly stronger escape response, distinct from both controls ($p<0.001$) and all other wavelengths ($p<0.01$); while IR wavelengths produced an opposite, attractive response ($p<0.001$). All time points are significantly different from controls ($p<0.001$) by two-way ANOVA, except for red at 1.5 minutes ($p<0.01$) and 2 minutes (not significant). Note the latter data indicate by 2 minutes worms have returned to the direct red light source in Q1.

different from) blue escape responses (Fig.12), in contrast to overall photophobic response (Fig.10) where white light was more similar to green. This may be related to the spectral composition of white light LEDs that typically contain several broad peaks, including notable amounts of energy in the blue range.

For IR light, the escape index (Fig.12) at all time points was significantly different from controls as well as all other wavelengths. This is in contrast to the overall photophobic response to IR light (Fig.10), which was not statistically different from controls even at the earlier 30 second time point. In particular, the escape index showed that IR wavelengths produced an opposite phototactic response, where worms were initially more likely to remain under direct light (Q1) than controls. This suggests the possibility that planarian responses to IR might be slightly photopositive, a hypothesis that would first need to be investigated in much greater detail. These data also indicate that the planarian visual system may be able to respond to IR wavelengths in some as yet unknown manner.

Most surprisingly, at 30 seconds the escape index for red light was significantly different from controls ($p<0.001$), illustrating an early visual behavioral response that was not different from the intermediate response noted above for green, blue and white. This was particularly unexpected given that the overall photophobic response to red at 2 minutes was not different than controls (Fig.12). Closer examination of the escape responses to red light revealed that responses remained significantly different at 1 minute ($p<0.001$), and at 1.5 minutes ($p<0.01$), but were no longer statistically different from controls by 2 minutes (Fig.12). This reflects the observation that at 2 minutes, worms that previously left Q1 returned, despite the continued presence of the red light exposure. When overall photophobic response (Fig.12) across all quadrants was examined at earlier time points, this pattern of an initial photophobic response to red light that

decreased over time was again observed: significant at 30 seconds ($p<0.02$) and at 1 minute ($p<0.01$), marginal at 1.5 minutes ($p<0.05$), and not significant at 2 minutes. These data suggest that after an initial photophobic response worms subsequently stopped responding to red wavelengths.

Planarians Have Both General and Wavelength-Specific Photophobic Responses

The overall photophobic response data, combined with escape index analyses, suggested that while planarians displayed different responses to different wavelengths (with UV causing the most robust responses), there may also exist a separate, wavelength-independent photophobic response to being placed under direct light such as might be expected with broadly-tuned visual pigments. In order to test this idea, we examined avoidance responses to different wavelengths (Fig.13). Whereas previously we examined whether or not planarians would move away from light exposure, our avoidance assay tested the reverse behavior: whether or not worms would choose to enter a light source. However, the LED wands we used in our previous assay produced a field of light that was too large to record worm movement from outside the field into the light. Therefore, we switched to the use of tiny spots of laser light under high magnification (under a stereomicroscope). We covered the end of a laser pointer with a piece of tape that had a single pinhole in the center, thus obtaining a much smaller coherent circle of light. For illustration, compare the relative size of the light field versus a single worm in our photophobia assay (UV 360 panels in Fig.10A) and in our avoidance assay (Fig.13). We chose red, green and UV laser lights as representative of the range used in our photophobia assay. We expected that if wavelength-specific responses existed, worms would respond with increasing severity to avoid entering regions lit by red, green and UV wavelengths, respectively.

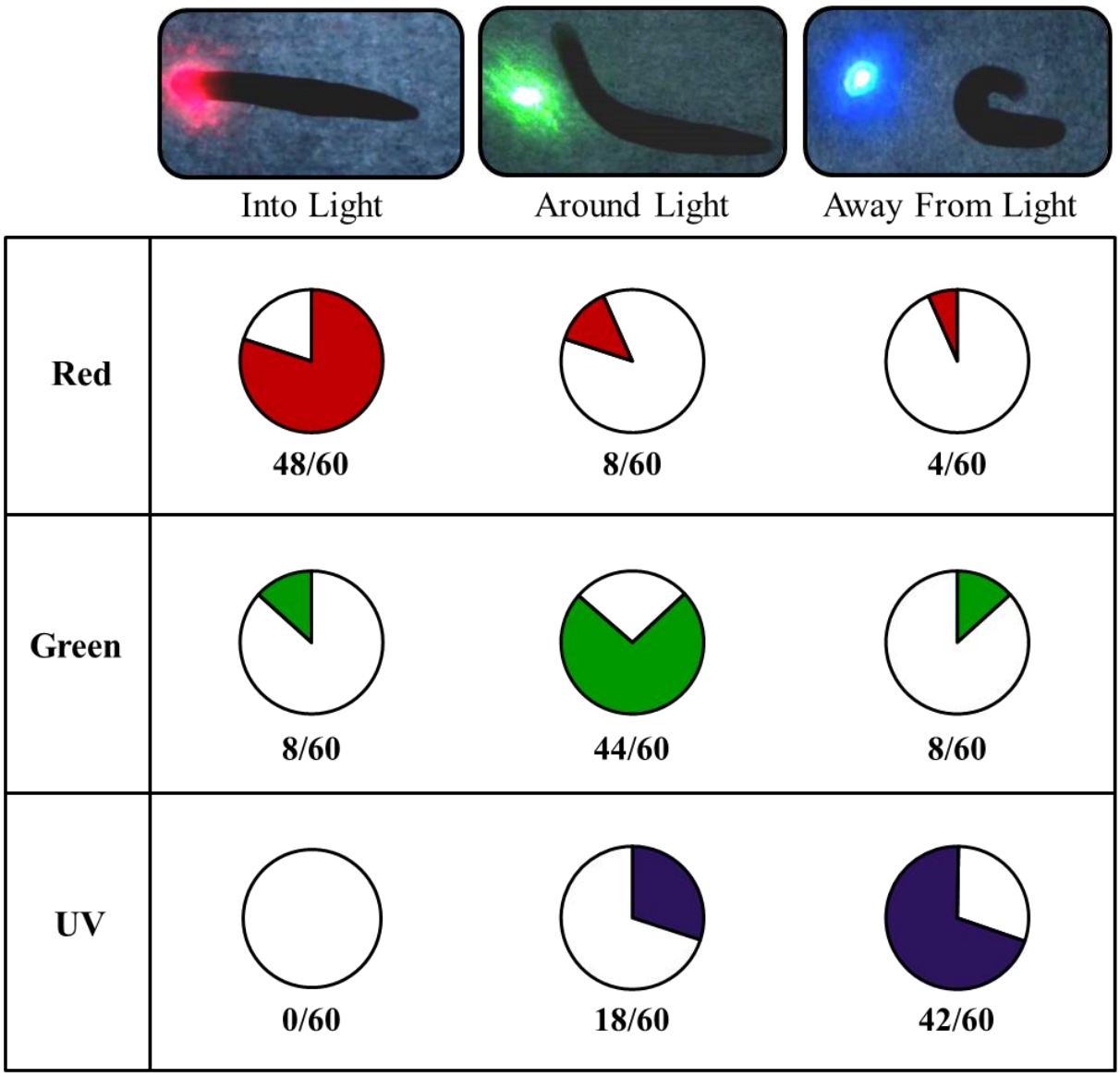

Figure 13. Light Avoidance Responses Vary by Wavelength. Avoidance assay to test worm responses when approaching areas of direct light. Red (top row), green (middle row), and UV (bottom row) wavelengths of laser light were placed in the worm's path (photos), resulting in three distinct behaviors (shaded areas): worms moved into the light (left column), went around the light (middle column), or avoided the light by making 90-180 degree turns (right column).

To test for light avoidance, the laser was pointed directly in front of a worm's path at a distance roughly equal to one diameter of the circle of light. This ensured that worms began the assay outside the direct light source but was close enough that worms continued moving in the direction of the light. Three distinct behaviors were observed. As worms approached the light source they either 1) did not respond and continued moving directly into the light, 2) moved around the light by making a slight directional change to one side without crossing into the light, or 3) abruptly made a 90-180 degree turn in the opposite direction of the light (photos in Fig.13). Consistent with our previous data, when exposed to the red laser the majority of worms (80%) were not affected and continued moving directly through the light (top row of Fig.13). When confronted with the green light, the majority (73.33%) of worms chose to go around either the right or left side of the light without entering the most luminous spot (middle row of Fig.13). Strikingly, as worms approached the UV light their reaction was even more dramatic with 70% of the animals suddenly changing direction at a 90-180 degree angle in order to avoid the light and directing movement away from it (bottom row of Fig.13). Furthermore, not a single worm chose to travel into the UV light, even though 13.33% of worms did so with green light.

These results are consistent with our previous data showing that planarians exhibited differential responses to different ranges of wavelengths of light. They also confirmed that not only did UV light produce the strongest photophobic responses and most robust initial responses, but that an intermediate and less severe photophobic response occurs with wavelengths within the visible spectrum such as green. Furthermore, these results demonstrated that planarians lack a red wavelength-specific behavioral response, suggesting that the escape response we observed to red light reflects instead an initial wavelength-independent photophobic response (Fig.14A).

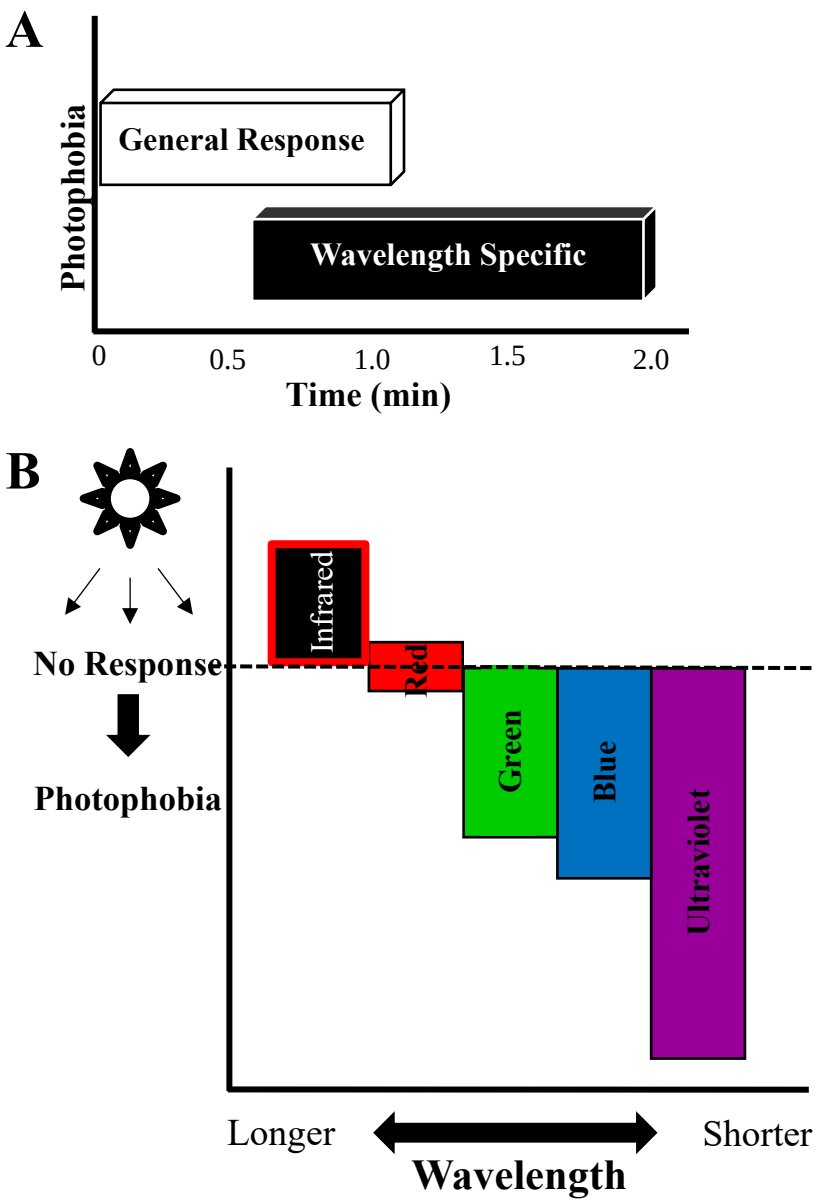

Figure 14. Planarian Photophobic Behavior is Hierarchal. (A) Graph showing the likely relationship between the two types of photophobic responses uncovered by our data: the general photophobic response, which occurs immediately after exposure to any wavelength, and the wavelength-specific responses. **(B)** Graph depicting the inverse relationship between photophobic responses and wavelength.

Discussion

Our results support the hypothesis that planarians do possess differential behavioral responses to light across a range of wavelengths. Our data also reveal that planarian phototactic responses occurred in a behavioral hierarchy (Fig.14B), where the shortest wavelengths (in this case near UV light) caused the most intense photophobic responses while longer wavelengths produced no effect (for red) or even opposite effects (in the case of IR). Thus, an inverse relationship appears to exist between the wavelength and the intensity of the worm's photophobia. These results highlight the importance of the spectral composition of light for planarian behavior and suggest that the current standard use of poorly characterized white light in planarian phototactic studies may mask more complex behaviors.

Unexpectedly, our data also suggested that planarian photophobic behavior may involve two different response types: a general photophobic response to luminal contrast (for example a rapid phasic change in luminosity) and more wavelength-specific photophobic responses (Fig. 14A). The general photophobic response occurred immediately after light exposure and drove planarians to escape the light source regardless of wavelength (except for IR). This initial response may be due to the change in contrast that occurs when worms are suddenly exposed to light after leaving their preferred low/no light environment and presumes either broadly-tuned photopigments or some unknown aspect of phototransduction. In contrast, the wavelength-specific responses encompass specific behavioral reactions that vary depending on the wavelengths involved. The difference between the general and wavelength-specific responses can be seen in the planarian response to red light. Although worms displayed an initial general response to escape the light source, they quickly adapted to it in order to return into the direct light (Fig.12). This lack of a red-specific negative light response was confirmed in both our main

photophobic assay (Fig.10B) and our avoidance assay (Fig.13). Together, these data illustrate that planarian photophobic behavior is complex and coordinated and not just the result of simple general light avoidance.

In this hierarchy, planarian responses to near IR light were the most surprising as worms appeared to be attracted to it. While worm localization across all quadrants was not statistically different from controls (illustrating a lack of photophobic response, Fig.10B), the escape indices for IR were significantly different at all time points ($p<0.001$, Fig.12) highlighting a slight but apparently real worm preference for remaining under direct IR light. The visual detection of IR has not been examined in planarians, although a few studies have shown that IR radiation causes increased stem cell proliferation (de Souza et al., 2005; Wu and Persinger, 2011). Our data seem to suggest that planarians may be able to detect IR by some mechanism. Although alternative explanations cannot be ruled out (for instance, IR may create a shadow effect by reducing the activation of opsin, thus making the IR quadrant appear darker than the ambient room lighting), IR detection is found in various parts of the animal kingdom. For example, some snakes and bats possess IR receptors called pit organs that are capable of sensing thermal stimuli (Campbell et al., 2002). Additionally, the visual systems of freshwater fish (such as the common carp, tilapia, zebrafish, green swordtail, and guppies) are also able to detect IR, an ability that may be directly related to their environmental conditions and/or circadian cycles (Matsumoto and Kawamura, 2005; Shcherbakov et al., 2013; Shcherbakov et al., 2012). The spectral absorption of water depends largely on the concentration of suspended particles such as dissolved oxygen and organic material, which enhance scattering and absorption of short- and mid-wavelengths (Hargreaves, 2003; Osburn and Morris, 2003; Shcherbakov et al., 2013). Therefore, fish living in turbid water have sensitivity to slightly longer wavelengths (Bowmaker, 1995). IR detection

could also be an adaption for nocturnally active animals as both moonlight and starlight consist of longer wavelengths (Matsumoto and Kawamura, 2005), at least in very shallow water environments where there might be some IR penetrance.

Our data demonstrate that, like leeches and *C. elegans*, planarians are strongly photophobic to short wavelengths of light, with UV causing the greatest responses(Edwards et al., 2008; Jellies, 2014a, b). Differential responses to specific wavelengths are well documented in the literature and reveal that an animal's sensitivity to each wavelength depends largely on its natural habitat and physiological needs. Fish that live in the ocean are typically most sensitive to blue wavelengths due to the fact that 470 nm blue light penetrates the greatest (Bowmaker, 1995; Shcherbakov et al., 2013). For example, zebrafish are more positively phototactic to UV and blue than green light (Orger and Baier, 2005). In contrast, the majority of flying or foraging insects are attracted to UV and green light, which they use in characterizing and identifying food sources (Aksoy and Camlitepe, 2012; Gao et al., 2008; Peitsch et al., 1992). For planarians, predator avoidance cues are likely to be the most crucial for survival, as they have few natural defenses and consist solely of soft tissues with no exoskeleton, venom, teeth, or claws. Thus, it makes sense that they would display strong photophobic behavior, particularly to daylight-related UV wavelengths. Furthermore, UV exposure causes significant damage to nucleic acids and proteins (Sinha and Hader, 2002); in planarians prolonged exposure to UV radiation damages their protective mucosal layer and leads to visible wounds (Kalafatić et al., 2006). Thus, a robust UV avoidance might offer a significant adaptive advantage.

UV detection is very common among animals, but the mechanisms used vary greatly. For example, several species of birds, fish, and insects have UV-sensitive photopigments (Briscoe and Chittka, 2001; Jacobs, 1992), while other animals use oil droplets or screening pigments

(Honkavaara et al., 2002; Jacobs, 1992). Additionally, it has been shown that when exposed to UV, invertebrate opsins can be converted to an intermediate that can regenerate the original UV opsin, which prevents bleaching and allows for continued detection of UV light (Nolte and Brown, 1972a, b). The damaging effects of UV exposure are so important that some animals also have general dermal methods to detect UV. *Drosophila* larvae possess neurons that cover their body wall and detect UV light using a chemosensory G-protein coupled receptor pathway (Xiang et al., 2010) distinct from the more commonly understood photopigments. *C. elegans* detect UV using a receptor called LITE-1, which is a member of the invertebrate Gustatory receptor family (Edwards et al., 2008). The photophobic response to UV is so robust in *C. elegans* that illumination of only a few neurons causes behavior (Edwards et al., 2008). Extraocular detection of UV has also recently been discovered in the leech (Jellies, 2014a, b). Extraocular or dermal photoreception has been noted previously in planarians in the historical literature (Steven, 1963). Confirming these reports, our initial behavioral observations found 98% of planarians (n=15) tried to move away from UV light placed on the tail alone. Future experiments should focus on investigating the mechanisms involved, as these are currently unknown. In summary, our results strongly support the notion that visual responses in planaria may be more complex than previously understood.

All data and figures presented in chapter III were published in the journal *PLoS One* with the title, “Planarian Phototactic Assay Reveals Differential Behavioral Responses Based on Wavelength” (Paskin et al., 2014).

CHAPTER IV: THE PLANARIAN TRPA1 HOMOLOG MEDIATES EXTRAOCULAR BEHAVIORAL RESPONSES TO NEAR ULTRAVIOLET LIGHT

Introduction

The ability to detect and respond to light is a fundamental characteristic of living organisms. Ocular photoreception (or vision) is what is most commonly associated with light detection and image formation, an ability which requires central nervous system processing from cells found specifically in the eye organ. However, many animals also have the ability to detect light using light-sensitive structures outside of the eye. Such extraocular photoreception (also known as dermal phototransduction, dispersed photoreception, or non-ocular photoreception) describes a type of "non-visual" light detection that it is not involved in image formation.

While the molecular basis of ocular phototransduction is extensively studied, the mechanisms involved in extraocular photoreception and transduction are not as well understood. This is despite the fact that the ability to detect light outside of the eye is widely distributed throughout the animal kingdom. Both vertebrate and invertebrate extraocular photoreception has been documented (Cronin and Johnsen, 2016; Lees, 1948; Porter, 2016; Steven, 1963). For example, mollusks and Cnidaria use extraocular photoreception for phototaxis and/or shadow-induced withdrawal (Lukowiak and Jacklet, 1972; Pankey et al., 2010; Ramirez et al., 2011; Taddei-Ferretti and Musio, 2000); leeches use extraocular photoreceptors for dorsal-ventral body orientation (Jellies, 2014b); in amphibians, extraocular photoreceptors are required for detection of polarized light and magnetic orientation (Adler and Taylor, 1973; Phillips et al., 2001); while birds possess photoreceptors in the hypothalamus that regulate their circadian and reproductive cycles (Menaker, 1968).

The mechanisms involved in classical ocular phototransduction are well characterized and appear to be highly conserved throughout the Bilateria (Arendt, 2003). Phototransduction occurs when a photon of light activates a light-sensitive photopigment, which consists of a chromophore and an opsin (Wald, 1968). Opsins are G-protein coupled receptors that are responsible for ocular light detection in all animals. Opsins are typically located within either rhabdomeric or ciliary photoreceptor cells, where they activate r-opsin or c-opsin signal transduction cascades, respectively (Arendt, 2003). C-opsins initiate a pathway that closes CNG ion channels (Kaupp and Seifert, 2002), while r-opsins lead to the opening of TRPC channels (Hardie, 2001). Both cascades result in signals that are interpreted by the brain to produce behavioral responses in the animal.

Although planarian eyes are simpler than vertebrate eyes, they still possess several phylogenetically conserved features. For example, eye development in many animals, including both planarians and vertebrates, relies on common genes such as *Sine oculis*, *Eyes absent*, and *Otx* (Mannini et al., 2004; Martín-Durán et al., 2012; Pineda et al., 2000). Planarian eyes are located on the dorsal side of the body and consist of two cell types: pigment cells and photoreceptor cells. Pigment cells form a semi-lunar optic cup and function to absorb photons of light, which creates shade and provides directional information about incoming light (Nilsson, 2009). Photoreceptor cell bodies are found outside of the optic cup and project axons posteriorly to the brain, with some fibers forming a partial optic chiasma (Agata et al., 1998; Carpenter et al., 1974; Okamoto et al., 2005). Photoreceptor cell dendrites extend into the optic cup making a rhabdomeric structure where opsin accumulates (Azuma and Shinozawa, 1998; Orii et al., 1998). Similar to rhabdomeric photoreceptors in other invertebrates, planarian photoreceptors express two r-opsin orthologs (Lapan and Reddien, 2012; Orii et al., 1998). Interestingly, transcriptome

analysis has also shown that planarian eyes contain genes that are typically associated with the phototransduction pathway found in ciliary photoreceptors, such as CNG (Lapan and Reddien, 2012). However, the roles of these genes in planarian vision is not currently known.

In contrast to ocular photoreception, the mechanisms used for extraocular photoreception have not been as extensively studied, and the few molecular pathways identified are more wide-ranging. Some animals appear to reuse the same ocular phototransduction receptors and pathways for extraocular photoreception. Cuttlefish and pond snails use c- and r-opsins, respectively, for extraocular photoreception (Mathger et al., 2010; Pankey et al., 2010); while Cnidarians use Gs-opsins (or "cnidops"), which in *Hydra* are believed to activate CNG channels (Plachetzki et al., 2010). Although poorly characterized, "RGR/Go-opsins" are another group of opsins known to have extraocular function (Feuda et al., 2012; Porter, 2016; Raible et al., 2006).

In addition to these opsin-based mechanisms, a few other mechanisms unique to extraocular photoreception have been identified. Cryptochromes are UV- and blue-light sensitive proteins that have been shown to regulate a variety of different light responses, including circadian rhythms in both plants and animals (Chaves et al., 2011; Haug et al., 2015) and magnetoreception (Bazalova et al., 2016; Gegear et al., 2008). There have also been pathways identified that center on gustatory-related receptor proteins. In *C. elegans*, two gustatory-related receptor genes, LITE-1 and GUR-3, have been found to elicit UV light avoidance and together also inhibit feeding behavior (Bhatla and Horvitz, 2015; Edwards et al., 2008). Similar to *C. elegans*, *Drosophila* larvae exhibit avoidance behavior to blue and UV light using the gustatory receptor, GR28b (its closest homolog to LITE-1), which is found in the neurons that tile the body wall. This mechanism also involves the ion channel TRPA1 (Xiang et al., 2010). The existence

of such variable mechanisms utilized for extraocular photoreception opens up questions about its evolutionary origins.

Furthermore, there can be conflicting evidence for the existence of extraocular photoreception in certain species, as is the case for planaria. Planarians are free-living flatworms that make excellent models for investigating the basic features of eye biology and evolution due to their relatively simple yet phylogenetically conserved visual systems(Lapan and Reddien, 2012; Orii et al., 1998). Historical studies recorded the planarian extraocular ability to respond to light (along with most other aquatic animals surveyed) (Steven, 1963). Early experiments that used surgical ablation to remove both eyes showed that eyeless planarians are negatively phototaxic and will change direction in response to white light (Parker, 1900; Taliaferro, 1920). However, more recent studies that also specifically removed the eyes failed to observe any behavioral responses to white light (Arees, 1986; Azuma and Shinozawa, 1998). We hypothesize that planarians are in fact capable of extraocular photoreception, and that previous reports may have disagreed due to the use of different sources of white light (which had different spectral compositions). White light is composed of many wavelengths, and our previous work has demonstrated that planarian behavioral responses vary by wavelength (Paskin et al., 2014). We set out to investigate whether planarians possess extraocular photoreception. Finding that planarians did respond to extraocular light cues, we then investigated if this response was wavelength-specific and what possible genetic mechanisms might be involved.

Materials and Methods

Animals and Colony Care

An asexual strain of *Schmidtea mediterranea* was used and maintained as previously described (Paskin et al., 2014), with worm water comprised of 0.5 g/L of Instant Ocean salts (Spectrum Brands, Blacksburg, VA, USA). Worms used were 7-9 mm in length and were starved at least one week prior to experimentation.

Light Sources

Behavioral assays were conducted using commercially available red, green, and near UV laser pointers with nominal peak wavelengths of 650 nm, 532 nm, and 405 nm (+/- 10 for all), respectively. A laser power meter (LaserBee A 2-Watt Laser Power Meter/Thermopile, J. BAUER electronics, CANADA) was used to determine the absorbed power for each laser: red = 85 mW, green = 29 mW, and UV = 54 mW. The power was then used to calculate the intensity (Watts/Area of light) of each wavelength: red = 0.68 W/cm^2, green = 0.23 W/cm^2, near UV = 0.43 W/cm^2. A piece of tape was placed on the end of the laser and punctured to create a pinhole that was smaller than the worm itself and produced a circle of light with a diameter of approximately 2.5 mm. The power of each laser with the pinhole was also examined but all were below the level of thermopile detection (<1 mW).

Avoidance Assay

Ocular responses were tested using an avoidance assay we previously developed (Paskin et al., 2014). A 100 mm Petri dish filled with 20 mL of worm water was positioned over a white

piece of paper and placed on the microscope stage. The white paper enables the laser light to be seen. The base brightfield light of the microscope was set to the lowest possible setting that allowed for video recording of worm position (~275 lux). This was considered our "ambient" light level, and all experiments were performed under this setting. Individual worms were transferred to the middle of the Petri dish and recording was started when the worm began traveling in a straight line. The laser beam was directed in front of the animal at a distance equal to one diameter of the circle of light (~2.5 mm), and held stationary while the worm traveled. Recording was stopped after worms either passed through the light (no response) or responded (avoided the light). Worms were tested in order of decreasing wavelength (red, then green, then near UV). For each wavelength, 30 worms were tested 4 times for a total of 120 trials per wavelength. Control "no light" experiments were performed without the laser light cue being presented (30 worms were tested 3 times for a total of 90 control trials). The recording time for no light controls was 2.5 seconds (the average time required to elicit a behavioral response in a random sample of red, green, and near UV trials, plus 0.3 seconds).

Behavioral responses were determined as follows: No response (movement of the worm through any part of the light); Moderate response (movement around the light at an angle less than 90 degrees from the worm's original trajectory); and Severe response (movement in the opposite direction of the light at an angle of 90 degrees or greater). Since worms randomly explore new environments (*i.e.*, do not always travel in a straight line), the amount of "responses" (either moderate or severe) recorded in no light controls represents the level of background noise (random turning) in the assay. Significance was determined by calculating the percent of worms that exhibited each of the 3 responses followed by a two sample *t*-test between

percents using the Statistics Calculator software (StatPac, V. 4.0, StatPac Inc., Northfield, MN, USA) with $p<0.0001$ significant.

Extraocular Assay

Extraocular responses to light were tested using the microscope, Petri dish, and laser pointer set-up as described for our avoidance assay. The same worms tested for ocular responses were tested for extraocular responses to allow for a comparison of ocular and extraocular responses in the same individual. As worms moved across the dish, the laser light was shone directly on the tail (midway between the tip of the tail and the pharynx), with the light coming from behind the worm to avoid involvement of the eyes. The light's position on the tail was maintained by moving the laser light with the worm (so that the light remained on the tail) until after a response was observed or for 5 seconds if no response was observed. No light controls were recorded for 5 seconds as worms moved. Behavioral extraocular responses were determined by the presence of tail thinning.

To assess tail thinning, we analyzed an image of the worm just before the light was positioned ("Before"), as well as an image when the tail appeared thinnest ("After"). When no thinning was apparent, the "After" image used was at 3 seconds after the spot of light was positioned (the average time it took for peak thinning in animals with a response). The two pictures ("Before" and "After") were then analyzed in Photoshop (Adobe Systems, San Jose, CA, USA) by measuring the width of the tail (in pixels) halfway between the most posterior part of the pharynx and the tip of the tail. Thinning responses were expressed as the percent of the animal that had thinned: the width of the "After" image was divided by the width of the "Before" image, and this value was subtracted from 1. Significance between the average percent thinned in

no light control animals versus red, green, or near UV wavelengths was determined using a Student's *t*-test with $p<0.0001$ significant.

Neutral Density Filters

Filters used were 25.4 mm diameter nickel chromium coated fused silica (7980) as previously described (Jellies, 2014b). A holder was designed from a small PVC pipe to position the laser pointer above the filter such that all emitted light passed through the filter. Neutral density filters attenuating 75% of light (optical density=0.6), 95% of light (optical density=1.3), and 99% of light (optical density=2.0) were used. Significance between the average percent thinned in animals exposed to full near UV light versus near UV attenuated light was determined using a Student's *t*-test with $p<0.0001$ significant.

Worm Fragment Assay

Amputations were performed as previously described (Beane et al., 2013). 1/5 fragments (head, pre-pharynx, pharynx, post-pharynx, and tail) were generated by cutting just posterior to the auricles, just anterior to the pharynx, just posterior to the pharynx, and midway between the pharynx and the tail. Fragments were transferred to non-treated tissue-culture welled plates, and worm water was changed immediately following surgery. After 1-2 hours of recovery, fragments were tested for extraocular responses as described above with the following exceptions: only no light controls and near UV laser light trials were performed (n=20 for each); the near UV laser pointer was positioned using a clamp stand approximately 2 inches above the worm, with the light positioned on the center of the fragment; and each fragment was recorded for 45 seconds or until it had moved out of the laser light, whichever occurred first.

To assess extraocular responses in fragments, an image when the light was first positioned ("Before") and an image when the worm first moved out of the field of light ("After") were analyzed. For no light controls, an image at 45 seconds was used for "After." "Before" and "After" images from each fragment trial were overlaid in Photoshop, and the distance between the most posterior edge of the fragment in each image was measured (in pixels). Using this distance measurement and the time it took for the fragment to leave the light (or 45 seconds for control), the rate of movement was calculated. Significance was determined using a Student's *t*-test with $p<0.001$ significant.

Eye Ablation Assay

Double eye ablations and sham ablations were performed as previously described (Deochand et al., 2016). After 24 hours, behavioral responses to green and near UV light were tested and analyzed using the avoidance assay described above. For each wavelength, n=50 for the sham ablated group and n=30 for the double eye ablated group. Significance was determined using a two sample *t*-test between percents using StatPac (V. 4.0) with $p<0.05$ significant.

Cloning

Homologs to Cyclic Nucleotide-Gated channel A (CNG-A) and LITE-1 (NP_509043.3) were used to search (tBlastn) the *Schmidtea mediterranea* Genome Database (Robb et al., 2015; Robb et al., 2008). To confirm identity, the resulting candidate sequences were used to search (tBlastx) NCBI (http://blast.ncbi.nlm.nih.gov/Blast.cgi). Previously identified planarian sequences to Transient Receptor Potential Cation channel, subfamily A (*Smed-TrpA*) (Wenemoser et al., 2012), and Opsin homologs (Lapan and Reddien, 2012; Sánchez Alvarado

and Newmark, 1999) were identified from the literature. An *S. mediterranea* cDNA library (from intact worms) was used to generate initial gene fragments by PCR with primers designed using Primer3plus (http://www.bioinformatics.nl/cgi-bin/primer3plus/primer3plus.cgi/). PCR fragments were ligated into pCRII-TOPO (Invitrogen, Carlsbad, CA, USA) and confirmed by sequencing. Protein domain analyses were performed using the NCBI Conserved Domains Database (http://www.ncbi.nlm.nih.gov/cdd) (Marchler-Bauer et al., 2015). Primer sequences used were:

TrpA:

Smed-TrpA-forward 5'-CAACTCGACACCTTTGCACTA-3'

Smed-TrpA-reverse 5'-CAACCTCCCAAATGAGTCTGT-3'

CNGA:

Smed-CNGA3-Forward 5'-GATTCAGAATGGATGCTT-3'

Smed-CNGA3-Reverse 5'-TGTGCCAATTAAAACTCC-3'

Smed-CNGA3-Like-Forward 5'-AACATTCTCGTGAATCGGAAC-3'

Smed-CNGA3-Like-Reverse 5'-TAACTCCCAAATTCGTTCTGG-3'

Opsin:

Smed-opsin-Homolog-1 Forward 5'-TCTTTTGGTTTTGGTGGACAG-3'

Smed-opsin-Homolog-1 Reverse 5'-TCCATCAACACAATGGCACTA-3'

Smed-opsin-Homolog-2 Forward 5'- GGTTTCATCGGTGGTCTTTT-3'

Smed-opsin-Homolog-2 Reverse 5'-ACCCGTTTTCATGGAAGTTG-3'

RNA interference (RNAi)

RNAi was performed as previously described (Rouhana et al., 2013). In summary: double-stranded RNA (dsRNA) was generated by using the above pCRII-TOPO constructs to make linearized templates via PCR (using T7 and SP6 primer sequences). This PCR template was used for *in vitro* dsRNA synthesis with T7 and SP6 RNA polymerases (Promega P2075, P1085, N2511, P1221, M6101; Promega, Madison, WI, USA). An RNAi mixture of 100 ng/μL in liver puree (Creekstone Farms, Arkansas City, KS, USA) plus 1% red food coloring was made. Worms were fed RNAi in Petri dishes (5 μL per worm) three times over eight days before being used on day 14 (from first feeding) to test behavioral responses as described above (avoidance and extraocular assays). Significance was determined for avoidance trials using a two sample *t*-test between percents with $p<0.05$ significant. For the extraocular assay, a one-way ANOVA with Tukey's multiple comparisons test with $p<0.0001$ was used for significance.

In situ *hybridization*

Whole-mount *in situ* hybridization was performed as described in (Pearson et al., 2009), with modifications as described in (Deochand et al., 2016) except samples were incubated in formamide-bleaching solution for 4 hours as described in (King and Newmark, 2013). *Smed-TrpA* probe was used at 4 ng/μL. Anti-digoxigenin-AP (Roche, Basel, Switzerland) was used at 1:3000.

Image Collection

All images were collected using a Zeiss V20 fluorescent stereomicroscope with AxioCam MRc or MRm camera and Zen Lite software (Zeiss, Oberkochen, Germany).

Results

Planarians Possess Both Ocular and Extraocular Responses to Light

Planarian behavioral responses to light are complex. Dorsal eye spots (ocelli) regulate a strong photophobic avoidance across a wide spectrum of light wavelengths (Brown et al., 1968; Paskin et al., 2014). Additionally, studies have suggested that planarians possess the ability to respond to light via extraocular mechanisms and will display avoidance behaviors following surgical removal of the eyes (Parker, 1900; Taliaferro, 1920). Our previous research has shown that different wavelengths elicit different behavioral responses in planarians (Paskin et al., 2014). However, these studies did not separate out any contribution that may have been made by extraocular photoreception to the behaviors observed. Therefore, we modified our previously described light avoidance assay (Paskin et al., 2014) in order to investigate extraocular responses to different wavelengths of light.

We set out to test both ocular and extraocular behavioral responses in the same individuals. To measure ocular responses to light, we performed our avoidance assay where a point of red, green, or near UV laser light is placed directly in front of a worms' path (Fig.15) (Paskin et al., 2014). Planarians display three distinct behaviors: 1) no response, with continued movement directly through the light; 2) a moderate response, with a directional change to avoid the light; and 3) a severe response, with an abrupt turn of ≥ 90 degrees away from the light. Negative controls, with no laser light, were also performed (Fig.15). Consistent with our previous findings, the majority of worms (>80%) had no response to red light (which was not significantly different from controls), while 75.83% displayed a moderate response to green light

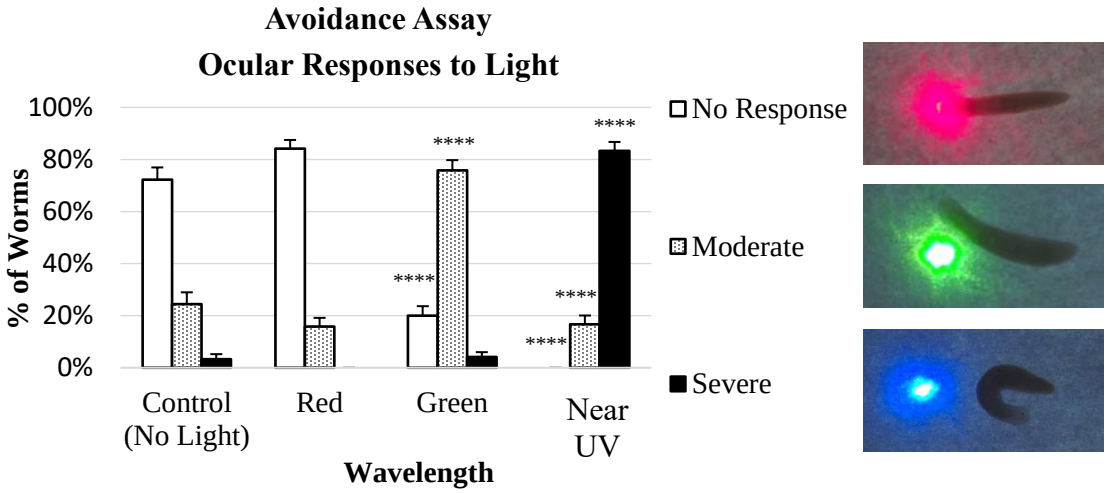

Figure 15. Planarians possess complex ocular photoresponses. The planarian species *Schmidtea mediterranea was used to* examine ocular behavioral responses to red, green, and near UV wavelengths using our avoidance assay. When approaching a spot of light, three distinct behaviors are observed: worms move through the light (no response), worms avoid the light by moving around it (moderate response), or worms make a 90-180 angle turn away from the light (severe). Note that worms fail to respond to red light, display moderate responses to green light, and have severe responses to near UV light. n=120 for red, green, and near UV, n=90 for control. Statistics: two sample *t*-test between percents, **** = $p<0.0001$ (as compared to no light controls), error bars = SD.

and >80% displayed a severe response to near UV light (Fig.15). The near UV severe response is so penetrant that no animals traveled through the near UV light (100%). These results demonstrate that this population of planarians responded as predicted with wildtype reactions to each different wavelength of light (and the shorter near UV wavelengths causing the strongest photophobic reactions).

Having established this baseline, we next used these same animals to examine extraocular behavioral responses. For our extraocular assay, either red, green, or near UV laser light was placed directly on the animals' tail (Fig.16). The same diameter of light used in our avoidance assay was positioned on the most posterior part of the worm (the tail) without ever illuminating the head or eyes. Using this method, we observed responses to some extraocular light sources of a "thinning" of the tail (Fig.16), presumably to reduce the surface area exposed to the light source, followed by swift movement (pulling of the tail) out of the spot of light. This response was analyzed by measuring the width of the tail halfway between the most posterior part of the pharynx and the tip of the tail (star in Fig.16) and was expressed as the percent of tail thinned. We observed no behavioral responses to either red or green wavelengths with responses not significantly different from no light controls ($p \geq 0.45$, Fig.16). However, exposure to near UV light resulted in a marked thinning of the tail, with an average decrease in tail width of 40.15% ($p < 0.0001$, Fig.16). These results demonstrate that planarians are in fact capable of extraocular photoreception and furthermore that their extraocular light detection is specific to near UV wavelengths. We next wanted to determine if any confounding variables might be contributing to the behavioral responses we observed. First, we repeated the extraocular assay using near UV light in combination with neutral density filters to determine whether or not there was a linear correlation between the light source and the behaviors observed (Fig.17A). Since neutral density

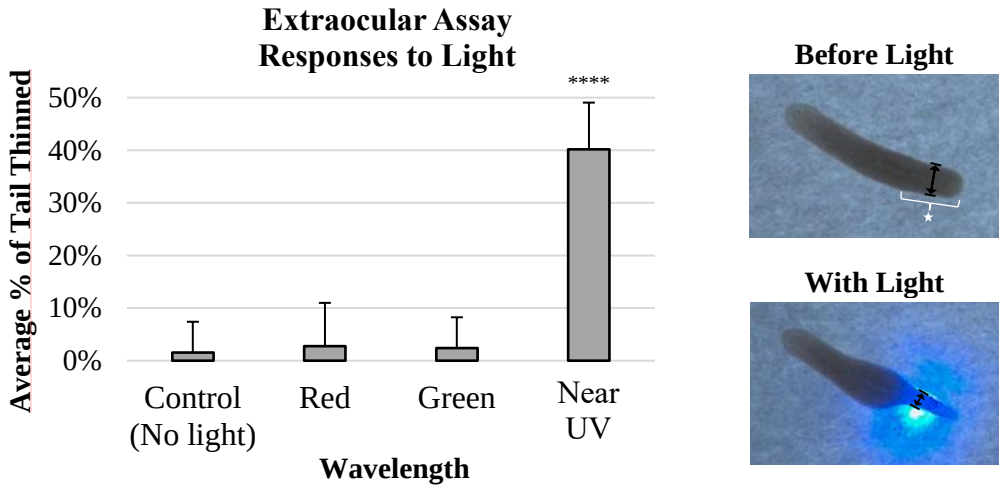

Figure 16. Planarians possess extraocular photoreception. Graph of extraocular responses to light using our extraocular assay. A spot of light was placed on the worm's tail, and the presence of the photophobic "tail thinning" response was assessed. Thinning was determined by measuring the width of the tail (midway between the posterior edge of the pharynx and tip of tail) both before and after exposure to red, green, and near UV laser light. Inset photos: starred bracket designates the tail; double headed black arrows designate the width measurement. Note that significant tail thinning was observed only with near UV wavelengths. N=40 for control, red, and green; n=120 for near UV. Statistics: two-tailed independent *t*-test, **** = $p<0.0001$ (as compared to no light controls), error bars = SD.

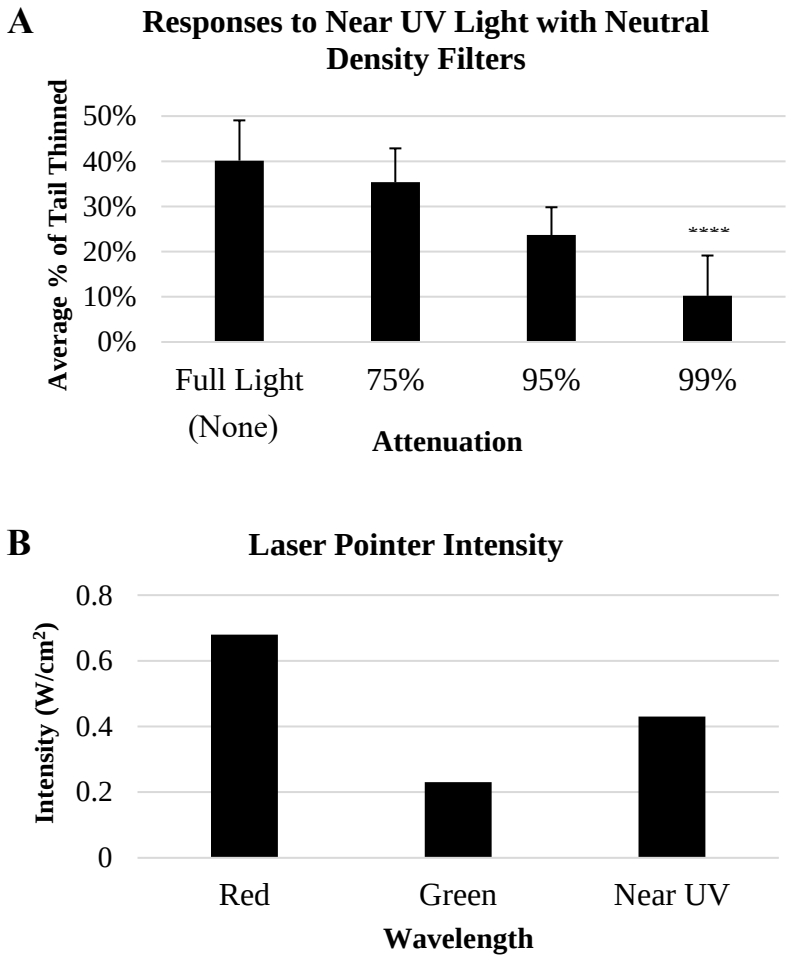

Figure 17. Extraocular behavioral responses result from detection of near UV light stimulus. **(A)** Graph showing extraocular behavioral responses with increasingly attenuated light, as measured by amount of tail thinning when exposed to near UV laser light ($n \geq 40$). Worms were exposed to full light, 75%, 95%, and 99% attenuated light (or optical densities of 0, 0.6, 1.3 and 2.0 respectively). The trend shows extraocular behaviors decrease with diminished light stimulus. Statistics: two-tailed independent *t*-test, **** = $p<0.0001$ (as compared to full light responses), error bars = SD. **(B)** Graph showing red, green, and near UV laser light intensities (W/cm^2). The light intensities do not correlate with planarian behavior as the most intense light, red, elicits no response.

filters attenuate light, which is our relevant stimulus, we would expect tail thinning to decrease in correlation with an increase in light attenuation. In the first trial, the near UV laser light was attenuated to 75%, meaning only 25% of the light reached the animal. For the second trial 95% of the light was attenuated, while in the last trial the near UV light was attenuated to 99%. Our results revealed a steady decrease in behavioral responses to near UV light (tail thinning) with increased light attenuation, such that with both 95% and 99% attenuation tail thinning was significantly less than full power near UV light controls (Fig.17A). Furthermore, there was a significant decrease in responses between each neutral density filter trial ($p \leq 0.01$). These data confirm that extraocular responses to near UV light diminish in a predictable fashion as light attenuation increases. Second, we used a laser power meter and confirmed that the laser light emitted from the pinhole produced very little power (and therefore heat) with levels below the threshold of the thermopile (<1 mW). Finally, we calculated the intensities of the full power of each laser light (no pinhole) and found that the red laser pointer actually produced the most power per unit area (Fig.17B), even though worms had no response to red light (Figs.15, 16). Together, these data suggest that neither heat nor light intensity are factors involved in the behavioral responses observed and that tail thinning is a result of near UV light detection.

Extraocular Light Responses Occur Across the Entire Body

Our extraocular assay showed that the post pharyngeal tissues of the tail possess extraocular photoreception. However, the nature of the assay (using whole worms) means that we could not rule out the possibility that animals were still receiving a small amount of ocular input, which could be contributing to the observed response. Furthermore, our previous assay did not allow us to evaluate whether the extraocular response to near UV occurs along the entire

anterior-posterior axis of the worm (as opposed to being confined to just the tail region). Planarians have the ability to survive and regenerate when cut into multiple fragments, including the movement of new fragments lacking any brain tissues in response to stimuli (Beane et al., 2011). We used this unique planarian characteristic to perform a worm fragment assay to confirm that extraocular responses do not require the eyes, as well as to examine if extraocular responses also occur in other regions of the body.

For our worm fragment assay, each worm was cut into 5 sections: head fragments, pre-pharynx fragments, pharynx fragments, post-pharynx fragments, and tail fragments (Fig.18A). Because new worm fragments do not move as much as whole worms (and typically not without a stimulus), we modified our extraocular assay and analyses to accommodate fragments. Behavioral responses for each fragment were recorded for 1 minute with no laser light (controls) and again with near UV laser light with the spot of light placed directly in the center of each fragment (Fig.18B). From these data, we calculated the speed at which each fragment moved out of the near UV light from the time and distance the fragment had moved (Fig.18B). Our results demonstrate that while control fragments (with no light stimulus) moved very little as expected, exposure to near UV light caused a significant increase in speed for all fragments tested ($p \leq 0.001$, Fig.18C). These data show that extraocular responses to near UV occur across the entire body of the planarian. Additionally, our results suggest that detecting and responding to near UV light does not require either ocular input or the brain.

Extraocular Behavioral Responses Require TrpA

Together our data from the extraocular assay and worm fragment assay demonstrate that planarians are capable of extraocular detection of light. Furthermore, our results show that these

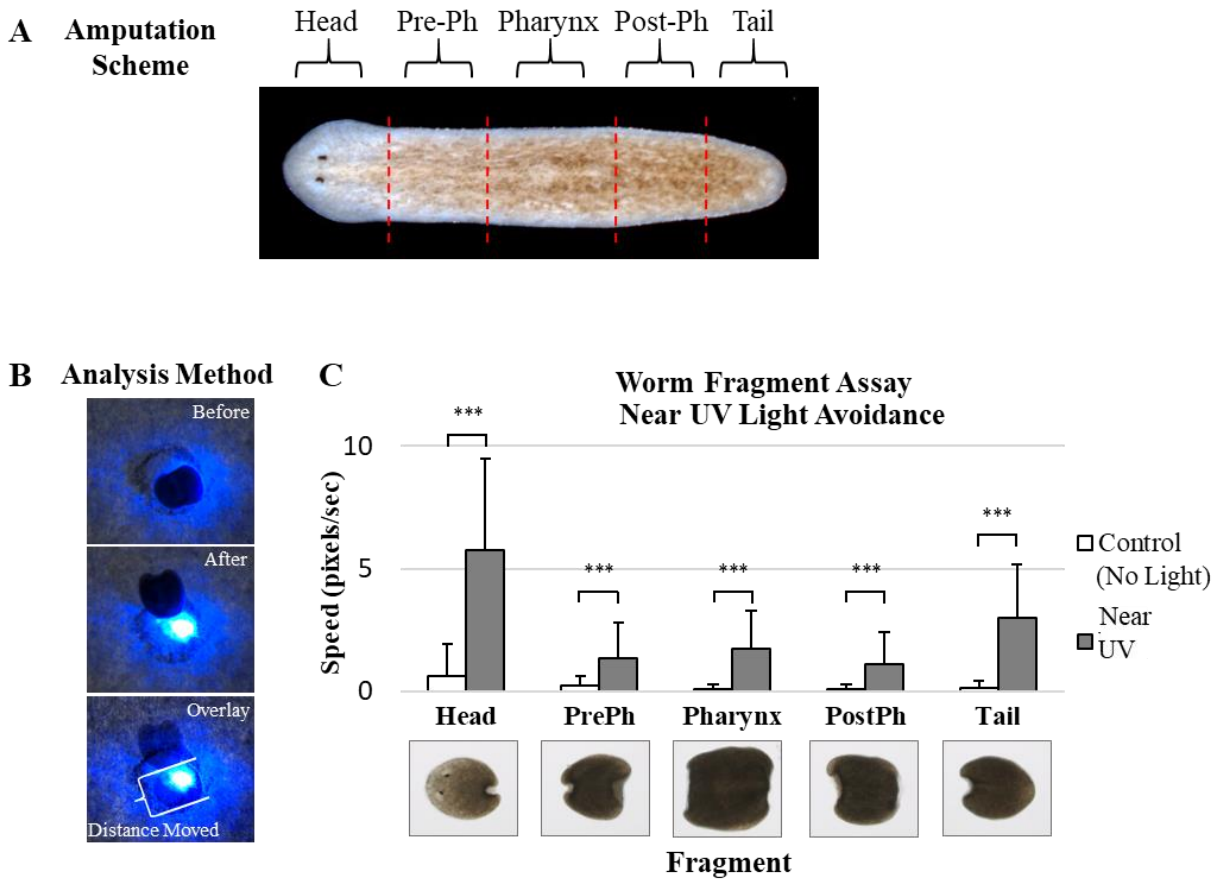

Figure 18. Extraocular photoreception occurs along the entire body. Worm fragment assay where worms were cut into 5 fragments along the anterior-posterior axis and individual fragments were tested at 1-2 hours post amputation for extraocular photophobic behavioral responses to near UV light. **(A)** Diagram of amputation scheme and resulting fragments. **(B)** Photophobia was assessed by analyzing the speed of fragments moving out of the cone of light [distance moved by the most posterior edge of the fragment (bracket) divided by time]. **(C)** Graph of near UV light avoidance in worm fragments showing that near UV light causes a significant increase in speed for all fragments (n=20). PrePh: pre-pharyngeal. PostPh: Post-pharyngeal. Statistics: two-tailed independent *t*-test, *** = $p<0.001$ (as compared to no light controls), error bars = SD.

responses are specific to near UV wavelengths and occur along the entire anterior-posterior axis of the animal. However, the genetic mechanism(s) for extraocular photoreception in planarians are unknown. We took a candidate gene approach to uncover potential mechanisms by searching the *S. mediterranea* genome (Robb et al., 2015; Robb et al., 2008) and the literature for planarian homologs to genes that regulate extraocular photoreception in other animals: CNG channels, Opsin, Lite-1, and TRPA1 (Bhatla and Horvitz, 2015; Edwards et al., 2008; Mathger et al., 2010; Pankey et al., 2010; Plachetzki et al., 2010; Xiang et al., 2010). We found no potential homologs for the *C. elegans* Lite-1 gene; however, *S. mediterranea* homologs for the other extraocular photoreception genes were identified (Table 1). Therefore, using RNAi we examined the role of the two planarian opsin orthologs (Lapan and Reddien, 2012; Sánchez Alvarado and Newmark, 1999), two CNG-A homologs, and the TRPA1 homolog (*Smed-TrpA*) (Wenemoser et al., 2012) in mediating planarian extraocular responses.

Table 1: List of Extraocular Photoreception Genes Tested.

GENE	Planarian Homolog	Planarian Homolog ID
CNG-A	CNG-A3/TAX-4	SMU15017470
	CNG-A3-Like	SMU15028995
Opsin	R-Opsin homolog 1 (Lapan and Reddien, 2012)	SMU15026624
	R-Opsin homolog 2 (Sanchez Alvarado and Newmark, 1999)	AF112361.1*
Lite-1	none found	--
TRPA1	*Smed-TrpA* (Wenemoser et al., 2012)	SMU15032241

CNG-A is subunit A. SMU numbers are unique gene identifiers from the Smed genome database (Robb et al., 2015). * is an NCBI accession number.

Treating whole worms with dsRNA made to the five identified homologs from Table 1, we found that only *Smed-TrpA(RNAi)* influenced extraocular behavioral responses to near UV

wavelengths (Fig.19A). TRPA1 is an ion channel that has been shown to be required for extraocular photoreception of UV light in *Drosophila* larvae (Xiang et al., 2010). Protein domain analysis between *Drosophila* TRPA1 and planarian *Smed-TrpA* shows the two genes to be highly conserved. In our extraocular assay using near UV laser light, the amount of tail thinning in both CNG-A(RNAi) homologs and r-opsin(RNAi) homologs were not significantly different from wildtype (Fig.19A). However, *Smed-TrpA(RNAi)* animals showed a significant decrease in tail thinning (Fig.19A,B2), as compared to wildtype worms ($p<0.0001$, Fig.19A,B1). These data suggest that, similar to *Drosophila* larvae, TRPA1 is required for planarian extraocular behavioral responses to near UV wavelengths. *In situ* hybridization of *Smed-TrpA* transcripts revealed that planarian TRPA1 is expressed throughout the entire anterior-posterior axis (Fig.19C1). These data are consistent with our worm fragment assay findings that planarians possess extraocular photoreception along their entire body. Furthermore, punctate *Smed-TrpA* expression was observed in dorsal tissues (Fig.19C2), reminiscent of the dorsal (sub)epidermal expression patterns of planarian body pigment synthesis genes, such as KMO-1, ALAS, ALAD-1, and PBGD-1 (Stubenhaus et al., 2016). These data suggest that *Smed-TrpA* is in the right place to mediate planarian extraocular behavioral responses.

To more closely assess the role of *Smed-TrpA* in mediating extraocular versus ocular photoreception, we compared "blind" (double eye ablated) animals to *Smed-TrpA(RNAi)* animals using our avoidance assay (Fig.20). For these experiments, we used an eye ablation technique we previously developed that removes the eyes without disturbing the underlying brain tissues (Deochand et al., 2016). We found that sham surgery controls (where two pieces of anterior tissue outside the eye field were excised) displayed similar responses to uninjured wildtype for both green ($p = 0.98$, Fig.20B) and near UV ($p = 0.67$, Fig.20C) wavelengths. As expected,

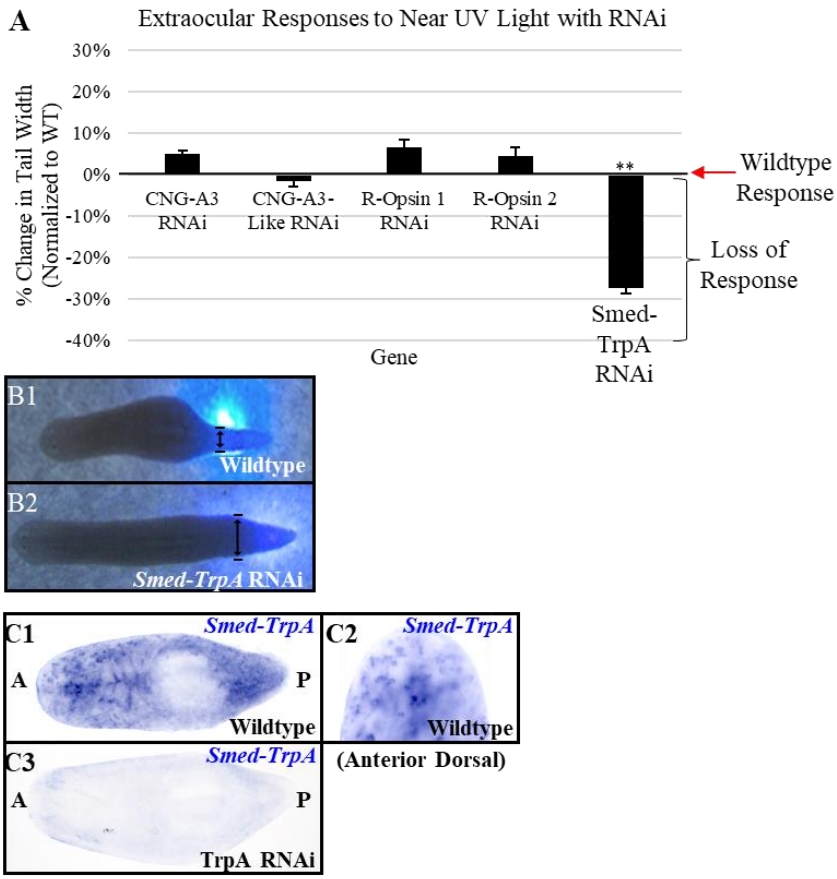

Figure 19. *Smed-TrpA* is required for extraocular behavioral responses to near UV light. (A) Graph of extraocular behavioral responses to near UV light following RNA interference (RNAi). Genes known to regulate extraocular photoreception in other animals (homologs to CNG channels, opsins, and TRPA1) were knocked down following dsRNA feeding then tested for tail thinning response. Graph is normalized to wildtype response. Tail thinning was significantly decreased only in *Smed-TrpA(RNAi)* animals (n≥21). Statistics: One-way ANOVA with Tukey's multiple comparisons test, **** = $p<0.0001$ (as compared to wildtype responses), error bars = SEM. **(B)** Images showing wildtype thinning response (B1) and lack of response in *Smed-TrpA(RNAi)* animals (B2). **(C)** *In situ* hybridization for *Smed-TrpA*. Wildtype worms express *Smed-TrpA* along the entire length of the planarian body (C1), particularly in dorsal tissues (C2), while expression is lost following *Smed-TrpA(RNAi)* (C3). (n≥13) A=anterior, P=posterior.

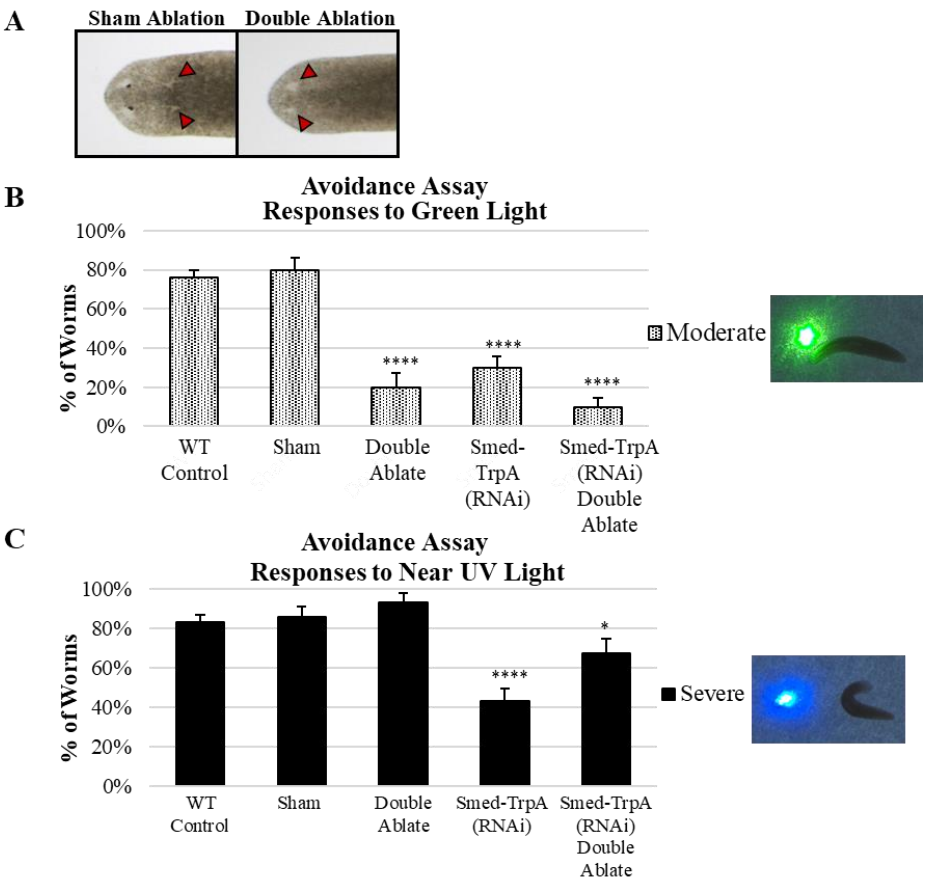

Figure 20. Both ocular and extraocular behavioral responses involve *Smed-TrpA*. (A) Representative examples of eye ablation assay. Surgery sham controls had tissue removed posterior to the eyes, while eyes were surgically removed in experimental groups (double eye ablation). Both groups were tested 24 hours post-surgery. Red arrows: resected tissue. **(B-C)** Graphs showing avoidance responses to green (B) and near UV (C) laser light across different treatment groups (n≥30). Double eye ablated worms showed a significant decrease in responses to green light while near UV light avoidance remained similar to controls, suggesting that eyes are needed for photoreception of green (but not near UV) wavelengths. *Smed-TrpA(RNAi)* significantly reduced responses to both green and near UV light, suggesting a role for *Smed-TrpA* in both ocular and extraocular behavioral responses. Statistics: two sample *t*-test between percents. **** = $p<0.0001$, * = $p<0.05$ (as compared to wildtype responses), error bars = SD.

double eye ablated animals had significantly reduced responses to green light ($p < 0.05$, Fig.20B). Double ablation of the eyes had no effect on the worm's ability to respond to near UV light as compared to wildtype ($p = 0.32$, Fig.20C). These data are consistent with our findings that planarians possess extraocular photoreception of near UV wavelengths.

We found that *Smed-TrpA(RNAi)* animals had significantly reduced responses to both green and near UV light ($p < 0.05$; Figs.20B,C). Our finding that, unlike wildtype , *Smed-TrpA(RNAi)* animals largely failed to respond to green wavelengths in our avoidance assay (typically used to measure ocular responses) was unexpected, given our data showed that planarians have no extraocular responses to green light (Fig.16). Furthermore, responses to green light after double eye ablation of *Smed-TrpA(RNAi)* animals were not significantly different from responses after double eye ablation alone ($p = 0.24$, Fig.20B). These data suggest the possibility that behavioral responses to ocular photoreception may be mediated in part by *Smed-TrpA*. Together, our ablation assay data suggest that planarian responses to green light are largely driven by ocular photoreception, whereas behavioral responses to near UV light are largely driven by extraocular photoreception. In summary, our data demonstrate that *Smed-TrpA* is required for behavioral responses to light, and specifically extraocular responses to near UV light, in planarians.

Discussion

Our results support the hypothesis that planarians are in fact capable of extraocular photoreception and that light detection occurs along the entire body. Furthermore, similar to *C. elegans* and *Drosophila* larvae, extraocular photoreception in planarians is specific to near UV wavelengths. We found that extraocular exposure to either red or green wavelengths did not

elicit photophobic responses, unlike the significant tail thinning that was observed when planarians were exposed to near UV light. In addition to our behavioral studies, we also discovered that *Smed-TrpA* is involved in planarian extraocular avoidance behavior to near UV light. Like *Drosophila* larvae, we found that a TRPA1 ion channel homolog is required for wildtype tail thinning responses in planarians and that normal photophobic responses to near UV light are significantly decreased when *Smed-TrpA* is knocked down.

TRPA1 is a nonselective cation channel that is permeable to Ca^{2+}, K^{+}, and Na^{+} ions and is a member of the large TRP family of ion channels. TRPA1 has been found in a variety of vertebrates and invertebrates, including humans, mice, rats, dogs, chickens, zebrafish, snakes, frogs, fruit flies, planarians, and *C. elegans* (Inoue et al., 2014; Laursen et al., 2015; Nilius et al., 2012). TRPA1 is unique in that it functions mainly to detect signals that cause pain and inflammation, such as noxious chemicals and both mechanical and thermal stimuli (Bautista et al., 2013; Hill and Schaefer, 2009; Kwan et al., 2006; Zygmunt and Högestätt, 2014). It has also been determined that the TRPA1 gene is activated in response to reactive electrophiles (which are tissue-damaging agents with aversive effects in both invertebrates and vertebrates) an activity that has been highly conserved for ~500 million years (Kang et al., 2010). Electrophiles that activate TRPA1 are incredibly diverse and range from chemicals found in mustard and cinnamon to formaldehyde and acrolein, the latter of which is found in tear gas and vehicle exhaust. In addition to external irritants, TRPA1 is also sensitive to endogenous agents such as reactive oxygen species (ROS) that are released by cells in response to tissue damage and inflammation (Bautista et al., 2013; Bessac and Jordt, 2008; Viana, 2016). Some of the ROS known to be TRPA1 activators include hypochlorite, H_2O_2, and ozone (O_3) (Takahashi and Mori, 2011).

We found that while planarians possess photophobic ocular responses to green light, they display no extraocular responses to green light. Although the majority of double eye ablated "blind" animals had no response to green light, a small percentage were still able to respond. While this avoidance could have been the result of residual eye tissue after surgery, planarians may also possess different types of extraocular photoreceptors in the head and tail. Interestingly, the majority of *Smed-TrpA(RNAi)* animals also had no response to green light (Fig.20). These data suggest that TRPA1 is required for ocular behavioral responses to green. This would appear to be the first recorded instance of TRPA1 involvement in ocular (visual) behavioral responses, although it does not rule out the possibility of off target or compensatory effects. In addition, our data reveal that *Smed-TrpA* is required for extraocular responses specifically to near UV wavelengths. Light-initiated behavioral responses (whether ocular or extraocular) involve photon capturing and phototransduction of light information to the nervous system (signal input), as well as translation of that input into specific behaviors (signal output). The data presented here do not distinguish between a role for *Smed-TrpA* in actual phototransduction as opposed to a role in the signal output controlling behavior.

While our data does not exclude the possibility that *Smed-TrpA* is involved in converting photons into electrical signals (traditional phototransduction), alternate mechanisms have been proposed in both *Drosophila* larvae and human melanocytes. It has long been known that UV light exposure generates cellular ROS, including H_2O_2; and, there is now evidence linking UV light-induced H_2O_2 production and activation of TRPA1 channels (Hill and Schaefer, 2009; McCormick et al., 1976). *Drosophila* larvae are capable of extraocular photoreception of UV light using cells found along their body wall (Xiang et al., 2010). A subsequent study identified two *Drosophila* TRPA1 isoforms that are directly activated by UV-produced H_2O_2 (Guntur et al.,

2015). Similarly, it has been shown in humans that epidermal melanocytes detect UV light (resulting in melanin synthesis), where phototransduction appears to involve a G protein-coupled receptor cascade that activates downstream TRPA1 channels (Bellono et al., 2014). These data implicate TRPA1 in mediating light-induced responses downstream of light detection.

The results of our neutral density filter experiments show that there is an inverse relationship between light attenuation and extraocular behavioral responses to near UV light. We observed a steady decrease in tail thinning as light attenuation increased. We ruled out the possibility of contributions by either heat or differences in light intensity, suggesting that it is the light stimulus itself causing the behavioral responses. However, our data do not eliminate the possibility that the animals are responding to pain, or nociception. Given that UV light can cause detrimental biological effects and TRPA1 is known to respond to reactive electrophiles, including UV-induced H_2O_2, it is possible that planarian extraocular behavioral responses to near UV light could be due to nociception.

Sensitivity to UV light is common in the animal kingdom, with its function ranging from mate selection in birds to feeding behavior in fish (Cronin and Bok, 2016; Hunt et al., 2001a; Hunt et al., 2001b). It has also been suggested that in zooplankton, mainly crustaceans and some mollusks, avoidance of UV radiation is the driving force of diel vertical migrations (Gehring and Rosbash, 2003). A range of other invertebrates also display negative phototaxis to UV light, including *Daphnia*, *C. elegans*, *Drosophila* larvae, and planarians (Edwards et al., 2008; Paskin et al., 2014; Storz and Paul, 1998; Xiang et al., 2010). It is well known that UV light causes significant damage to nucleic acids and proteins (Sinha and Hader, 2002). In planarians, extended exposure to UV radiation also causes damage to their protective mucosal layer and

leads to visible wounds (Kalafatić et al., 2006). Therefore, in animals like planarians that have few natural defenses, avoidance of UV light might offer significant adaptive advantages.

In the current study, our results clearly demonstrate that planarians are indeed capable of extraocular photoreception. Conversely, a few studies have reported that they failed to observe extraocular behavioral responses in planarians (Arees, 1986; Azuma and Shinozawa, 1998), despite several accounts of planarian extraocular photoreception in the historical literature (Parker, 1900; Steven, 1963; Taliaferro, 1920). The discrepancy between our results (demonstrating extraocular responses) and those that reported a lack of extraocular responses could be due to several factors. First, these other studies used different planarian species, specifically in the genus *Dugesia*, whereas our study examined *Schmidtea mediterranea.* Therefore, the observed differences could be merely species-related. However, since *Schmidtea* and *Dugesia* are closely related, a more likely explanation would be differences in the light source(s) used. Our results show that extraocular photoreception is specific to near UV wavelengths and that planarians do not respond to longer wavelengths without eyes. These previous studies examining extraocular responses have used white light only, which is a combination of many different wavelengths, whose composition varies widely between light sources. Therefore, it is impossible to know the exact composition of wavelengths used from each study. Thus, the most likely explanation is that the white light source used in those early, historical experiments may have contained a greater percentage of UV wavelengths than the more recent studies.

Our data suggests that, similar to *Drosophila*, extraocular near UV light avoidance in planarians is mediated by TRPA1. This opsin-independent mechanism for extraocular photoresponses is intriguing because it suggests a separate evolutionary origin from opsin-based

phototransduction. Additionally, the fact that several other extraocular mechanisms seem to be sensitive to UV light, including cryptochromes and the *C. elegans* gustatory-related receptors (Bhatla and Horvitz, 2015; Chaves et al., 2011; Edwards et al., 2008; Haug et al., 2015), might reflect the evolution of early life in aquatic environments where short wavelengths penetrate water more substantially than long wavelengths (Gehring and Rosbash, 2003). However, a true understanding of the evolution of extraocular photoreception will require investigation into the mechanisms in many other species, both among different planarian species as well as in other invertebrates and vertebrates.

All data and figures presented in chapter IV were published in the *Journal of Experimental Biology* with the title, "The planarian TRPA1 homolog mediates extraocular behavioral responses to near ultraviolet light" (Birkholz and Beane, 2017).

CHAPTER V: CONSERVED MECHANISMS OF EYE REGENERATION

Introduction

Although the human eye has very limited regenerative ability, there are several animals that are capable of regenerating lost eye tissue. An important part of current research in regenerative medicine is to determine evolutionarily conserved signaling pathways required for regeneration. This can be difficult, however, since animals vary drastically in their regenerative capacity with many animals only capable of regenerating specific tissues. *Hydra* (Chera et al., 2009) and planarians (Beane et al., 2011) can regenerate their entire head while *C. elegans* have limited regenerative capabilities. Even among closely related species regenerative abilities can be variable. For example, newts (Kumar et al., 2007) and axolotls (Kragl et al., 2009) can regenerate complete limbs while adult frogs only regenerate a cartilaginous spike-like structure (Dent, 1962). For these reasons, uncovering conserved regenerative mechanisms between very diverse species, i.e. vertebrates and invertebrates, has been difficult. However, if we can identify a set of signals used during regeneration in two highly divergent species (i.e. invertebrate and vertebrate), it is more likely that these signals are evolutionarily conserved. It is important to understand the cellular and molecular dynamics involved during regeneration in a wide range of species because it is plausible that regeneration mechanisms were selected for early in evolution and may be conserved in higher animals, such as mammals. Any such identified pathways could be used to develop therapies for human regeneration.

The vertebrate eye is a highly complex structure and molecular studies have shown that many features of the eye are evolutionarily conserved. For example, there are two main

photoreceptor neuron types (rhabdomeric and ciliary) that both rely on opsins for phototransduction (Arendt, 2003). Eye development also involves several highly conserved genes such as *Pax-6* (Gehring and Ikeo, 1999), *Sin oculis* (Hanson, 2001), *Eyes absent* (Bonini et al., 1993), and *Otx* (Leuzinger et al., 1998). Additionally, individual eye tissues are known to be regenerative in different animals; lens regeneration occurs in salamanders (Henry and Tsonis, 2010) and zebrafish have the ability to regenerate retina (Brockerhoff and Fadool, 2011). However, historically only a few invertebrates, including the planarian (Deochand et al., 2016) and mystery snail (Bever and Borgens, 1988), were known to be able to regenerate all eye tissues. Recently, it has been discovered that the developing *Xenopus laevis* embryo is also capable of regenerating the entire eye (Kha et al., 2018). This makes the planarian and embryonic *Xenopus* excellent models for identifying underlying conserved mechanisms in eye regeneration.

Our preliminary data suggests that a common signaling pathway regulated by Vacuolar ATPases (V-ATPases) may be used during eye regeneration in both *Xenopus* embryos and adult planarians. V-ATPases are ATP driven proton pumps that have a highly conserved structure among all eukaryotic cells (Pamarthy et al., 2018). V-ATPase consists of multiple subunits that are arranged into two complexes: the peripheral V1 domain and the integral membrane domain V0 (Forgac, 2007). V-ATPases function to acidify vesicular, luminal, and extracellular environments and are therefore involved in numerous cellular functions (Holliday, 2014). Within the cell, V-ATPase is found on the surface of endosomes, where acidification is crucial for uncoupling of internalized ligand-receptor complexes as well as for the recycling of receptors back to the plasma membrane after signaling initiation (Maxfield and McGraw, 2004). In lysosomes and other degradative organelles, a low pH is required for enzymes to degrade

internalized macromolecules (Saftig and Klumperman, 2009). V-ATPases are also found on the plasma membrane where they are important for renal acidification, bone resorption, sperm maturation, and pH homeostasis (Pamarthy et al., 2018).

V-ATPases have been shown to play a role in a large number of biological contexts, including both regeneration and eye development. In zebrafish, V-ATPase plays a key role in regulating eye growth, neuronal survival and photoreceptor morphogenesis (Nuckels et al., 2009). V-ATPases also play an important role in the proper development of the ocular system in flies (Pyza et al., 2004). In regenerative models, V-ATPase activity has been shown to be required for adult zebrafish fin regeneration (Monteiro et al., 2014), as well as *Xenopus* tail regeneration (Adams et al., 2007).

In the current study, we used two divergent model organisms that both have the capacity to regrow the entire eye organ: embryonic *Xenopus* and adult planarians (Deochand et al., 2016; Kha et al., 2018). This allowed us to investigate conserved mechanisms of eye regeneration between vertebrates and invertebrates. We hypothesize that a conserved signaling pathway that involves V-ATPases, Notch, and apoptosis is required for eye regeneration in these two regenerative animal models.

Materials and Methods

Animals and Colony Care

An asexual strain of *Schmidtea mediterranea* was used and maintained as previously described (Paskin et al., 2014), with worm water comprised of 0.5 g/L of Instant Ocean salts

(Spectrum Brands, Blacksburg, VA, USA). Worms used were 5-7 mm in length and were starved at least one week prior to experimentation.

Microsurgeries

Worms were immobilized via chilling on a custom Peltier plate covered with a moist Kimwipe topped by white filter paper (Whatman #2). Using a scalpel, animals were cut just above and below the pharynx (for pharynx fragments) or midway between the head and tail (bisected). Removal of eyes was performed by scooping the eye out with the beveled tip of a 31-gauge insulin needle (5/16" in length), where the syringe was used as a handle. Following surgery, worms were placed into fresh worm water and allowed to regenerate at 20◦C in the dark.

Histology

Worms were fixed using Carnoy's, stored in EtOH at −20◦C, and processed as previously described (Stevenson and Beane, 2010). Worms were embedded in paraffin wax and cut into 7-μmsections with a microtome (Leitz 1512, Leica, Wetzlar, Germany). Slides were removed of wax and rehydrated with a series of washes in xylene and alcohol, respectively. Tissues were stained with hematoxylin and eosin (Fisher, Waltham, MA) and mounted with Permount (Fisher) following standard protocols.

RNAi and Pharmacology

For RNAi experiments, dsRNA was generated and injected as previously described (Beane et al., 2013). Whole worms were injected with dsRNA to H^+,K^+-ATPase on days 1-3 and scored at 8 weeks. Chemicals and working concentrations used include: 450 nM bafilomycin A1

(Cayman Chemical, Ann Arbor, MI), 50 nM concanamycin A (Cayman Chemical, Ann Arbor, MI), 200 µM LY411575 (Cayman Chemical, Ann Arbor, MI), 10 µM MG-132 (Sigma Aldrich, St. Louis, MO), 10 µM NS3694 (Sigma Aldrich, St. Louis, MO), and 1 µM ivermectin (Sigma I8898) was made and used as previously described (Beane et al., 2011). Worms were presoaked in 1 µM ivermectin for 3 days prior to decapitation when Ivermectin was refreshed and worms were scored on day 7. Stock solutions were made with dimethyl sulfoxide (DMSO; ATCC, Manassas, VA) and stored at -20°C. Working concentrations were made by diluting stock concentrations with worm water. DMSO concentration of working solutions did not exceed 10 µl/ml.

Regeneration Assay

Pharynx fragments or tail fragments (as described above) from *S. mediterranea* were placed in drug in 6-well untreated culture plates immediately after surgery. On any new treatment day, a control group was also included that were cut then exposed to the highest DMSO concentration of that day (never to exceed 10 µl/ml). Water was not changed during the course of treatment. Eye regeneration was examined and photographed after 7 days of drug exposure. Phenotypes observed included the following: wild-type (where animals were undistinguishable from untreated controls), complete loss of eye regeneration, eye regeneration that occurred in the pigment of old tissue instead of blastema, several tiny eyes that regenerated in the middle of the head (these eyes were much smaller than control eyes and formed a line in the middle of the head), and reduced or absent blastema (with minimal or no eye regeneration). All phenotypes described above (other than wild-type) were grouped together for analysis and considered to have "reduced eye regeneration." Additionally, a few DMSO control animals (3/98

total) as well as a few drug-treated animals (9/138 total treated) regenerated with additional pigment cells. However, there was not statistical significance in this phenotype, and therefore, these were not included in the analysis of our reduced eye regeneration phenotype.

Image Collection and Statistical Analysis

All images were collected using a Zeiss V20 fluorescent stereomicroscope with AxioCam MRc camera and Zen Lite software (Zeiss, Oberkochen, Germany). Adobe Photoshop was used to orient, scale, and improve clarity of images. Data were neither added nor subtracted; original images available upon request.

Significance was determined by the number of animals that had a "reduced eye regeneration phenotype" (described above). The percent of animals that had the described phenotype was calculated in each drug group and compared with the corresponding DMSO vehicle control group (group with same DMSO concentration as drug). A two sample *t*-test between percents was used to determine significance with the Statistics Calculator software (StatPac, V. 4.0, StatPac Inc., Northfield, MN, USA) with $p<0.05$ significant.

Results

Evidence for Conserved Eye Regeneration Mechanisms

It has recently been demonstrated that both developing *Xenopus* (Kha et al., 2018) and adult planarians (Deochand et al., 2016) are capable of directed eye repair following eye removal. We first wanted to confirm eye regeneration using our previously described eye

ablation technique where one eye was removed (red arrowheads, Fig. 21) while the other eye was left intact as an internal control (n≥15) (Deochand et al., 2016).

We found that our eye ablation assay successfully removed all eye tissues (red arrowheads, Fig. 21A2, 21B2). The regenerating eye appeared similar to the control eye at 14 days (yellow arrowhead, Fig. 21A3) and by day 28, the ablated and control eyes were nearly identical with regards to size and shape (Fig. 21A4, 21B3). In *Xenopus*, the ablated eye was similar to the intact control eye by 5 days after ablation (data not shown, personal communication Dr. Tseng, UNLV).

These results show that after eye ablation, *Xenopus* and planarians are both able to completely regenerate all eye tissues. Although the regeneration of individual eye tissue has been documented in other animals, the ability to regenerate the entire eye is very rare and, to our knowledge is limited to animals with eye talks, such as the mystery snail (Bever and Borgens, 1988), and planarians and *Xenopus*. Therefore, these two evolutionarily divergent animals are ideal for investigating conserved mechanisms of eye regeneration.

V-ATPase is Required for Eye Regeneration in Planarians

Our primary goal was to elucidate conserved mechanisms required for eye regeneration in both *Xenopus* and planarians. The proton pump, V-ATPase, has been shown to be involved in both eye development and regeneration (Adams et al., 2007; Monteiro et al., 2014; Nuckels et al., 2009; Pyza et al., 2004). Therefore, we decided to investigate V-ATPase as a potential conserved mechanism for eye regeneration. Following head amputation in planarians, V-ATPase activity was pharmacologically inhibited by exposing animals to either bafilomycin A1

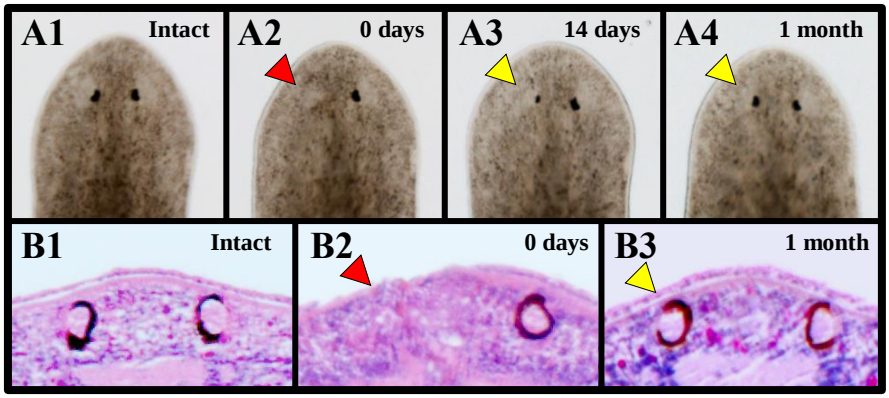

Figure 21. Characterization of Planarian Eye Regrowth Following Eye Ablation. (A-D) Planarian eyes were similar to control by 14 days. Eye tissues visualized with hematoxylin and eosin staining. n≥15 for each. Yellow arrowheads = regenerating eye. Red arrowheads = ablation site.

or concanamycin A and regeneration was examined 7 dpa.

Exposure to 50 nM concanamycin (Fig. 22A2) resulted in significantly disrupted eye regeneration in planarians, with treated animals having much smaller eyes that frequently regenerated within the pigment of the old tissue instead of the blastema. In addition, these animals regenerated with smaller blastemas than controls. The same phenotype was also observed using a different V-ATPase inhibitor, bafilomycin. Again, after 7 days of exposure to 450 nM bafilomycin, a significant number of animals regenerated with both smaller eyes and blastema (Fig. 22A3). Similar to planarians, inhibition of V-ATPase with concanamycin in *Xenopus* also impairs eye regeneration (data not shown, personal communication Dr. Tseng, UNLV). Together, this data suggests that V-ATPase is a conserved mechanism required for eye regeneration in both *Xenopus* and planarians.

Our data revealed that when V-ATPase is inhibited, eye regeneration is disrupted. One possibility for how V-ATPase affects eye regeneration could be through its regulation of membrane voltage. V-ATPase is a proton pump that on the plasma membrane functions to pump positive hydrogen ions out of the cell (Pamarthy et al., 2018). A net negative charge inside the cell leads to hyperpolarization, while depolarization results from a net positive charge. Therefore, it is possible that the role of V-ATPase during eye regeneration involves hyperpolarization. Membrane voltage has been shown to be required for eye induction during *Xenopus* embryogenesis, as modulation either inhibits eye formation (with depolarization) or produces ectopic eye formation (with hyperpolarization) (Pai et al., 2012). Therefore, we decided to examine the role of membrane voltage during eye regeneration.

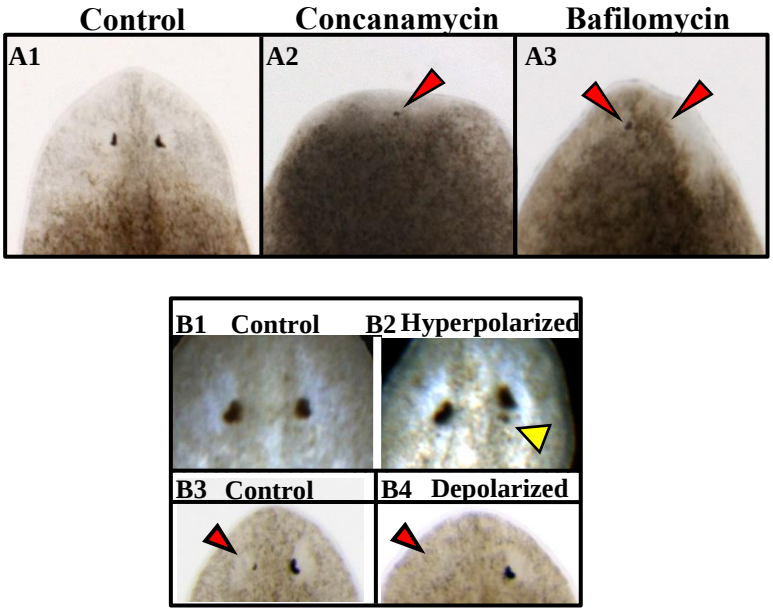

Figure 22. V-ATPase and Hyperpolarization Are Required for Eye Regeneration (A) Planarian eye regeneration was significantly impaired 7 dpa with V-ATPase inhibition using either 50 nM concanamycin A (n=15, $p<0.01$)(A2) or 450 nM bafilomycin A1 (n=30, $p<0.0001$)(A3) compared to DMSO vehicle controls ($n\geq19$ for each group)(A1). **(B)** Ectopic hyperpolarization with H^+,K^+-ATPase RNAi resulted in ectopic eye formation (B2). In contrast, depolarization (using 1 µM ivermectin) following eye ablation inhibited planarian eye regeneration (B4). Yellow arrowheads = ectopic eye growth. Red arrowheads = eye regrowth inhibition.

We found that similar to *Xenopus* embryogenesis, hyperpolarization via H^+,K^+-ATPase inhibition led to ectopic eye growth in planarians (Fig. 22B1, 22B2). Additionally, depolarization (via ivermectin treatment) inhibited eye regeneration (Fig. 22B3, 22B4). A similar phenotype is observed with hyperpolarization in *Xenopus* where overexpression of a voltage-gated sodium channel also results in ectopic eye growth (data not shown, personal communication Dr. Tseng, UNLV). These results are consistent with V-ATPase playing a hyperpolarizing role during eye regeneration since inhibition of V-ATPase led to a reduction of eye regeneration.

Notch is Required for Eye Regeneration

Another mechanism that has been shown to be involved in both the visual system and regeneration is the Notch signaling pathway. The Notch signaling pathway is a highly conserved cellular communication pathway that is involved in cell fate determination, differentiation, and patterning in a wide variety of developmental processes (Artavanis-Tsakonas et al., 1999). The Notch pathway is initiated when the extracellular region of the Notch receptor binds with Delta or Serrate/Jagged ligands on neighboring cells. Following binding, the receptor is cleaved for activation by γ-secretase, which generates the Notch intracellular domain (NICD) (Lai, 2004). The NICD then translocates into the nucleus to modify transcription of target genes (Kopan, 2002).

Notch signaling is important for eye development in several different animals. For example, Notch is required for the determination of glia cells in the retina of rodents and zebrafish (Furukawa et al., 2000; Scheer et al., 2001), regulating eye disc development in *Drosophila* (Cagan and Ready, 1989), and is also involved in cell fate specification in the developing *Xenopus* retina (Dorsky et al., 1995). It addition to the visual system, Notch has also

been shown to play a fundamental role during regeneration. Notch is required for blastema proliferation and differentiation during zebrafish fin regeneration (Münch et al., 2013), is required for retina regeneration in both goldfish (Sullivan et al., 1997) and newts (Kaneko et al., 2001), and also plays a role in hydra head regeneration (Münder et al., 2013).

Due to its function in eye development and regeneration, we next investigated the role of Notch in planarian eye regeneration. We found that Notch inhibition with 10 µM MG-132 caused 90% of the animals to regenerate with markedly reduced eyes and blastema size (Fig. 23A, 23B). Although this phenotype was similar to V-ATPase inhibition, in contrast, the eyes typically regenerated in the blastema instead of in the old tissue as was observed with V-ATPase inhibition (Fig. 22A3). Additionally, we found that when Notch was inhibited using a different drug, 200 µM LY411575, there was also a significant number of worms with reduced eye regeneration (Fig. 23C). However, the phenotype with LY411575 exposed animals was slightly different than previously observed phenotypes. The eyes that regenerated were considerably smaller than control and several of these tiny eyes regenerated in the middle of the head in the shape of a line. Also, the blastema appeared slightly larger than with other drug treatments. These results are likely due to differences in the mechanism of Notch inhibition between the drugs.

Similar to planarians, it has also been found that Notch inhibition disrupted eye regeneration in *Xenopus*. When *Xenopus* were exposed to MG-132 following eye ablation, there was significant reduction of eye regrowth (data not shown, personal communication Dr. Tseng, UNLV). Together, these results suggest that Notch is a conserved signaling pathway required for eye regeneration in both *Xenopus* and planarians.

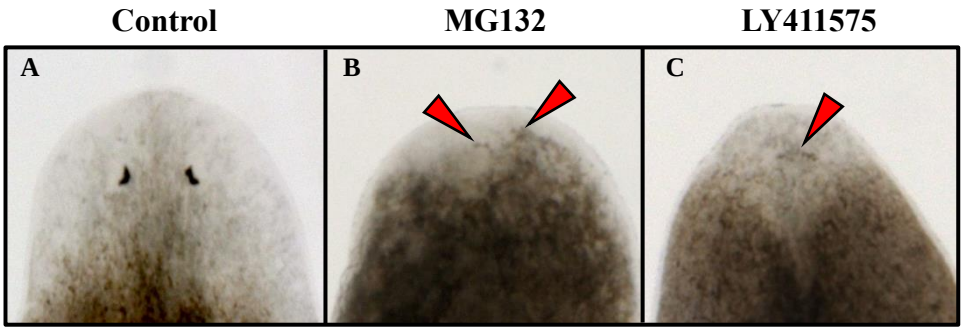

Figure 23. Notch is Required for Eye Regeneration. (A-C) Seven days following decapitation, planarian eye regeneration was impaired when Notch was inhibited with 10 μM MG-132 ($n=20$, $p<0.0001$) or 200 μM LY411575 ($n=20$, $p<0.01$) (DMSO control, $n=20$ per drug). Red arrowhead = eye growth with inhibitor treatment.

Apoptosis is Required for Eye Regeneration

Although it may seem counterintuitive, apoptosis, or programmed cell death, also plays a critical role in many regenerative contexts. Apoptosis is driven by a family of cysteine proteases, called caspases, that can cleave cellular substrates and ultimately leads to the death of the cell (Elmore, 2007). Regeneration of damaged or lost tissue often requires compensatory proliferation within surviving tissue and multiple studies have shown that the initiation of apoptosis commonly drives this increase in mitotic activity (Fogarty and Bergmann, 2017). Apoptosis-induced proliferation is required for both tail and eye regeneration in *Xenopus* (Kha et al., 2018; Tseng et al., 2007), *Hydra* head regeneration (Chera et al., 2009), and also plays a role in wound healing and liver regeneration in mice (Li et al., 2010).

During planarian regeneration, there are two main waves of apoptosis. The first apoptotic peak is part of the generic wound response and does not appear to regulate proliferation (González-Estévez and Saló, 2010; Pellettieri et al., 2010). However, the second apoptotic wave that occurs 3 days post amputation is required for apoptosis-induced proliferation and regeneration (Beane et al., 2013).

Previous studies have already shown that apoptosis is required for eye regeneration in *Xenopus* (Kha et al., 2018). Therefore, we examined the role of apoptosis in planarian eye regeneration. We found that when apoptosis was pharmacologically inhibited with 10 µM NS3694 for 7 days following amputation, planarians regenerated with a phenotype similar to what was observed with V-ATPase and Notch inhibition where both eyes and blastema regenerated much smaller than control (Fig. 24A). Furthermore, we also saw that like V-ATPase inhibition, several of the eyes regenerated in the old tissue instead of within the regenerating blastema. These results suggest that, like *Xenopus*, planarian eye regeneration requires apoptosis.

A Apoptosis Inhibited

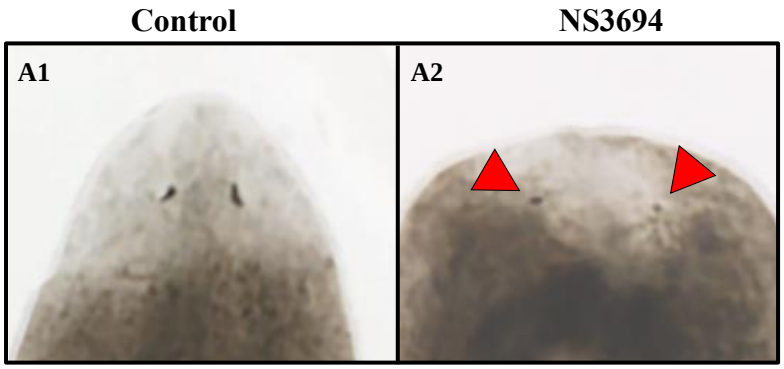

B Proposed Pathway

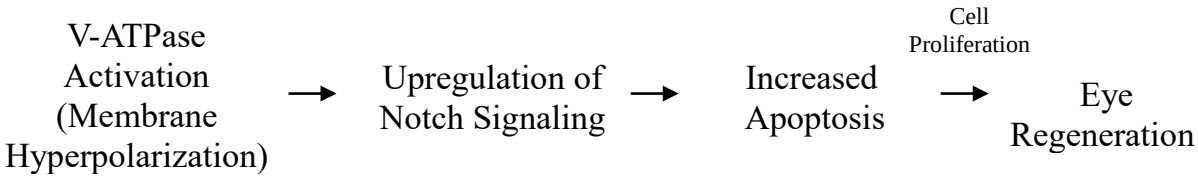

Figure 24. Apoptosis, Notch, and V-ATPase are Required for Proposed Eye Regeneration Signaling Pathway (A) Planarian eye regeneration is reduced at 7 days when apoptosis is inhibited with 10 μM NS3694 (n=49) (DMSO control, n=19). $P < 0.05$. Red arrowhead = eye growth with inhibitor treatment. **(B)** Proposed signaling pathway required for eye regeneration in both planarian and *Xenopus*.

Discussion

The results from this study confirm our previous work showing that adult planarians (Deochand et al., 2016) and *Xenopus* embryos (Kha et al., 2018) are capable of eye regeneration. Targeted removal of the eye in planarians results in complete eye repair after 14 days (Fig. 21). Furthermore, we identified several mechanisms that were required for eye regeneration, including the ion channel, V-ATPase (Fig. 22), Notch (Fig. 23), and apoptosis (Fig. 24A).

Our results suggest that V-ATPase, Notch, and apoptosis are conserved mechanisms of eye regeneration since pharmacological inhibition of each inhibits eye regeneration in both planarians and *Xenopus* (data not shown, personal communication Dr. Tseng, UNLV). Furthermore, the current body of literature indicates a relationship exists between these mechanisms. Based on this information, we propose the following cell signaling pathway is involved in eye regeneration: eye removal activates V-ATPase ion channels (and subsequent hyperpolarization of tissue), which causes Notch upregulation. Notch then signals an increase in apoptosis that leads to apoptosis-induced proliferation of cells needed for eye regeneration (Fig. 24B).

Although further experiments will be needed to confirm the epistatic relationship between V-ATPase, Notch, and apoptosis during eye regeneration, there is already evidence that V-ATPase activity is upstream of Notch. V-ATPases have a known role in regulating signaling pathways, especially in pathways that depend on the endolysosomal route, like the Notch signaling pathway (Le Borgne, 2006). Following ligand binding, the Notch receptor is taken into the cell via endocytosis and studies have shown that V-ATPases are needed to produce an acidic environment for γ-secretase activity and Notch cleavage (Vaccari et al., 2010; Yan et al., 2009).

Additionally, V-ATPases are required for Notch receptor degradation in lysosomes (Baron, 2012).

Examples for the requirement of V-ATPase in Notch signaling have been reported in *Drosophila* eye discs (Yan et al., 2009), the developing mouse cortex (Lange et al., 2011), and astrocytes found in the optic nerve in rats (Valapala et al., 2013). V-ATPase has also been shown to play a role upstream of apoptosis. In fact, V-ATPase inhibitors have been a target in cancer research for many years due to their known role in apoptosis and tumor reduction (Izumi et al., 2003). This evidence is consistent with our proposed V-ATPase signaling pathway where V-ATPase is required for upregulation of Notch and subsequent increased apoptosis.

We further hypothesize that Notch is acting upstream of apoptosis during planarian and *Xenopus* eye regeneration based on current research implicating Notch in regulating apoptotic cell death in the eyes and nervous system of other animals. For example, in the developing retinas of both *Drosophila* (Miller and Cagan, 1998) and zebrafish (Scheer et al., 2001), Notch activation promotes apoptosis. Similarly, inhibition of Notch during mouse development results in reduced apoptosis of early neural progenitor cells (Yang et al., 2004). Together, these studies support a hypothetical signaling pathway where V-ATPase activates the Notch pathway, which in turn signals apoptosis and cell proliferation.

One of the most important issues in regenerative medicine is finding conserved mechanisms of regeneration in many different animals with the ultimate goal being able to understand these processes so that they can be applied to human health matters. Historically, studies tend to compare regenerative mechanisms between two closely related species. In contrast, we hypothesize that identifying conserved mechanisms between extremely different organisms (a vertebrate and an invertebrate) is more likely to identify mechanisms that will

translate into a wider range of species. Understanding ancestral processes involved in directed eye repair could ultimately assist in developing treatments to stimulate eye regeneration in humans with degenerative eye disease or severe eye injuries.

CHAPTER VI: GENERAL DISCUSSION AND FUTURE DIRECTIONS

Summary of Results

The eyes are sensitive organs that are highly susceptible to traumatic injury. In the United States, 2.4 million ocular injuries occur every year, making traumatic eye injury the leading cause of unilateral blindness (McGwin and Owsley, 2005; Scruggs et al., 2012). Understanding the mechanisms that are required for eye regeneration is critical if we want to promote eye regeneration in non-regenerative species, like mammals.

Although some vertebrates can regenerate individual eye tissues (Brockerhoff and Fadool, 2011; Henry and Tsonis, 2010), the ability to regenerate the entire eye organ is limited to only a few animal models, including planarians. Planarians make excellent models for studying eye regeneration for many reasons. In addition to their regenerative abilities, planarians share many of the same eye developmental genes as vertebrates (Lapan and Reddien, 2012), they are small and relatively easy to care for in the lab, and some species such as *S. mediterranea* have a completely sequenced genome (Robb et al., 2015). Although much work has been done in determining the genes that are involved in planarian eye regeneration, there was still some critical foundational knowledge that was lacking regarding the planarian visual system. The purpose of this work was to increase our understanding of the basic properties of the planarian visual system, as well as develop some essential tools that were needed to effectively study eye regeneration in planarians.

A major problem in previous eye regeneration studies was the use of white light to determine functional recovery of the eyes. White light consists of many different wavelengths

and these studies did not take into consideration that different wavelengths could affect behaviors. Therefore, in our work from chapter III, we developed an easily reproducible behavioral assay and found that planarians do possess differential behavioral responses to different wavelengths of light, including UV and IR. Furthermore, we found that these behaviors have an inverse relationship with wavelength where the shortest wavelengths (UV) caused the most intense photophobic responses while the longest wavelengths resulted in no response (red) or even an opposite photophilic response (IR). These results demonstrate the importance of spectral composition on planarian behavior and suggest that the previous use of white light in regeneration studies may be masking complex behaviors or even confounding results.

Another fundamental characteristic of the planarian visual system that was never taken into consideration in regeneration assays was their ability to respond to light using mechanisms outside of the eye, or extraocular photoreception. This might be partly due to the fact that historical studies show conflicting evidence for planarian extraocular photoreception. While early studies found that eyeless planarians are negatively phototactic (Parker, 1900; Steven, 1963; Taliaferro, 1920), more recent studies failed to observe behavioral responses to white light following eye removal (Arees, 1986; Azuma and Shinozawa, 1998). We found that similar to leeches (Jellies, 2014a), *Drosophila* (Xiang et al., 2010), and *C. elegans* (Edwards et al., 2008), planarians do respond to UV wavelengths using mechanisms outside of the eye. Furthermore, we found that these extraocular responses are mediated in part by the TRPA1 ion channel. The results of this study might help to explain the contradictory results from older studies as the white light composition in some experiments, but not others, may have extended into the UV range. In future studies, we can now make sure this is taken into account so that dermal responses can be excluded when testing for functional eye recovery during regeneration.

The ultimate goal of our work was to look at mechanisms involved in regenerating eyes *in situ*. Although we know a lot about the genes involved in stem cell differentiation during eye regeneration (Lapan and Reddien, 2012), this alone does not explain all the important details involved in the complex process of regeneration. For example, following decapitation how do planarians know to regenerate two eyes in the correct location? This relatively new field, called regenerative morphology, describes how an animal reestablishes overall shape during regeneration. Regenerative morphology is completely distinct from the signaling pathways that are more commonly studied but is just as important to consider when examining how regeneration is established.

Although it may not seem immediately apparent, regenerative morphology is critical for planarian eye regeneration. Following decapitation, the eyes have to regenerate completely *de novo*. This means that the animal must decide which specific tissue to regenerate (eyes and brain, not tail or pharynx), produce the correct number of new cells, position the new eyes in the correct location, make sure the eyes are the correct shape and are scaled to the appropriate size, and know when to stop regenerating. If the eyes do not regenerate with the correct shape or number of cells, this could disrupt their ability to detect the direction of incoming light, which is critical for an animal with very few defenses.

Our data suggests that one of the mechanisms that planarians might use to regenerate eyes in the correct location is V-ATPase and hyperpolarization. Our results showed that when V-ATPase is inhibited, (most likely causing depolarization), eye regeneration is disrupted and eyes do not regenerate in the correct location. These data suggest that just understanding the genes involved in stem cell differentiation is not sufficient for understanding all of eye regeneration and it is critical to also consider regenerative morphology and how these mechanisms interact.

Future Directions

Electrophysiological Recordings

In chapter III, we found that planarians display differential behavioral responses to different wavelengths of light, including UV and IR. However, our data did not provide direct evidence that photophobic responses were a result of the activation of a phototransduction cascade within the eye. Therefore, it would be interesting to take electrophysiological recordings during exposure to different wavelengths, in particular UV and IR, to determine if the behavioral responses we observed were actually from the detection of photons of light or from a secondary variable that the light produced (i.e. heat or ROS)). Our results show that planarians are intensely photophobic to UV wavelengths and can also respond to UV using mechanisms outside of the eye. Therefore, it is possible that all negative phototactic behavior observed to UV light was a result of extraocular mechanisms. Examination of action potentials produced within the eye during UV light exposure would show us if the planarian eye has opsins capable of detecting UV wavelengths.

Electrophysiological recordings would also be useful for examining how the planarian eye responds to IR wavelengths. We found that planarians actually preferred IR light to dim background lighting but, again, we do not know if this was actually due to light detection or another mechanism. For example, the control background lighting was not completely dark, and it is possible that IR wavelengths could function to reduce opsin activation, making the IR light appear darker. Another possibility is that the IR energy could be producing a small amount of

heat that the animals might prefer. This could also be tested by developing an assay to examine temperature preference.

Wavelength and Eye Regeneration

Since we know that planarians display different behavioral responses to individual wavelengths, it might also be interesting to examine if eye regeneration is also affected by different wavelengths. This would be a relatively easy experiment where we would either decapitate or remove only eye tissue then place animals under a specific wavelength. After 1-2 weeks we could examine eye regeneration both morphologically and functionally (to see if wavelength-specific responses are affected). It is possible that, similar to our behavioral results, regenerative capacity when exposed to different wavelengths could occur in a hierarchy and be correlated with wavelength (highly regenerative under IR light and inhibited under UV light). IR wavelengths have been shown to increase stem cell proliferation during planarian regeneration (Wu and Persinger, 2011). It seems as though under stressful conditions, like UV light exposure, proliferation and eye regeneration could very well be compromised.

TRPA1 Activation by H_2O_2 and ROS

Our results from chapter IV show that planarians behaviorally respond to UV light using extraocular photoreception and this response is mediated in part by the ion channel TRPA1. Although it has been known for some time that UV light generates cellular ROS (including H_2O_2), it has also been demonstrated that in *Drosophila*, UV light-induced H_2O_2 production activates TRPA1 channels (Guntur et al., 2015). Furthermore, a recent study in planarians found that the activation of *Smed-TrpA* (planarian homologue of TRPA1) is mediated by H_2O_2 and

ROS (Arenas et al., 2017). I think it would be interesting to expand on these results by directly exposing planarians to a concentrated stream of H_2O_2 to see if they react with a similar behavioral response as UV light exposure (tail thinning). We could also use a general oxidative stress indicator dye, 5-(and-6) chloromethyl-2',7'- dicholorodihydrofluorescein diacetate, to examine ROS production during UV light exposure. Additionally, it might also be possible to pharmacologically inhibit ROS using the drug diphenyleneiodonium chloride (DPI) then examine if this reduces extraocular responses to UV light in a similar manner as *Smed-TrpA* RNAi.

Role of V-ATPase, Notch, and Apoptosis During Eye Regeneration

The results of our data show that V-ATPase, Notch, and apoptosis are mechanisms that are required for regeneration and correct morphology during eye regeneration in planarians. I think an important next step would be to confirm the roles of V-ATPase and Notch during eye regeneration by inhibiting each with RNAi to provide us with an alternative mechanism of inhibition. Therefore, if RNAi produces the same eye phenotype as we observed in chapter V during regeneration, we can be confident that pharmacological inhibition did not cause any secondary cytotoxic effects.

Another future direction to confirm the roles of V-ATPase, Notch, and apoptosis during eye regeneration will be to determine innervation and visualize photoreceptor cells using anti-arrestin staining. This will be important because our current results are limited to overall morphology and since we can only directly observe pigment cells, we do not know how the regeneration of photoreceptor neurons are affected by pathway inhibition.

V-ATPase Signaling Pathway

Although our current data suggests a role for V-ATPase, Notch, and apoptosis individually, additional experiments will be needed to determine the epistatic relationship between them. Following planarian decapitation, each mechanism will be inhibited individually (V-ATPase, Notch, and apoptosis), then we will examine if the other pathway components are present with *in situ* hybridization. For example, if our hypothesis is correct that V-ATPase is upstream of Notch, which is upstream of apoptosis, then inhibiting Notch should not affect V-ATPase expression, but will cause a decrease in apoptosis (determined by caspase staining) compared to expression levels in regenerating controls.

Eye Regeneration and Hyperpolarization

Finally, we would like to further investigate the role of membrane voltage during eye regeneration using a voltage-sensitive dye called $DiBAC_4(3)$. The dye consists of negatively charged molecules that enter and bind to a positively charged membrane in depolarized cells. When the membrane is negative, or hyperpolarized, the molecules leave the cell and are no longer fluorescent (Adams and Levin, 2013). This will allow us to track the **relative** membrane voltage in control animals and during regeneration. Our data suggests that membrane hyperpolarization is needed for eye regeneration and the proton pump V-ATPase may be required for hyperpolarizing cells. To confirm this, we will examine eye regeneration and membrane voltage using $DiBAC_4(3)$ when V-ATPase is inhibited and compare this to the membrane voltage during eye regeneration in control animals (not V-ATPase inhibited).

REFERENCES

Adams, D.S., Levin, M., 2013. Endogenous voltage gradients as mediators of cell-cell communication: strategies for investigating bioelectrical signals during pattern formation. Cell and Tissue Research 352, 95-122.

Adams, D.S., Masi, A., Levin, M., 2007. H+ pump-dependent changes in membrane voltage are an early mechanism necessary and sufficient to induce *Xenopus* tail regeneration. Development 134, 1323-1335.

Adams, D.S., Robinson, K.R., Fukumoto, T., Yuan, S., Albertson, R.C., Yelick, P., Kuo, L., McSweeney, M., Levin, M., 2006. Early, H+-V-ATPase-dependent proton flux is necessary for consistent left-right patterning of non-mammalian vertebrates. Development 133, 1657-1671.

Adell, T., Cebrià, F., Saló, E., 2010. Gradients in planarian regeneration and homeostasis. Cold Spring Harb Perspect Biol 2, a000505.

Adell, T., Saló, E., Boutros, M., Bartscherer, K., 2009. Smed-Evi/Wntless is required for beta-catenin-dependent and -independent processes during planarian regeneration. Development 136, 905-910.

Adler, C.E., Sánchez Alvarado, A., 2015. Types or States? Cellular Dynamics and Regenerative Potential. Trends Cell Biol 25, 687-696.

Adler, K., Taylor, D.H., 1973. Extraocular Perception of Polarized-Light by Orienting Salamanders. J Comp Physiol 87, 203-212.

Agata, K., Soejima, Y., Kato, K., Kobayashi, C., Umesono, Y., Watanabe, K., 1998. Structure of the planarian central nervous system (CNS) revealed by neuronal cell markers. Zoolog Sci 15, 433-440.

Aksoy, V., Camlitepe, Y., 2012. Behavioural analysis of chromatic and achromatic vision in the ant Formica cunicularia (Hymenoptera: Formicidae). Vision research 67, 28-36.

Almuedo-Castillo, M., Crespo-Yanez, X., Seebeck, F., Bartscherer, K., Salò, E., Adell, T., 2014. JNK controls the onset of mitosis in planarian stem cells and triggers apoptotic cell death required for regeneration and remodeling. PLoS genetics 10, e1004400.

Arees, E.A., 1986. Absence of light response in eyeless planaria. Physiology & behavior 36, 445-449.

Arenas, O.M., Zaharieva, E.E., Para, A., Vásquez-Doorman, C., Petersen, C.P., Gallio, M., 2017. Activation of planarian TRPA1 by reactive oxygen species reveals a conserved mechanism for animal nociception. Nature neuroscience 20, 1686-1693.

Arendt, D., 2003. Evolution of eyes and photoreceptor cell types. The International journal of developmental biology 47, 563-571.

Artavanis-Tsakonas, S., Rand, M.D., Lake, R.J., 1999. Notch signaling: cell fate control and signal integration in development. Science (New York, N.Y.) 284, 770-776.

Asano, Y., Nakamura, S., Ishida, S., Azuma, K., Shinozawa, T., 1998. Rhodopsin-like proteins in planarian eye and auricle: detection and functional analysis. The Journal of experimental biology 201 (Pt 9), 1263-1271.

Azuma, K., Shinozawa, T., 1998. Rhodopsin-like proteins in planarian eye and auricle: detection and functional analysis. The Journal of experimental biology 201 (Pt 9), 1263-1271.

Baguñá, J., Romero, R., 1981. Quantitative analysis of cell types during growth, degrowth and regeneration in the planarians Dugesia mediterranea and Dugesia tigrina. Hydrobiologia 84, 181-194.

Baguñà, J., Saló, E., Auladell, C., 1989. Regeneration and pattern formation in planarians. III. Evidence that neoblasts are totipotent stem cells and the source of blastema cells. Development 107, 77-86.

Baguñà, J., Saló, E., Romero, R., Garcia-Fernàndez, J., Bueno, D., Muñoz-Marmol, A.M., Bayascas-Ramirez, J.R., Casali, A., 1994. Regeneration and pattern formation in planarians: cells, molecules and genes. Zoological Science 11, 781-795.

Barghouth, P.G., Thiruvalluvan, M., Oviedo, N.J., 2015. Bioelectrical regulation of cell cycle and the planarian model system. Biochimica et Biophysica Acta (BBA) - Biomembranes 1848, 2629-2637.

Baron, M., 2012. Endocytic routes to Notch activation. Seminars in cell & developmental biology 23, 437-442.

Bautista, D.M., Pellegrino, M., Tsunozaki, M., 2013. TRPA1: A gatekeeper for inflammation. Annual review of physiology 75, 181-200.

Bazalova, O., Kvicalova, M., Valkova, T., Slaby, P., Bartos, P., Netusil, R., Tomanova, K., Braeunig, P., Lee, H.J., Sauman, I., Damulewicz, M., Provaznik, J., Pokorny, R., Dolezel, D., Vacha, M., 2016. Cryptochrome 2 mediates directional magnetoreception in cockroaches. Proceedings of the National Academy of Sciences of the United States of America 113, 1660-1665.

Beane, W.S., Morokuma, J., Adams, D.S., Levin, M., 2011. A Chemical Genetics Approach Reveals H,K-ATPase-Mediated Membrane Voltage Is Required for Planarian Head Regeneration. Chemistry & Biology 18, 77-89.

Beane, W.S., Morokuma, J., Lemire, J.M., Levin, M., 2013. Bioelectric signaling regulates head and organ size during planarian regeneration. Development 140, 313-322.

Beane, W.S., Tseng, A.S., Morokuma, J., Lemire, J.M., Levin, M., 2012. Inhibition of planar cell polarity extends neural growth during regeneration, homeostasis, and development. Stem Cells Dev 21, 2085-2094.

Bellono, N.W., Najera, J.A., Oancea, E., 2014. UV light activates a Galphaq/11-coupled phototransduction pathway in human melanocytes. The Journal of general physiology 143, 203-214.

Bergmann, A., Steller, H., 2010. Apoptosis, stem cells, and tissue regeneration. Science signaling 3, 1-16.

Bessac, B.F., Jordt, S.E., 2008. Breathtaking TRP channels: TRPA1 and TRPV1 in airway chemosensation and reflex control. Physiology (Bethesda, Md.) 23, 360-370.

Bever, M.M., Borgens, R.B., 1988. Eye regeneration in the mystery snail. J Exp Zool 245, 33-42.

Bhatla, N., Horvitz, H.R., 2015. Light and hydrogen peroxide inhibit C. elegans Feeding through gustatory receptor orthologs and pharyngeal neurons. Neuron 85, 804-818.

Birkholz, T.R., Beane, W.S., 2017. The planarian TRPA1 homolog mediates extraocular behavioral responses to near-ultraviolet light. The Journal of experimental biology 220, 2616-2625.

Birkholz, T.R., Van Huizen, A.V., Beane, W.S., 2018. Staying in shape: Planarians as a model for understanding regenerative morphology. Seminars in cell & developmental biology.

Blackiston, D.J., McLaughlin, K.A., Levin, M., 2009. Bioelectric controls of cell proliferation: ion channels, membrane voltage and the cell cycle. Cell Cycle 8, 3527-3536.

Blassberg, R.A., Felix, D.A., Tejada-Romero, B., Aboobaker, A.A., 2013. PBX/extradenticle is required to re-establish axial structures and polarity during planarian regeneration. Development 140, 730-739.

Bonini, N.M., Leiserson, W.M., Benzer, S., 1993. The eyes absent gene: Genetic control of cell survival and differentiation in the developing Drosophila eye. Cell 72, 379-395.

Bowmaker, J.K., 1995. The visual pigments of fish. Progress in retinal and eye research 15, 1-31.

Briscoe, A.D., Chittka, L., 2001. The evolution of color vision in insects. Annual review of entomology 46, 471-510.

Brockerhoff, S.E., Fadool, J.M., 2011. Genetics of photoreceptor degeneration and regeneration in zebrafish. Cellular and molecular life sciences : CMLS 68, 651-659.

Brown, H.M., Ito, H., Ogden, T.E., 1968. Spectral sensitivity of the planarian ocellus. The Journal of general physiology 51, 255-260.

Cagan, R.L., Ready, D.F., 1989. Notch is required for successive cell decisions in the developing Drosophila retina. Genes Dev 3, 1099-1112.

Campbell, A.L., Naik, R.R., Sowards, L., Stone, M.O., 2002. Biological infrared imaging and sensing. Micron (Oxford, England : 1993) 33, 211-225.

Carpenter, K.S., Morita, M., Best, J.B., 1974. Ultrastructure of the photoreceptor of the planarian Dugesia dorotocephala. I. Normal eye. Cell Tissue Res 148, 143-158.

Cebrià, F., 2016. Planarian Body-Wall Muscle: Regeneration and Function beyond a Simple Skeletal Support. Front Cell Dev Biol 4, 8.

Cebrià, F., Guo, T., Jopek, J., Newmark, P.A., 2007. Regeneration and maitenance of the planarian midline is regulated by a slit orthologue. Developmental biology 307, 394-406.

Cebrià, F., Kobayashi, C., Umesono, Y., Nakazawa, M., Mineta, K., Ikeo, K., Gojobori, T., Itoh, M., Taira, M., Sánchez Alvarado, A., Agata, K., 2002. FGFR-related gene nou-darake restricts brain tissues to the head region of planarians. Nature 419, 620-624.

Chan, J.D., Agbedanu, P.N., Zamanian, M., Gruba, S.M., Haynes, C.L., Day, T.A., Marchant, J.S., 2014. 'Death and axes': unexpected Ca(2)(+) entry phenologs predict new anti-schistosomal agents. PLoS Pathog 10, e1003942.

Chan, J.D., Zhang, D., Liu, X., Zarowiecki, M., Berriman, M., Marchant, J.S., 2017. Utilizing the planarian voltage-gated ion channel transcriptome to resolve a role for a Ca(2+) channel in neuromuscular function and regeneration. Biochim Biophys Acta 1864, 1036-1045.

Chaves, I., Pokorny, R., Byrdin, M., Hoang, N., Ritz, T., Brettel, K., Essen, L.O., van der Horst, G.T., Batschauer, A., Ahmad, M., 2011. The cryptochromes: blue light photoreceptors in plants and animals. Annual review of plant biology 62, 335-364.

Chen, C.C., Wang, I.E., Reddien, P.W., 2013. pbx is required for pole and eye regeneration in planarians. Development 140, 719-729.

Chera, S., Ghila, L., Dobretz, K., Wenger, Y., Bauer, C., Buzgariu, W., Martinou, J.-C., Galliot, B., 2009. Apoptotic Cells Provide an Unexpected Source of Wnt3 Signaling to Drive Hydra Head Regeneration. Developmental Cell 17, 279-289.

Child, C.M., 1911. Studies on the dynamics of morphogenesis and inheritance in experimental reproduction. II. Physiological dominance of anterior over posterior regions in the regulation of Planaria dorotocephala. Journal of Experimental Zoology 11, 187-220.

Chong, T., Stary, J.M., Wang, Y., Newmark, P.A., 2011. Molecular markers to characterize the hermaphroditic reproductive system of the planarian Schmidtea mediterranea. BMC Developmental Biology 11, 69.

Conlon, I., Raff, M., 1999. Size Control in Animal Development. Cell 96, 235-244.

Cronin, T.W., Bok, M.J., 2016. Photoreception and vision in the ultraviolet. The Journal of experimental biology 219, 2790-2801.

Cronin, T.W., Johnsen, S., 2016. Extraocular, Non-Visual, and Simple Photoreceptors: An Introduction to the Symposium. Integrative and comparative biology 56, 758-763.

Currie, K.W., Pearson, B.J., 2013. Transcription factors lhx1/5-1 and pitx are required for the maintenance and regeneration of serotonergic neurons in planarians. Development 140, 3577-3588.

Cutie, S., Hoang, A.T., Payumo, A.Y., Huang, G.N., 2017. Unconventional Functions of Muscles in Planarian Regeneration. Dev Cell 43, 657-658.

Dalyell, J.G.S., 1814. Observations on some interesting phenomena in animal physiology, exhibited by several species of Planariae : illustrated by coloured figures of living animals / by John Graham Dalyell. Archibald Constable, Edinburgh :.

Dasheiff, B.D., Dasheiff, R.M., 2002. Photonegative response in brown planaria (Dugesia tigrina) following regeneration. Ecotoxicology and environmental safety 53, 196-199.

Davidson, C., Prados, J., Gibson, C.L., Young, A.M., Barnes, D., Sherlock, R., Hutchinson, C.V., 2011. Shedding light on photosensitive behaviour in brown planaria (Dugesia Tigrina). Perception 40, 743-746.

de Souza, S.C., Munin, E., Alves, L.P., Salgado, M.A., Pacheco, M.T., 2005. Low power laser radiation at 685 nm stimulates stem-cell proliferation rate in Dugesia tigrina during regeneration. Journal of photochemistry and photobiology. B, Biology 80, 203-207.

Delroisse, J., Ullrich-Luter, E., Ortega-Martinez, O., Dupont, S., Arnone, M.I., Mallefet, J., Flammang, P., 2014. High opsin diversity in a non-visual infaunal brittle star. BMC genomics 15, 1035.

Dent, J.N., 1962. Limb regeneration in larvae and metamorphosing individuals of the South African clawed toad. Journal of Morphology 110, 61-77.

Deochand, M.E., Birkholz, T.R., Beane, W.S., 2016. Temporal regulation of planarian eye regeneration. Regeneration (Oxford, England) 3, 209-221.

Dhanasekaran, D.N., Reddy, E.P., 2017. JNK-signaling: A multiplexing hub in programmed cell death. Genes & Cancer 8, 682-694.

Dorsky, R.I., Rapaport, D.H., Harris, W.A., 1995. Xotch inhibits cell differentiation in the Xenopus retina. Neuron 14, 487-496.

Durant, F., Lobo, D., Hammelman, J., Levin, M., 2016. Physiological controls of large-scale patterning in planarian regeneration: a molecular and computational perspective on growth and form. Regeneration (Oxford, England) 3, 78-102.

Edwards, S.L., Charlie, N.K., Milfort, M.C., Brown, B.S., Gravlin, C.N., Knecht, J.E., Miller, K.G., 2008. A novel molecular solution for ultraviolet light detection in Caenorhabditis elegans. PLoS biology 6, e198.

Eisenhoffer, G.T., Kang, H., Sánchez Alvarado, A., 2008. Molecular analysis of stem cells and their descendants during cell turnover and regeneration in the planarian Schmidtea mediterranea. Cell stem cell 3, 327-339.

Elliott, S.A., Sánchez Alvarado, A., 2013. The history and enduring contributions of planarians to the study of animal regeneration. Wiley Interdiscip Rev Dev Biol 2, 301-326.

Elmore, S., 2007. Apoptosis: A review of programmed cell death. Toxicol Pathol 35, 495-516.

Emmons-Bell, M., Durant, F., Hammelman, J., Bessonov, N., Volpert, V., Morokuma, J., Pinet, K., Adams, D.S., Pietak, A., Lobo, D., Levin, M., 2015. Gap Junctional Blockade Stochastically Induces Different Species-Specific Head Anatomies in Genetically Wild-Type Girardia dorotocephala Flatworms. Int J Mol Sci 16, 27865-27896.

Felix, D.A., Aboobaker, A.A., 2010. The TALE class homeobox gene Smed-prep defines the anterior compartment for head regeneration. PLoS genetics 6, e1000915.

Ferreira, F., Luxardi, G., Reid, B., Zhao, M., 2016. Early bioelectric activities mediate redox-modulated regeneration. Development (Cambridge, England) 143, 4582-4594.

Feuda, R., Hamilton, S.C., McInerney, J.O., Pisani, D., 2012. Metazoan opsin evolution reveals a simple route to animal vision. Proceedings of the National Academy of Sciences of the United States of America 109, 18868-18872.

Fogarty, C.E., Bergmann, A., 2017. Killers creating new life: caspases drive apoptosis-induced proliferation in tissue repair and disease. Cell death and differentiation 24, 1390-1400.

Forgac, M., 2007. Vacuolar ATPases: rotary proton pumps in physiology and pathophysiology. Nature Reviews Molecular Cell Biology 8, 917.

Forsthoefel, D.J., Park, A.E., Newmark, P.A., 2011. Stem cell-based growth, regeneration, and remodeling of the planarian intestine. Developmental biology 356, 445-459.

Forsthoefel, D.J., Waters, F.A., Newmark, P.A., 2014. Generation of cell type-specific monoclonal antibodies for the planarian and optimization of sample processing for immunolabeling. BMC Dev Biol 14, 45.

Fraguas, S., Barberán, S., Iglesias, M., Rodríguez-Esteban, G., Cebrià, F., 2014. egr-4, a target of EGFR signaling, is required for the formation of the brain primordia and head regeneration in planarians. Development 141, 1835-1847.

Furukawa, T., Mukherjee, S., Bao, Z.Z., Morrow, E.M., Cepko, C.L., 2000. rax, Hes1, and notch1 promote the formation of Muller glia by postnatal retinal progenitor cells. Neuron 26, 383-394.

Gao, S., Takemura, S.Y., Ting, C.Y., Huang, S., Lu, Z., Luan, H., Rister, J., Thum, A.S., Yang, M., Hong, S.T., Wang, J.W., Odenwald, W.F., White, B.H., Meinertzhagen, I.A., Lee, C.H., 2008. The neural substrate of spectral preference in Drosophila. Neuron 60, 328-342.

Gauron, C., Rampon, C., Bouzaffour, M., Ipendey, E., Teillon, J., Volovitch, M., Vriz, S., 2013. Sustained production of ROS triggers compensatory proliferation and is required for regeneration to proceed. Scientific reports 3, 2084.

Gaviño, M.A., Reddien, P.W., 2011. A Bmp/Admp regulatory circuit controls maintenance and regeneration of dorsal-ventral polarity in planarians. Current biology : CB 21, 294-299.

Gegear, R.J., Casselman, A., Waddell, S., Reppert, S.M., 2008. Cryptochrome mediates light-dependent magnetosensitivity in Drosophila. Nature 454, 1014-1018.

Gehring, W., Rosbash, M., 2003. The coevolution of blue-light photoreception and circadian rhythms. Journal of molecular evolution 57 Suppl 1, S286-289.

Gehring, W.J., Ikeo, K., 1999. Pax 6: mastering eye morphogenesis and eye evolution. Trends in Genetics 15, 371-377.

González-Estévez, C., Felix, D.A., Aboobaker, A.A., Saló, E., 2007. Gtdap-1 promotes autophagy and is required for planarian remodeling during regeneration and starvation.

Proceedings of the National Academy of Sciences of the United States of America 104, 13373-13378.

González-Estévez, C., Felix, D.A., Rodríguez-Esteban, G., Aboobaker, A.A., 2012. Decreased neoblast progeny and increased cell death during starvation-induced planarian degrowth. The International journal of developmental biology 56, 83-91.

González-Estévez, C., Saló, E., 2010. Autophagy and apoptosis in planarians. Apoptosis 15, 279-292.

Grebe, E., Schaeffer, D.J., 1991. Planarians in toxicology, standardization of a rapid neurobehavioral toxicity test using phenol in a crossover study. Bulletin of environmental contamination and toxicology 46, 866-870.

Grohme, M.A., Schloissnig, S., Rozanski, A., Pippel, M., Young, G.R., Winkler, S., Brandl, H., Henry, I., Dahl, A., Powell, S., Hiller, M., Myers, E., Rink, J.C., 2018. The genome of Schmidtea mediterranea and the evolution of core cellular mechanisms. Nature 554, 56-61.

Guntur, A.R., Gu, P., Takle, K., Chen, J., Xiang, Y., Yang, C.H., 2015. Drosophila TRPA1 isoforms detect UV light via photochemical production of H2O2. Proceedings of the National Academy of Sciences of the United States of America 112, E5753-5761.

Gurley, K.A., Elliott, S.A., Simakov, O., Schmidt, H.A., Holstein, T.W., Sánchez Alvarado, A., 2010. Expression of secreted Wnt pathway components reveals unexpected complexity of the planarian amputation response. Developmental biology 347, 24-39.

Gurley, K.A., Rink, J.C., Sánchez Alvarado, A., 2008. B-Catenin defines head versus tail identity during planarian regeneration and homeostasis. Science (New York, N.Y.) 319, 323-327

Hanson, I.M., 2001. Mammalian homologues of the Drosophila eye specification genes. Seminars in cell & developmental biology 12, 475-484.

Harden Jones, F.R., 1971. The response of the planarian Dendrocoelum lacteum to an increase in light intensity. Animal Behaviour 19, 269-276.

Hardie, R.C., 2001. Phototransduction in Drosophila melanogaster. The Journal of experimental biology 204, 3403-3409.

Hargreaves, B., 2003. Water column optics and penetration of UVR, in: Helbling, E.W., Zagarese, H. (Eds.), UV Effects in Aquatic Organisms and Ecosystems. Cambridge: The Royal Society of Chemistry, pp. 61-105.

Haug, M.F., Gesemann, M., Lazović, V., Neuhauss, S.C.F., 2015. Eumetazoan Cryptochrome Phylogeny and Evolution. Genome Biology and Evolution 7, 601-619.

Hayashi, T., Motoishi, M., Yazawa, S., Itomi, K., Tanegashima, C., Nishimura, O., Agata, K., Tarui, H., 2011. A LIM-homeobox gene is required for differentiation of Wnt-expressing cells at the posterior end of the planarian body. Development 138, 3679-3688.

Henry, J.J., Tsonis, P.A., 2010. Molecular and cellular aspects of amphibian lens regeneration. Progress in retinal and eye research 29, 543-555.

Hill, E.M., Petersen, C.P., 2015. Wnt/Notum spatial feedback inhibition controls neoblast differentiation to regulate reversible growth of the planarian brain. Development 142, 4217-4229.

Hill, K., Schaefer, M., 2009. Ultraviolet light and photosensitising agents activate TRPA1 via generation of oxidative stress. Cell calcium 45, 155-164.

Holliday, L.S., 2014. Vacuolar H+-ATPase: An Essential Multitasking Enzyme in Physiology and Pathophysiology. New Journal of Science 2014, 21.

Honkavaara, J., Koivula, M., Korpimäki, E., Siitari, H., Viitala, J., 2002. Ultraviolet vision and foraging in terrestrial vertebrates. Oikos 98, 505-511.

Hunt, D.M., Wilkie, S.E., Bowmaker, J.K., Poopalasundaram, S., 2001a. Vision in the ultraviolet. Cellular and molecular life sciences : CMLS 58, 1583-1598.

Hunt, S., Cuthill, I.C., Bennett, A.T., Church, S.C., Partridge, J.C., 2001b. Is the ultraviolet waveband a special communication channel in avian mate choice? The Journal of experimental biology 204, 2499-2507.

Hwang, J.S., Kobayashi, C., Agata, K., Ikeo, K., Gojobori, T., 2004. Detection of apoptosis during planarian regeneration by the expression of apoptosis-related genes and TUNEL assay. Gene 333, 15-25.

Iglesias, M., Gómez-Skarmeta, J.L., Saló, E., Adell, T., 2008. Silencing of Smed-betacatenin1 generates radial-like hypercephalized planarians. Development 135, 1215-1221.

Inoue, T., Kumamoto, H., Okamoto, K., Umesono, Y., Sakai, M., Sánchez Alvarado, A., Agata, K., 2004. Morphological and functional recovery of the planarian photosensing system during head regeneration. Zoolog Sci 21, 275-283.

Inoue, T., Yamashita, T., Agata, K., 2014. Thermosensory signaling by TRPM is processed by brain serotonergic neurons to produce planarian thermotaxis. The Journal of neuroscience : the official journal of the Society for Neuroscience 34, 15701-15714.

Ishii, S., 1980. The ultrastructure of the protonephridial flame cell of the freshwater planarian Bdellocephala brunnea. Cell Tissue Res 206, 441-449.

Izumi, H., Torigoe, T., Ishiguchi, H., Uramoto, H., Yoshida, Y., Tanabe, M., Ise, T., Murakami, T., Yoshida, T., Nomoto, M., Kohno, K., 2003. Cellular pH regulators: potentially

promising molecular targets for cancer chemotherapy. Cancer Treatment Reviews 29, 541-549.

Jacobs, G.H., 1992. Ultraviolet Vision in Vertebrates. American Zoologist 32, 544-554.

Jäger, R., Fearnhead, H.O., 2012. "Dead Cells Talking": The Silent Form of Cell Death Is Not so Quiet. Biochem Res Int 2012, 453838.

Jellies, J., 2014a. Detection and selective avoidance of near ultraviolet radiation by an aquatic annelid: the medicinal leech. The Journal of experimental biology 217, 974-985.

Jellies, J., 2014b. Which way is up? Asymmetric spectral input along the dorsal-ventral axis influences postural responses in an amphibious annelid. Journal of comparative physiology. A, Neuroethology, sensory, neural, and behavioral physiology 200, 923-938.

Jellies, J., Kueh, D., 2012. Centrally patterned rhythmic activity integrated by a peripheral circuit linking multiple oscillators. Journal of comparative physiology. A, Neuroethology, sensory, neural, and behavioral physiology 198, 567-582.

Kalafatić, M., Kovacević, G., Franjević, D., 2006. Resistance of two planarian species to UV-irradiation. Folia biologica 54, 103-108.

Kaneko, Y., Hirota, K., Matsumoto, G., Hanyu, Y., 2001. Expression pattern of a newt Notch homologue in regenerating newt retina. Brain research. Developmental brain research 128, 53-62.

Kang, K., Pulver, S.R., Panzano, V.C., Chang, E.C., Griffith, L.C., Theobald, D.L., Garrity, P.A., 2010. Analysis of Drosophila TRPA1 reveals an ancient origin for human chemical nociception. Nature 464, 597-600.

Kaupp, U.B., Seifert, R., 2002. Cyclic nucleotide-gated ion channels. Physiological reviews 82, 769-824.

Kha, C.X., Son, P.H., Lauper, J., Tseng, K.A.-S., 2018. A model for investigating developmental eye repair in Xenopus laevis. Experimental Eye Research 169, 38-47.

King, R.S., Newmark, P.A., 2013. *In situ* hybridization protocol for enhanced detection of gene expression in the planarian *Schmidtea mediterranea*. BMC Dev Biol. 13, 1-16.

Kobayashi, C., Saito, Y., Ogawa, K., Agata, K., 2007. Wnt signaling is required for antero-posterior patterning of the planarian brain. Developmental biology 306, 714-724.

Kopan, R., 2002. Notch: a membrane-bound transcription factor. Journal of cell science 115, 1095-1097.

Kragl, M., Knapp, D., Nacu, E., Khattak, S., Maden, M., Epperlein, H.H., Tanaka, E.M., 2009. Cells keep a memory of their tissue origin during axolotl limb regeneration. Nature 460, 60.

Kumar, A., Godwin, J.W., Gates, P.B., Garza-Garcia, A.A., Brockes, J.P., 2007. Molecular Basis for the Nerve Dependence of Limb Regeneration in an Adult Vertebrate. Science (New York, N.Y.) 318, 772-777.

Kwan, K.Y., Allchorne, A.J., Vollrath, M.A., Christensen, A.P., Zhang, D.S., Woolf, C.J., Corey, D.P., 2006. TRPA1 contributes to cold, mechanical, and chemical nociception but is not essential for hair-cell transduction. Neuron 50, 277-289.

Labbé, R.M., Irimia, M., Currie, K.W., Lin, A., Zhu, S.J., Brown, D.D., Ross, E.J., Voisin, V., Bader, G.D., Blencowe, B.J., Pearson, B.J., 2012. A comparative transcriptomic analysis reveals conserved features of stem cell pluripotency in planarians and mammals. Stem cells (Dayton, Ohio) 30, 1734-1745.

Lai, E.C., 2004. Notch signaling: control of cell communication and cell fate. Development 131, 965-973.

Lander, R., Petersen, C.P., 2016. Wnt, Ptk7, and FGFRL expression gradients control trunk positional identity in planarian regeneration. Elife 5.

Lange, C., Prenninger, S., Knuckles, P., Taylor, V., Levin, M., Calegari, F., 2011. The H(+) vacuolar ATPase maintains neural stem cells in the developing mouse cortex. Stem Cells Dev 20, 843-850.

Lapan, S.W., Reddien, P.W., 2011. dlx and sp6-9 Control optic cup regeneration in a prototypic eye. PLoS genetics 7, e1002226.

Lapan, S.W., Reddien, P.W., 2012. Transcriptome analysis of the planarian eye identifies ovo as a specific regulator of eye regeneration. Cell reports 2, 294-307.

Laursen, W.J., Anderson, E.O., Hoffstaetter, L.J., Bagriantsev, S.N., Gracheva, E.O., 2015. Species-specific temperature sensitivity of TRPA1. Temperature (Austin, Tex.) 2, 214-226.

Le Borgne, R., 2006. Regulation of Notch signalling by endocytosis and endosomal sorting. Current Opinion in Cell Biology 18, 213-222.

Lees, A.D., 1948. The Sensory Physiology of the Sheep Tick, *Ixodes Ricinus*. Journal of Experimental Biology 25, 145-207.

Leuzinger, S., Hirth, F., Gerlich, D., Acampora, D., Simeone, A., Gehring, W.J., Finkelstein, R., Furukubo-Tokunaga, K., Reichert, H., 1998. Equivalence of the fly orthodenticle gene and the human OTX genes in embryonic brain development of Drosophila. Development 125, 1703-1710.

Levin, M., Pezzulo, G., Finkelstein, J.M., 2017. Endogenous Bioelectric Signaling Networks: Exploiting Voltage Gradients for Control of Growth and Form. Annu Rev Biomed Eng 19, 353-387.

Levin, M., Stevenson, C.G., 2012. Regulation of cell behavior and tissue patterning by bioelectrical signals: challenges and opportunities for biomedical engineering. Annu Rev Biomed Eng 14, 295-323.

Li, F., Huang, Q., Chen, J., Peng, Y., Roop, D.R., Bedford, J.S., Li, C.Y., 2010. Apoptotic cells activate the "phoenix rising" pathway to promote wound healing and tissue regeneration. Science signaling 3, ra13.

Lillie, F.R., 1900. Some Notes on Regeneration and Regulation in Planarians. The American Naturalist 34, 173-177.

Lillie, F.R., 1901. Some Notes on Regeneration and Regulation in Planarians. Am Jour Physiol 6, 129-141.

Lin, A.Y., Pearson, B.J., 2014. Planarian yorkie/YAP functions to integrate adult stem cell proliferation, organ homeostasis and maintenance of axial patterning. Development 141, 1197-1208.

Lin, A.Y.T., Pearson, B.J., 2017. Yorkie is required to restrict the injury responses in planarians. PLOS Genetics 13, e1006874.

Lukowiak, K., Jacklet, J.W., 1972. Habituation and dishabituation: interactions between peripheral and central nervous systems in Aplysia. Science (New York, N.Y.) 178, 1306-1308.

MacRae, E.K., 1967. The fine structure of sensory receptor processes in the auricular epithelium of the planarian, Dugesia tigrina. Zeitschrift fur Zellforschung und mikroskopische Anatomie (Vienna, Austria : 1948) 82, 479-494.

Mannini, L., Rossi, L., Deri, P., Gremigni, V., Salvetti, A., Saló, E., Batistoni, R., 2004. Djeyes absent (Djeya) controls prototypic planarian eye regeneration by cooperating with the transcription factor Djsix-1. Developmental biology 269, 346-359.

Marchler-Bauer, A., Derbyshire, M.K., Gonzales, N.R., Lu, S., Chitsaz, F., Geer, L.Y., Geer, R.C., He, J., Gwadz, M., Hurwitz, D.I., Lanczycki, C.J., Lu, F., Marchler, G.H., Song, J.S., Thanki, N., Wang, Z., Yamashita, R.A., Zhang, D., Zheng, C., Bryant, S.H., 2015. CDD: NCBI's conserved domain database. Nucleic acids research 43, D222-226.

Martín-Durán, J.M., Monjo, F., Romero, R., 2012. Morphological and molecular development of the eyes during embryogenesis of the freshwater planarian Schmidtea polychroa. Development genes and evolution 222, 45-54.

März, M., Seebeck, F., Bartscherer, K., 2013. A Pitx transcription factor controls the establishment and maintenance of the serotonergic lineage in planarians. Development 140, 4499-4509.

Mathews, J., Levin, M., 2017. Gap junctional signaling in pattern regulation: Physiological network connectivity instructs growth and form. Dev Neurobiol 77, 643-673.

Mathger, L.M., Roberts, S.B., Hanlon, R.T., 2010. Evidence for distributed light sensing in the skin of cuttlefish, Sepia officinalis. Biology letters 6, 600-603.

Matsumoto, T., Kawamura, G., 2005. The eyes of the common carp and Nile tilapia are sensitive to near-infrared. Fisheries Science 71, 350-355.

Maxfield, F.R., McGraw, T.E., 2004. Endocytic recycling. Nature reviews. Molecular cell biology 5, 121-132.

McConnell, J.V., 1967. A Manual of psychological experimentation on planarians.

McCormick, J.P., Fischer, J.R., Pachlatko, J.P., Eisenstark, A., 1976. Characterization of a cell-lethal product from the photooxidation of tryptophan: hydrogen peroxide. Science (New York, N.Y.) 191, 468-469.

McGwin, G., Jr., Owsley, C., 2005. Incidence of emergency department-treated eye injury in the United States. Archives of ophthalmology (Chicago, Ill. : 1960) 123, 662-666.

Menaker, M., 1968. Extraretinal light perception in the sparrow. I. Entrainment of the biological clock. Proceedings of the National Academy of Sciences of the United States of America 59, 414-421.

Miller, C.M., Newmark, P.A., 2012. An insulin-like peptide regulates size and adult stem cells in planarians. Int J Dev Biol 56, 75-82.

Miller, D.T., Cagan, R.L., 1998. Local induction of patterning and programmed cell death in the developing Drosophila retina. Development 125, 2327-2335.

Molina, M.D., Saló, E., Cebrià, F., 2007. The BMP pathway is essential for re-specification and maintenance of the dorsoventral axis in regenerating and intact planarians. Developmental biology 311, 79-94.

Monteiro, J., Aires, R., Becker, J.D., Jacinto, A., Certal, A.C., Rodriguez-Leon, J., 2014. V-ATPase proton pumping activity is required for adult zebrafish appendage regeneration. PloS one 9, e92594.

Morgan, T.H., 1898. Experimental studies of the regeneration of *Planaria maculata*. Arch. Entw. Mech. Org. 7, 364-397.

Morgan, T.H., 1900. Regeneration in planarians. Archiv. Entwick. Mech. 10, 58-119.

Morgan, T.H., 1901. Growth and regeneration in *Planaria lugubris*. Arch. Entw. Mech. Org. 13, 179-212.

Morgan, T.H., 1905. "Polarity" considered as a phenomenon of gradation of materials. J Exp Zool 2, 495-506.

Münch, J., González-Rajal, A., de la Pompa, J.L., 2013. Notch regulates blastema proliferation and prevents differentiation during adult zebrafish fin regeneration. Development 140, 1402-1411.

Münder, S., Tischer, S., Grundhuber, M., Büchels, N., Bruckmeier, N., Eckert, S., Seefeldt, C.A., Prexl, A., Käsbauer, T., Böttger, A., 2013. Notch-signalling is required for head regeneration and tentacle patterning in Hydra. Developmental biology 383, 146-157.

Nakazawa, M., Cebria, F., Mineta, K., Ikeo, K., Agata, K., Gojobori, T., 2003. Search for the evolutionary origin of a brain: planarian brain characterized by microarray. Molecular biology and evolution 20, 784-791.

Newmark, P.A., Sanchez Alvarado, A., 2002. Not your father's planarian: a classic model enters the era of functional genomics. Nature reviews. Genetics 3, 210-219.

Nilius, B., Appendino, G., Owsianik, G., 2012. The transient receptor potential channel TRPA1: from gene to pathophysiology. Pflugers Archiv : European journal of physiology 464, 425-458.

Nilsson, D.E., 2009. The evolution of eyes and visually guided behaviour. Philosophical transactions of the Royal Society of London. Series B, Biological sciences 364, 2833-2847.

Nogi, T., Levin, M., 2005. Characterization of innexin gene expression and functional roles of gap-junctional communication in planarian regeneration. Developmental biology 287, 314-335.

Nogi, T., Zhang, D., Chan, J.D., Marchant, J.S., 2009. A novel biological activity of praziquantel requiring voltage-operated Ca2+ channel beta subunits: subversion of flatworm regenerative polarity. PLoS neglected tropical diseases 3, e464.

Nolte, J., Brown, J.E., 1972a. Electrophysiological Properties of Cells in the Median Ocellus of Limulus. The Journal of general physiology 59, 167-185.

Nolte, J., Brown, J.E., 1972b. Ultraviolet-Induced Sensitivity to Visible Light in Ultraviolet Receptors of Limulus. The Journal of general physiology 59, 186-200.

Nuckels, R.J., Ng, A., Darland, T., Gross, J.M., 2009. The Vacuolar-ATPase Complex Regulates Retinoblast Proliferation and Survival, Photoreceptor Morphogenesis, and Pigmentation in the Zebrafish Eye. Investigative ophthalmology & visual science 50, 893-905.

Okamoto, K., Takeuchi, K., Agata, K., 2005. Neural projections in planarian brain revealed by fluorescent dye tracing. Zoolog Sci 22, 535-546.

Orger, M.B., Baier, H., 2005. Channeling of red and green cone inputs to the zebrafish optomotor response. Visual neuroscience 22, 275-281.

Orii, H., Katayama, T., Sakurai, T., Agata, K., Watanabe, K., 1998. Immunohistochemical detection of opsins in turbellarians. Hydrobiologia 383, 183-187.

Orii, H., Watanabe, K., 2007. Bone morphogenetic protein is required for dorso-ventral patterning in the planarian Dugesia japonica. Development, growth & differentiation 49, 345-349.

Osburn, C., Morris, D., 2003. Photochemistry of chromophoric dissolved organic matter in natural waters in: Helbing, E.W., Zagarese, H. (Eds.), UV Effects in Aquatic Organisms and Ecosystems. Cambridge: The Royal Society of Chemistry, pp. 187-217.

Oviedo, N.J., Morokuma, J., Walentek, P., Kema, I.P., Gu, M.B., Ahn, J.M., Hwang, J.S., Gojobori, T., Levin, M., 2010. Long-range neural and gap junction protein-mediated cues control polarity during planarian regeneration. Developmental biology 339, 188-199.

Oviedo, N.J., Newmark, P.A., Sánchez Alvarado, A., 2003. Allometric scaling and proportion regulation in the freshwater planarian Schmidtea mediterranea. Developmental dynamics : an official publication of the American Association of Anatomists 226, 326-333.

Pai, V.P., Aw, S., Shomrat, T., Lemire, J.M., Levin, M., 2012. Transmembrane voltage potential controls embryonic eye patterning in Xenopus laevis. Development 139, 313-323.

Pamarthy, S., Kulshrestha, A., Katara, G.K., Beaman, K.D., 2018. The curious case of vacuolar ATPase: regulation of signaling pathways. Molecular cancer 17, 41.

Pankey, S., Sunada, H., Horikoshi, T., Sakakibara, M., 2010. Cyclic nucleotide-gated channels are involved in phototransduction of dermal photoreceptors in Lymnaea stagnalis. Journal of comparative physiology. B, Biochemical, systemic, and environmental physiology 180, 1205-1211.

Parker, G.H.B., F.L., 1900. The reactions of planarians with and without eyes to light. Am Jour Physiol 4, 373-385.

Paskin, T.R., Jellies, J., Bacher, J., Beane, W.S., 2014. Planarian Phototactic Assay Reveals Differential Behavioral Responses Based on Wavelength. PloS one 9, e114708.

Pearson, B.J., Eisenhoffer, G.T., Gurley, K.A., Rink, J.C., Miller, D.E., Sánchez Alvarado, A., 2009. Formaldehyde-based whole-mount in situ hybridization method for planarians. Developmental dynamics : an official publication of the American Association of Anatomists 238, 443-450.

Peiris, T.H., Oviedo, N.J., 2013. Gap junction proteins: master regulators of the planarian stem cell response to tissue maintenance and injury. Biochim Biophys Acta 1828, 109-117.

Peitsch, D., Fietz, A., Hertel, H., de Souza, J., Ventura, D.F., Menzel, R., 1992. The spectral input systems of hymenopteran insects and their receptor-based colour vision. Journal of Comparative Physiology A 170, 23-40.

Pellettieri, J., Fitzgerald, P., Watanabe, S., Mancuso, J., Green, D.R., Sánchez Alvarado, A., 2010. Cell death and tissue remodeling in planarian regeneration. Developmental biology 338, 76-85.

Perathoner, S., Daane, J.M., Henrion, U., Seebohm, G., Higdon, C.W., Johnson, S.L., Nüsslein-Volhard, C., Harris, M.P., 2014. Bioelectric signaling regulates size in zebrafish fins. PLoS genetics 10, e1004080.

Pérez-Garijo, A., Steller, H., 2015. Spreading the word: non-autonomous effects of apoptosis during development, regeneration and disease. Development 142, 3253-3262.

Petersen, C.P., Reddien, P.W., 2008. Smed-Bcatenin-1 is required for anteroposterior blastema polarity in planarian regeneration. Science (New York, N.Y.) 319, 327-330.

Petersen, C.P., Reddien, P.W., 2009. A wound-induced Wnt expression program controls planarian regeneration polarity. Proceedings of the National Academy of Sciences of the United States of America 106, 17061-17066.

Petersen, C.P., Reddien, P.W., 2011. Polarized notum Activation at Wounds Inhibits Wnt Function to Promote Planarian Head Regeneration. Science (New York, N.Y.) 332, 852-855.

Phelan, P., 2005. Innexins: members of an evolutionarily conserved family of gap-junction proteins. Biochim Biophys Acta 1711, 225-245.

Phillips, J.B., Deutschlander, M.E., Freake, M.J., Borland, S.C., 2001. The role of extraocular photoreceptors in newt magnetic compass orientation: parallels between light-dependent magnetoreception and polarized light detection in vertebrates. The Journal of experimental biology 204, 2543-2552.

Pineda, D., Gonzalez, J., Callaerts, P., Ikeo, K., Gehring, W.J., Salo, E., 2000. Searching for the prototypic eye genetic network: Sine oculis is essential for eye regeneration in planarians. Proceedings of the National Academy of Sciences of the United States of America 97, 4525-4529.

Plachetzki, D.C., Fong, C.R., Oakley, T.H., 2010. The evolution of phototransduction from an ancestral cyclic nucleotide gated pathway. Proceedings. Biological sciences 277, 1963-1969.

Porter, M.L., 2016. Beyond the Eye: Molecular Evolution of Extraocular Photoreception. Integrative and comparative biology 56, 842-852.

Pra, D., Lau, A.H., Knakievicz, T., Carneiro, F.R., Erdtmann, B., 2005. Environmental genotoxicity assessment of an urban stream using freshwater planarians. Mutation research 585, 79-85.

Pyza, E., Borycz, J., Giebultowicz, J.M., Meinertzhagen, I.A., 2004. Involvement of V-ATPase in the regulation of cell size in the fly's visual system. Journal of insect physiology 50, 985-994.

Raible, F., Tessmar-Raible, K., Arboleda, E., Kaller, T., Bork, P., Arendt, D., Arnone, M.I., 2006. Opsins and clusters of sensory G-protein-coupled receptors in the sea urchin genome. Developmental biology 300, 461-475.

Ramirez, M.D., Speiser, D.I., Pankey, M.S., Oakley, T.H., 2011. Understanding the dermal light sense in the context of integrative photoreceptor cell biology. Visual neuroscience 28, 265-279.

Randolph, H., 1897. Observations and experiments on regeneration in Planarians. Arch. Entw. Mech. Org. 5, 352-372.

Reddien, P.W., 2013. Specialized progenitors and regeneration. Development 140, 951-957.

Reddien, P.W., Bermange, A.L., Kicza, A.M., Sánchez Alvarado, A., 2007. BMP signaling regulates the dorsal planarian midline and is needed for asymmetric regeneration. Development 134, 4043-4051.

Reddien, P.W., Sánchez Alvarado, A., 2004. Fundamentals of planarian regeneration. Annual review of cell and developmental biology 20, 725-757.

Reuter, H., März, M., Vogg, M.C., Eccles, D., Grífol-Boldú, L., Wehner, D., Owlarn, S., Adell, T., Weidinger, G., Bartscherer, K., 2015. Beta-catenin-dependent control of positional information along the AP body axis in planarians involves a teashirt family member. Cell reports 10, 253-265.

Reynierse, J.H., 1967. Reactions to light in four species of planaria. Journal of comparative and physiological psychology 63, 366-368.

Rink, J.C., 2013. Stem cell systems and regeneration in planaria. Development genes and evolution 223, 67-84.

Rink, J.C., Gurley, K.A., Elliott, S.A., Sánchez Alvarado, A., 2009. Planarian Hh signaling regulates regeneration polarity and links Hh Pathway evolution to cilia. Science (New York, N.Y.) 326, 1406-1410.

Rink, J.C., Vu, H.T.-K., Sánchez Alvarado, A., 2011. The maintenance and regeneration of the planarian excretory system are regulated by EGFR signaling. Development (Cambridge, England) 138, 3769-3780.

Robb, S.M., Gotting, K., Ross, E., Sánchez Alvarado, A., 2015. SmedGD 2.0: The Schmidtea mediterranea genome database. Genesis (New York, N.Y. : 2000) 53, 535-546.

Robb, S.M., Ross, E., Sánchez Alvarado, A., 2008. SmedGD: the Schmidtea mediterranea genome database. Nucleic acids research 36, D599-606.

Roberts-Galbraith, R.H., Brubacher, J.L., Newmark, P.A., 2016. A functional genomics screen in planarians reveals regulators of whole-brain regeneration. Elife 5.

Roberts-Galbraith, R.H., Newmark, P.A., 2015. On the organ trail: insights into organ regeneration in the planarian. Current opinion in genetics & development 32, 37-46.

Ross, K.G., Currie, K.W., Pearson, B.J., Zayas, R.M., 2017. Nervous system development and regeneration in freshwater planarians. Wiley Interdiscip Rev Dev Biol 6.

Rouhana, L., Tasaki, J., Saberi, A., Newmark, P.A., 2017. Genetic dissection of the planarian reproductive system through characterization of Schmidtea mediterranea CPEB homologs. Developmental biology 426, 43-55.

Rouhana, L., Weiss, J.A., Forsthoefel, D.J., Lee, H., King, R.S., Inoue, T., Shibata, N., Agata, K., Newmark, P.A., 2013. RNA interference by feeding in vitro-synthesized double-stranded RNA to planarians: methodology and dynamics. Developmental dynamics : an official publication of the American Association of Anatomists 242, 718-730.

Saftig, P., Klumperman, J., 2009. Lysosome biogenesis and lysosomal membrane proteins: trafficking meets function. Nature Reviews Molecular Cell Biology 10, 623.

Sakai, F., Agata, K., Orii, H., Watanabe, K., 2000. Organization and regeneration ability of spontaneous supernumerary eyes in planarians -eye regeneration field and pathway selection by optic nerves. Zoolog Sci 17, 375-381.

Sánchez Alvarado, A., Newmark, P.A., 1999. Double-stranded RNA specifically disrupts gene expression during planarian regeneration. Proceedings of the National Academy of Sciences of the United States of America 96, 5049-5054.

Scheer, N., Groth, A., Hans, S., Campos-Ortega, J.A., 2001. An instructive function for Notch in promoting gliogenesis in the zebrafish retina. Development 128, 1099-1107.

Scimone, M.L., Cote, L.E., Rogers, T., Reddien, P.W., 2016. Two FGFRL-Wnt circuits organize the planarian anteroposterior axis. Elife 5.

Scimone, M.L., Kravarik, K.M., Lapan, S.W., Reddien, P.W., 2014a. Neoblast specialization in regeneration of the planarian Schmidtea mediterranea. Stem Cell Reports 3, 339-352.

Scimone, M.L., Lapan, S.W., Reddien, P.W., 2014b. A forkhead transcription factor is wound-induced at the planarian midline and required for anterior pole regeneration. PLoS genetics 10, e1003999.

Scruggs, D., Scruggs, R., Stukenborg, G., Netland, P.A., Calland, J.F., 2012. Ocular injuries in trauma patients: an analysis of 28,340 trauma admissions in the 2003-2007 National Trauma Data Bank National Sample Program. The journal of trauma and acute care surgery 73, 1308-1312.

Shcherbakov, D., Knörzer, A., Espenhahn, S., Hilbig, R., Haas, U., Blum, M., 2013. Sensitivity Differences in Fish Offer Near-Infrared Vision as an Adaptable Evolutionary Trait. PloS one 8, e64429.

Shcherbakov, D., Knörzer, A., Hilbig, R., Haas, U., Blum, M., 2012. Near-infrared orientation of Mozambique tilapia Oreochromis mossambicus. Zoology 115, 233-238.

Shomrat, T., Levin, M., 2013. An automated training paradigm reveals long-term memory in planarians and its persistence through head regeneration. The Journal of experimental biology 216, 3799-3810.

Sinha, R.P., Hader, D.P., 2002. UV-induced DNA damage and repair: a review. Photochemical & photobiological sciences : Official journal of the European Photochemistry Association and the European Society for Photobiology 1, 225-236.

Skerrett, I.M., Williams, J.B., 2017. A structural and functional comparison of gap junction channels composed of connexins and innexins. Dev Neurobiol 77, 522-547.

Steven, D.M., 1963. The dermal light sense. Biological reviews of the Cambridge Philosophical Society 38, 204-240.

Stevens, N.M., 1909. Notes on regeneration in *Planaria simplicissima* and *Planaria morgani*. Arch. Entw. Mech. Org. 27, 610-621.

Stevenson, C.G., Beane, W.S., 2010. A low percent ethanol method for immobilizing planarians. PloS one 5, e15310.

Storz, U.C., Paul, R.J., 1998. Phototaxis in water fleas (Daphnia magna) is differently influenced by visible and UV light. Journal of Comparative Physiology A 183, 709-717.

Stubenhaus, B.M., Dustin, J.P., Neverett, E.R., Beaudry, M.S., Nadeau, L.E., Burk-McCoy, E., He, X., Pearson, B.J., Pellettieri, J., 2016. Light-induced depigmentation in planarians models the pathophysiology of acute porphyrias. Elife 5.

Stückemann, T., Cleland, J.P., Werner, S., Thi-Kim Vu, H., Bayersdorf, R., Liu, S.Y., Friedrich, B., Jülicher, F., Rink, J.C., 2017. Antagonistic Self-Organizing Patterning Systems

Control Maintenance and Regeneration of the Anteroposterior Axis in Planarians. Dev Cell 40, 248-263 e244.

Sullivan, S.A., Barthel, L.K., Largent, B.L., Raymond, P.A., 1997. A goldfish Notch-3 homologue is expressed in neurogenic regions of embryonic, adult, and regenerating brain and retina. Developmental genetics 20, 208-223.

Taddei-Ferretti, C., Musio, C., 2000. Photobehaviour of Hydra (Cnidaria, Hydrozoa) and correlated mechanisms: a case of extraocular photosensitivity. Journal of photochemistry and photobiology. B, Biology 55, 88-101.

Takahashi, N., Mori, Y., 2011. TRP Channels as Sensors and Signal Integrators of Redox Status Changes. Front Pharmacol 2, 58.

Takano, T., Pulvers, J.N., Inoue, T., Tarui, H., Sakamoto, H., Agata, K., Umesono, Y., 2007. Regeneration-dependent conditional gene knockdown (Readyknock) in planarian: demonstration of requirement for Djsnap-25 expression in the brain for negative phototactic behavior. Development, growth & differentiation 49, 383-394.

Taliaferro, W.H., 1920. Reactions to light in Planaria maculata, with special reference to the function and structure of the eyes. Journal of Experimental Zoology 31, 58-116.

Tseng, A., Levin, M., 2013. Cracking the bioelectric code: Probing endogenous ionic controls of pattern formation. Commun Integr Biol 6, e22595.

Tseng, A.S., Adams, D.S., Qiu, D., Koustubhan, P., Levin, M., 2007. Apoptosis is required during early stages of tail regeneration in Xenopus laevis. Developmental biology 301, 62-69.

Tseng, A.S., Beane, W.S., Lemire, J.M., Masi, A., Levin, M., 2010. Induction of vertebrate regeneration by a transient sodium current. The Journal of neuroscience : the official journal of the Society for Neuroscience 30, 13192-13200.

Tseng, A.S., Levin, M., 2012. Transducing bioelectric signals into epigenetic pathways during tadpole tail regeneration. Anat Rec (Hoboken) 295, 1541-1551.

Umesono, Y., Tasaki, J., Nishimura, K., Inoue, T., Agata, K., 2011. Regeneration in an evolutionarily primitive brain--the planarian Dugesia japonica model. The European journal of neuroscience 34, 863-869.

Umesono, Y., Watanabe, K., Agata, K., 1997. A planarian *orthopedia* homolog is specifically expressed in the branch region of both the mature and regenerating brain. Development, growth & differentiation 39, 723-727.

Vaccari, T., Duchi, S., Cortese, K., Tacchetti, C., Bilder, D., 2010. The vacuolar ATPase is required for physiological as well as pathological activation of the Notch receptor. Development 137, 1825-1832.

Valapala, M., Hose, S., Gongora, C., Dong, L., Wawrousek, E.F., Samuel Zigler, J., Jr., Sinha, D., 2013. Impaired endolysosomal function disrupts Notch signalling in optic nerve astrocytes. Nature communications 4, 1629.

Van Huizen, A.V., Tseng, A.S., Beane, W.S., 2017. Methylisothiazolinone toxicity and inhibition of wound healing and regeneration in planaria. Aquatic toxicology (Amsterdam, Netherlands) 191, 226-235.

van Wolfswinkel, J.C., Wagner, D.E., Reddien, P.W., 2014. Single-cell analysis reveals functionally distinct classes within the planarian stem cell compartment. Cell stem cell 15, 326-339.

Vásquez-Doorman, C., Petersen, C.P., 2014. zic-1 Expression in Planarian neoblasts after injury controls anterior pole regeneration. PLoS genetics 10, e1004452.

Viana, F., 2016. TRPA1 channels: molecular sentinels of cellular stress and tissue damage. The Journal of physiology 594, 4151-4169.

Vöcking, O., Kourtesis, I., Tumu, S.C., Hausen, H., 2017. Co-expression of xenopsin and rhabdomeric opsin in photoreceptors bearing microvilli and cilia. eLife 6, e23435.

Vogg, M.C., Owlarn, S., Pérez Rico, Y.A., Xie, J., Suzuki, Y., Gentile, L., Wu, W., Bartscherer, K., 2014. Stem cell-dependent formation of a functional anterior regeneration pole in planarians requires Zic and Forkhead transcription factors. Developmental biology 390, 136-148.

Wald, G., 1968. Molecular basis of visual excitation. Science (New York, N.Y.) 162, 230-239.

Wells, B.S., Yoshida, E., Johnston, L.A., 2006. Compensatory proliferation in *Drosophila* imaginal discs requires droc-dependent p53 activity. Current biology : CB 16, 1606-1615.

Wenemoser, D., Lapan, S.W., Wilkinson, A.W., Bell, G.W., Reddien, P.W., 2012. A molecular wound response program associated with regeneration initiation in planarians. Genes Dev 26, 988-1002.

Wenemoser, D., Reddien, P.W., 2010. Planarian regeneration involves distinct stem cell responses to wounds and tissue absence. Developmental biology 344, 979-991.

Witchley, J.N., Mayer, M., Wagner, D.E., Owen, J.H., Reddien, P.W., 2013. Muscle cells provide instructions for planarian regeneration. Cell reports 4, 633-641.

Wu, H.-P.P., Persinger, M.A., 2011. Increased mobility and stem-cell proliferation rate in Dugesia tigrina induced by 880nm light emitting diode. Journal of Photochemistry and Photobiology B: Biology 102, 156-160.

Wu, J.-P., Li, M.-H., 2018. The use of freshwater planarians in environmental toxicology studies: Advantages and potential. Ecotoxicology and environmental safety 161, 45-56.

Wurtzel, O., Cote, L.E., Poirier, A., Satija, R., Regev, A., Reddien, P.W., 2015. A Generic and Cell-Type-Specific Wound Response Precedes Regeneration in Planarians. Dev Cell 35, 632-645.

Xiang, Y., Yuan, Q., Vogt, N., Looger, L.L., Jan, L.Y., Jan, Y.N., 2010. Light-avoidance-mediating photoreceptors tile the Drosophila larval body wall. Nature 468, 921-926.

Yan, Y., Denef, N., Schupbach, T., 2009. The vacuolar proton pump, V-ATPase, is required for notch signaling and endosomal trafficking in Drosophila. Dev Cell 17, 387-402.

Yang, X., Kaj, K.J., Schwab, D.J., Collins, E.S., 2017. Coordination of size-control, reproduction and generational memory in freshwater planarians. Physical biology 14, 036003.

Yang, X., Klein, R., Tian, X., Cheng, H.T., Kopan, R., Shen, J., 2004. Notch activation induces apoptosis in neural progenitor cells through a p53-dependent pathway. Developmental biology 269, 81-94.

Zhang, D., Chan, J.D., Nogi, T., Marchant, J.S., 2011. Opposing roles of voltage-gated Ca2+ channels in neuronal control of regenerative patterning. The Journal of neuroscience : the official journal of the Society for Neuroscience 31, 15983-15995.

Zhu, S.J., Pearson, B.J., 2016. (Neo)blast from the past: new insights into planarian stem cell lineages. Current opinion in genetics & development 40, 74-80.

Zukauskas, A., Vaicekauskas, R., Ivanauskas, F., Vaitkevicius, H., Vitta, P., Shur, M.S., 2009. Statistical approach to color quality of solid-state lamps*. IEEE Journal of Selected Topics in Quantum Electronics 15, 1753-1762.

Zygmunt, P.M., Högestätt, E.D., 2014. TRPA1, in: Nilius, B., Flockerzi, V. (Eds.), Mammalian Transient Receptor Potential (TRP) Cation Channels. Springer-Verlag Berlin Heidelberg.